Lecture Notes on

Laser Physics

Mosbah Difallah

E-mail : mosbah-difallah@univ-eloued.dz

April 6, 2025

Contents

List of Figures

List of Tables

Chapter 1

Fundamentals of Lasers

1.1 A Brief History of Lasers

- LASER acronym for Light Amplification by Stimulated Emission of Radiation.The lasing process is based on *stimulated emission* which has to compete with the inverse process of *absorption*. The laser consists of a gain (amplifying) medium where the stimulated emission process occurs, a resonator made of fully and partial reflecting mirrors, and a pumping process, as seen in Fig. (1.1).

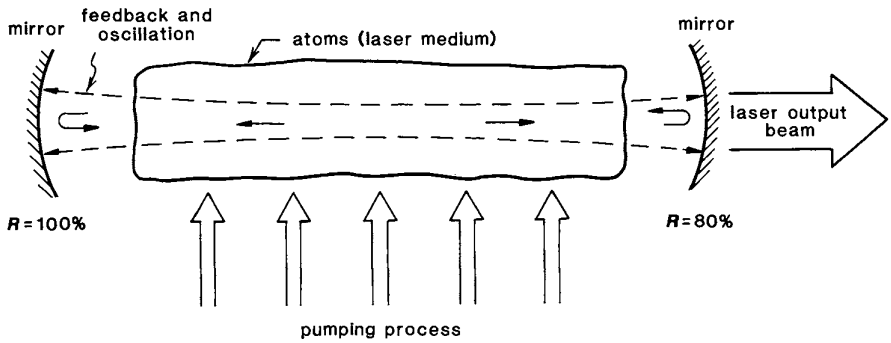

Fig. 1.1: Elements of a typical laser.

- 1917 Einstein used stimulated emission do derive Planck's equation for radiation.
- 1928 Ladenburg measured stimulated emission.
- 1954 Townes used stimulated emission for the amplification of radiation. He build a MASER (with microwaves).
- 1954 Basov and Prokhorov calculated MASERS.

- 1958 Schawlow and Townes build a resonator.
- 1959 Gould find a patent about lasers.
- 1960 Maiman build the first laser (ruby laser at 694 nm).
- 1961 Javan made the first He-Ne gas laser at 633 nm.
- 1964 Townes, Basov and Prokhorov received the Nobel Prize in physics for "fundamental work in the field of quantum electronics, which has led to the construction of oscillators and amplifiers based on the maser–laser principle".
- It's fascinating that only a few years after the first laser was developed, by the mid-1960s, laser activity had been observed in all types of media, including gases, liquids, semiconductors, and crystalline solids. However, the titanium sapphire laser, which holds significant economic importance, is a notable exception, as it wasn't developed until 1984.
- The range of laser types, technologies, and applications after forty years of research and development is so vast that a comprehensive list is nearly impossible. Applications span from the treatment of retina to laser-induced nuclear fusion, and from beam steering in tunnel construction to the study of ultrafast chemical processes with sub-10-fs pulses and quantum information transfer.

Materials	**Technologies**
1960 Maiman: Ruby laser (694 nm).	1961 Collins: Q-switch.
1961 Javan: He-Ne laser (1150 nm, 633 nm).	1965 Mocker and Collins: passive mode
1961 Snitzer: Nd^{3+} glass laser (1064 nm).	locking (ps pulses).
various: GaAS diode laser (840 nm).	1968 Bradley and Durrant: synchroneous pumping.
1964 Patel: CO_2 laser, Geusic: Nd:YAG laser.	1971 Kogelnik and Shank: distributed
1965 Kasper and Pimentel: chemical HCl laser.	feedback laser.
1966 Sorokin and Lankard: dye laser.	1985 Strickland and Mourou: chirped
1971 Basov: Excimer laser.	pulse amplification.
1985 Moulton: Ti-Sa laser (800 nm, pulsed).	1991 Spence: Kerr lens mode locking.

Table 1.1: Laser materials and technologies

1.2 Properties of Laser Radiation

- An ideal monochromatic source emits electromagnetic radiation at a single frequency as plane wave homogeneous electric field

$$\begin{aligned} \mathbf{E}(t) &= \mathbf{E}_0 \cos(\mathbf{k}\cdot\mathbf{r} - \omega t) && (1.1)\\ &= \mathbf{E}_0 \mathrm{Re}\{e^{i\phi}\},\ \phi = \mathbf{k}\cdot\mathbf{r} - \omega t && (1.2)\\ &= \mathbf{E}_0 \frac{e^{i\phi} + e^{-i\phi}}{2}. && (1.3) \end{aligned}$$

  Definitions:

  i) $\phi = \mathbf{k}\cdot\mathbf{r} - \omega t$ is the phase.

  ii) $k = 2\pi/\lambda$ is the wave vector.

  iii) $\omega = 2\pi\nu$ is the angular frequency.

- The electric field $\mathbf{E}$ is determined by the amplitude E_0 and the phase ϕ.

- The speed of light is $c = \lambda\nu = 299792458\,\mathrm{m/s}$.

- The photon energy is given by $E = h\nu = mc^2 = pc$, with the momentum $p = mc$, such that $p = h/\lambda$ is the momentum of light where $h = 6.626 \times 10^{-34}$J.s is Planck's constant.

- The intensity of the field reads

$$I(t) = \epsilon_0 c |\mathbf{E}(t)|^2, \tag{1.4}$$

  where $\epsilon_0 = 8.8 \times 10^{-12}\,\mathrm{A\,s/V\,m}$ is the dielectric constant. Since the photodetectors are too slow to measure $I(t)$ instantaneously, averaging over time yields

$$I = \frac{1}{2}\epsilon_0 c E_0^2. \tag{1.5}$$

1.3 Important Laser Parameters

- Parameters needed to describe a laser beam are:

  a) Spectral or temporal intensity distribution.

  b) Spatial intensity distribution.

c) Temporal and spatial coherence.

d) Polarization.

a) FOURIER transform connects spectrum to temporal behavior

$$\tilde{I}(\omega) = \int_{-\infty}^{+\infty} I(t) \mathrm{e}^{-\mathrm{i}\omega t} \mathrm{d}t \tag{1.6}$$

time-limited pulses have always a broad spectrum.

b) If a laser beam is not ideally symmetric as a GAUSSIAN beam, one uses for identifying the beam radius W the definition of the second moment (which is measurable quantity)

$$W^2(z) := \frac{\int\int r^2 I(r,\phi,z) r \mathrm{d}r \mathrm{d}\phi}{\int\int I(r,\phi,z) r \mathrm{d}r \mathrm{d}\phi} \tag{1.7}$$

The divergence angle is defined as

$$\theta := \frac{W_2 - W_1}{z_2 - z_1}. \tag{1.8}$$

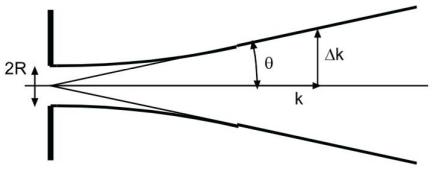

Fig. 1.2: The divergence of a collimated laser beam at an aperture.

- An intuitive connection between $W(z=0)$ and θ can be explained using particle-wave duality.

  1. **The particle character**: the photon is a particle that can transfer energy, angular momentum, or parity during an interaction.
  2. **The wave character**: the light is a wave when discussing interference, diffraction, beam propagation, etc.

- The *interference* phenomena that occurs for waves behind a double slit works as well for photons. The non-local character of a wave does not arise from the overlapping of many photons. The ability to interfere is not an ensemble property; indeed, the interference pattern of the double-slit setup arises even when the photon flux is so low that at any given time, no more than one photon is detected.

- The following example aims to illustrate particle-wave duality: One could detect an interference pattern behind a double slit, for instance, by using an arrangement of photomultipliers. Each photomultiplier is localized with an extent Δx in the plane perpendicular to the direction of photon propagation, and individual photons are detected by triggering an electron avalanche.

- The quantum nature of photons implies an uncertainty in momentum $\Delta x \Delta p = h/\pi$.[1] The distribution of photons is similar to the wave character. The uncertainty relation is also valid for particular propagation. For example an aperture with radius $R = \Delta x$ causes a distribution of momentum

$$R = \Delta x, \quad \Delta p = \hbar \Delta k \Longrightarrow \theta = \frac{\Delta k}{k} \geq \frac{\lambda}{R\pi}. \tag{1.9}$$

- This phenomenon is called *diffraction*. Due to diffraction, there cannot be a collimated laser beam over arbitrary distances. The finite diameter of the laser beam inevitably leads to divergence. Following the beam path in the opposite direction, one realizes that a corresponding laser beam cannot be focused into an infinitesimal point but only into a finite, diffraction-limited spot. In fact, this spot is at least 1.4 times larger than given in Eq. (1.9). This is related to the definition of beam width Δx, for which, conventionally, the $1/e^2$ width of the intensity distribution, equivalent to the $1/e$ width of the amplitude distribution, has been taken here. We will delve into the corresponding definitions for Gaussian beams and diffraction more precisely in Chapter 2, as well as the analogous uncertainty of time and frequency (energy) in treating short pulses in Chapter 4. The laser beam is diffraction-limited

$$\boxed{\theta \geq \frac{\lambda}{R\pi}.} \tag{1.10}$$

- Moreover the product of the divergence angle and the beam waist fulfills

$$\boxed{\theta W_0 \geq \frac{\lambda}{\pi},} \tag{1.11}$$

  where $W_0 = W(z = 0)$.

- For ideal Gaussian beams $\theta W_0 = \frac{\lambda}{\pi}$, and for real beams $\theta \overline{W}_0 > \frac{\lambda}{\pi}$. Let us define factor $Q = M^2$, called the beam propagation factor (M^2 factor), which indicates the beam quality of a real beam. One forms the quotient of the real beam radius $\overline{W}_0$ with the ideal beam radius

$$Q = M^2 = \frac{\overline{W}_0}{W_0} = \overline{W}_0 \frac{\pi\theta}{\lambda}. \tag{1.12}$$

[1] The exact form depends somewhat on the choice of wave functions and the precise definition of Δx and Δp.

- This value indicates by how much the beam diameter is larger compared to the ideal (GAUSSIAN) beam, while maintaining the same divergence angle. Therefore, it is a measure of the beam's ability to focus.

- Similarly, it indicates by how much the divergence angle Θ of a real beam is larger than the divergence angle θ of the ideal beam, given the same radius of the beam waist:

$$\Theta = M^2\theta. \tag{1.13}$$

  The term "beam quality factor" illustrates that divergence is a consequence of diffraction.

- For certain applications, such as material processing, the definition of *brightness* is meaningful. It is essentially the quotient of power and beam quality:

$$L = \frac{P}{(\Theta W_0)^2}. \tag{1.14}$$

- Finally, the *brilliance* takes into account the spectral distribution of the radiation and is defined as:

$$B(\lambda) = L\frac{\lambda/1000}{\Delta\lambda}. \tag{1.15}$$

c) Coherence

- The measurement of the phase of a wave emitted from a light source $E(\mathbf{r}, t)$ at two distinct points in space $(\mathbf{r}_1, \mathbf{r}_2)$ and time (t_1, t_2) reveals the coherence properties (temporal and spatial) of the light source.

- Suppose we measure this field at some point $\mathbf{r}_1$ and different times t_1, t_2. For stationary light source we define the first-order temporal correlation function

$$\begin{aligned} \Gamma^{(1)}(\mathbf{r}_1, t_1; \mathbf{r}_1, t_2) &= \Gamma^{(1)}(\mathbf{r}_1, \mathbf{r}_1, \tau) \\ &= \langle E^*(\mathbf{r}_1, t+\tau)E(\mathbf{r}_1, t)\rangle_{\text{ens}} \end{aligned} \tag{1.16}$$

  where $\langle\cdots\rangle_{\text{ens}}$ states for an ensemble average and $\tau = t_1 - t_2$ is some time delay.

- Assuming *ergodicity*, i.e., the ensemble average is equivalent to time average. Therefore

$$\Gamma^{(1)}(\mathbf{r}_1, \mathbf{r}_1, \tau) \equiv \Gamma^{(1)}(\tau) = \lim_{T\longrightarrow\infty}\frac{1}{T}\int_0^T E^*(\mathbf{r}_1, t+\tau)E(\mathbf{r}_1, t)\mathrm{d}t. \tag{1.17}$$

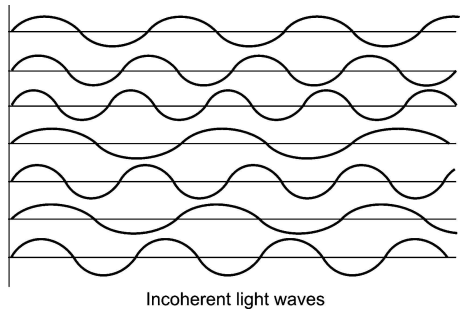

(a)

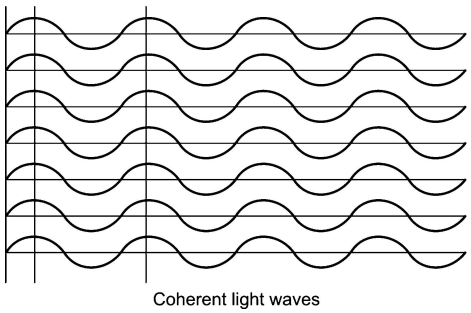

(b)

Fig. 1.3: Coherence.

- Moreover, the normalized coherence function can be written as

$$\begin{aligned} g^{(1)}(\tau) &= \frac{\langle E^*(\mathbf{r}_1, t+\tau)E(\mathbf{r}_1, t)\rangle}{\langle E^*(\mathbf{r}_1, t+\tau)E(\mathbf{r}_1, t+\tau)\rangle^{1/2}\langle E^*(\mathbf{r}_1, t)E(\mathbf{r}_1, t)\rangle^{1/2}} \\ &= \frac{\langle E^*(\mathbf{r}_1, t+\tau)E(\mathbf{r}_1, t)\rangle}{\langle I(\mathbf{r}_1, t)\rangle}. \end{aligned} \tag{1.18}$$

- $g^{(1)}(\tau)$ is the complex degree of temporal coherence, and its modulus $|g^{(1)}(\tau)|$ is the degree of temporal coherence.
- Properties of $g^{(1)}(\tau)$:
  1. $g^{(1)}(0) = 1$.
  2. $g^{(1)}(-\tau) = g^{(1)^*}(\tau)$.
  3. $|g^{(1)}(\tau)| \leq 1$.
- If $|g^{(1)}(\tau)| = 1, \forall\tau$, the beam is perfectly *coherent*.
- If $|g^{(1)}(\tau)| = 0, \forall\tau > 0$, the beam is completely *incoherent*.

- In the case of monochromatic wave $E(\mathbf{r},t) = E_0(\mathbf{r})\mathrm{e}^{-i\omega t}$

$$\begin{aligned}\Gamma^{(1)}(\mathbf{r}_1,\mathbf{r}_1,\tau) &= \lim_{T\longrightarrow\infty}\frac{1}{T}\int_0^T |E(\mathbf{r}_1)|^2\mathrm{e}^{\mathrm{i}\omega(t+\tau)}\mathrm{e}^{-\mathrm{i}\omega t}\mathrm{d}t \\ &= |E(\mathbf{r}_1)|^2\mathrm{e}^{\mathrm{i}\omega\tau} \\ &= I(\mathbf{r}_1)\mathrm{e}^{\mathrm{i}\omega\tau}, \end{aligned} \tag{1.19}$$

  so that

$$|g^{(1)}(\tau)| = 1, \quad \forall\tau, \tag{1.20}$$

  i.e., perfect coherence.

- Since $|g^{(1)}(\tau)|$ is symmetric in τ, the coherence time τ_{coh} is defined as

$$\tau_{\mathrm{coh}} = \int_{-\infty}^{+\infty} |g^{(1)}(\tau)|^2\mathrm{d}\tau, \tag{1.21}$$

  where $\tau_{\mathrm{coh}} \longrightarrow \infty$ in the case of *perfect coherence* and $\tau_{\mathrm{coh}} \longrightarrow 0$ for *complete incoherence*.

- The coherence length reads

$$L_{\mathrm{coh}} = c\tau_{\mathrm{coh}}. \tag{1.22}$$

- Michelson interferometer measures the degree of coherence of light waves. A light source impinges on 50:50 beam splitter, one part $E_1(t)$ propagates upward and reflected by a mirror and the other part $E_2(t)$ is transmitted by the beam splitter and reflected back by a movable mirror. The light field $E_2(t)$ is equivalent to $E_1(t+\tau)$ because it travels an excess amount of time $\tau = 2d/c$ whenever recombines to the beam splitter. Finally, the detector measures simultaneously the electric field at different times.

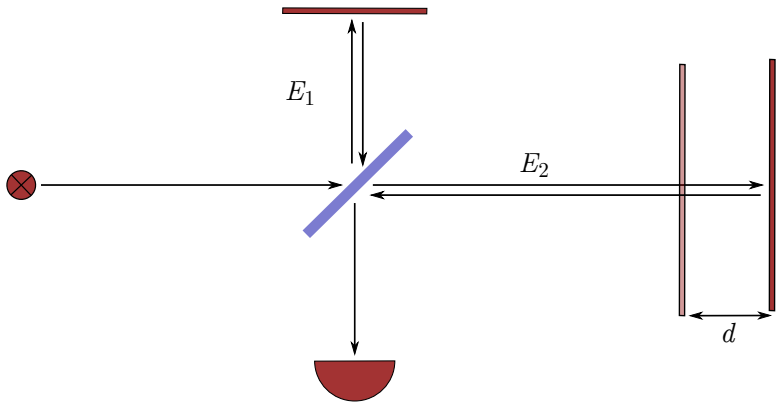

Fig. 1.4: Michelson interferometer.

- The electric field at the detector is

$$\begin{aligned} E(t) &= E_1(t) + E_2(t) \\ &= E_1(t) + E_1(t+\tau), \end{aligned} \tag{1.23}$$

hence the intensity would be

$$\begin{aligned} I(\tau) &= \left\langle \big(E_1(t) + E_2(t)\big)^* \big(E_1(t) + E_2(t)\big) \right\rangle \\ &= \langle E_1^*(t)E_1(t)\rangle + \langle E_2^*(t)E_2(t)\rangle + \langle E_1^*(t)E_2(t)\rangle + \langle E_2^*(t)E_1(t)\rangle \\ &= 2I_1 + 2\mathrm{Re}\,\langle E_1^*(t)E_2(t)\rangle \\ &= 2I_1 + 2\mathrm{Re}\,\Gamma^{(1)}(\mathbf{r},\mathbf{r},\tau). \end{aligned} \tag{1.24}$$

- For a monochromatic wave $E_1(t) = E_0 e^{-\mathrm{i}\omega t}$

$$\begin{aligned} I(\tau) &= 2I_1 + 2I_1 \mathrm{Re}\,\mathrm{e}^{\mathrm{i}\omega\tau} \\ &= 2I_1(1 + \cos\omega\tau) \\ &= 2I_1(1 + \mathrm{Re}\,g^{(1)}(\tau)). \end{aligned} \tag{1.25}$$

- For monochromatic light wave entering the interferometer, the intensity at the detector oscillates with frequency ω and period τ. Additionally, the amplitude of the intensity varies between 0 and $4I_1$.

- According to Eq. (1.24), the intensity amplitude is maximum/minimum at maximum/minimum $\mathrm{Re}\,\Gamma^{(1)}(\tau)$. The figure (1.5) shows the intensity at the detector for different light waves.

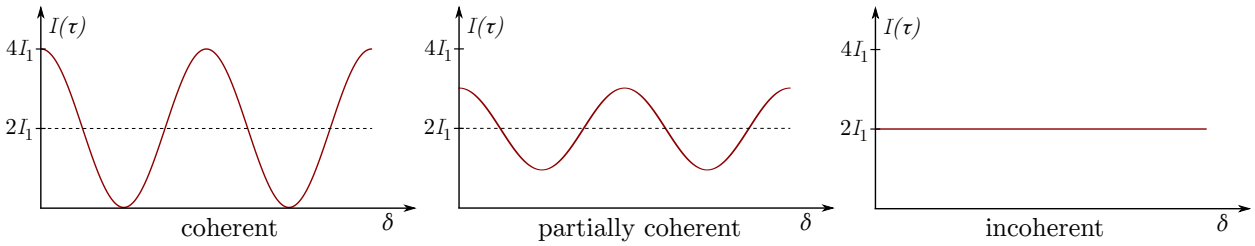

Fig. 1.5: Intensity of the signal for different light sources.

- The coherence order can also be quantified via the *fringe visibility*

$$V = \frac{I_{\max}(\tau_1) - I_{\min}(\tau_2)}{I_{\max}(\tau_1) + I_{\min}(\tau_2)}. \tag{1.26}$$

- Assuming that $\mathrm{Re}\,\Gamma^{(1)}(\tau_1) \approx -\mathrm{Re}\,\Gamma^{(1)}(\tau_2) \approx |\Gamma^{(1)}(\tau)|$, we find from (1.24) that

$$I_{\max}(\tau_1) = 2I_1 + 2|\Gamma^{(1)}(\tau)| \tag{1.27}$$
$$I_{\min}(\tau_2) = 2I_1 - 2|\Gamma^{(1)}(\tau)|, \tag{1.28}$$

  which implies that

$$\boxed{V(\tau) = |g^{(1)}(\tau)|.} \tag{1.29}$$

  Thus measuring the fringe visibility provides a direct access to the degree of temporal coherence.

- The spectrum of a stochastic light source is given by Fourier transform

$$\tilde{E}(\mathbf{r},\omega) = \int_{-\infty}^{+\infty} E(\mathbf{r},t)\mathrm{e}^{-\mathrm{i}\omega t}\mathrm{d}t, \quad \text{and} \quad \tilde{E}(\mathbf{r},\omega) = 0 \quad \text{for} \quad \omega < 0. \tag{1.30}$$

- The quantity $\left\langle |\tilde{E}(\mathbf{r},\omega)|^2 \right\rangle$ is called the *spectral energy density*.

- The expression (1.30) is not well-defined for monochromatic waves, hence cut-off at finite time T is needed for stationary light fields

$$\tilde{E}_T(\mathbf{r},\omega) = \int_{-T/2}^{+T/2} E(\mathbf{r},t)\mathrm{e}^{-\mathrm{i}\omega t}\mathrm{d}t, \tag{1.31}$$

  and the *spectral power density* reads

$$S(\omega) = \lim_{T\to\infty} \frac{1}{T} \left\langle \left|\tilde{E}_T(\mathbf{r},\omega)\right|^2 \right\rangle \quad \text{and} \quad S(\omega) = 0 \quad \text{for} \quad \omega < 0. \tag{1.32}$$

- The *average total intensity* is therefore

$$I(\omega) = \int_0^{\infty} S(\omega)\mathrm{d}\omega. \tag{1.33}$$

- The integral (1.32) is a *convolution* of electric fields and can be written as

$$\boxed{S(\omega) = \int_{-\infty}^{+\infty} \Gamma^{(1)}(\mathbf{r},\mathbf{r},\tau)\mathrm{e}^{-\mathrm{i}\omega\tau}\mathrm{d}\tau,} \tag{1.34}$$

  which is known as *Wiener-Khinchin theorem*.

Proof. We insert Eq. (1.30) into Eq. (1.32):

$$\begin{aligned} S(\omega) &= \lim_{T\to\infty}\frac{1}{T}\left\langle \tilde{E}_T^*(\mathbf{r},\omega)\tilde{E}_T(\mathbf{r},\omega)\right\rangle \\ &= \lim_{T\to\infty}\frac{1}{T}\left\langle \int_{-T/2}^{+T/2} E^*(\mathbf{r},t_2)\mathrm{e}^{\mathrm{i}\omega t_2}\mathrm{d}t_2 \int_{-T/2}^{+T/2} E(\mathbf{r},t_1)\mathrm{e}^{-\mathrm{i}\omega t_1}\mathrm{d}t_1 \right\rangle \\ &= \lim_{T\to\infty}\frac{1}{T}\int_{-T/2}^{+T/2}\int_{-T/2}^{+T/2} \mathrm{e}^{-\mathrm{i}\omega(t_1-t_2)}\left\langle E^*(\mathbf{r},t_2)E(\mathbf{r},t_1)\right\rangle \mathrm{d}t_1\mathrm{d}t_2 \\ &= \lim_{T\to\infty}\frac{1}{T}\int_{-T/2}^{+T/2}\int_{-T/2}^{+T/2} \mathrm{e}^{-\mathrm{i}\omega(t_1-t_2)}\Gamma^{(1)}(\mathbf{r},t_1;\mathbf{r},t_2)\mathrm{d}t_1\mathrm{d}t_2 \\ &= \lim_{T\to\infty}\frac{1}{T}\int_{-T/2}^{+T/2}\int_{-T/2-t_1}^{+T/2+t_1} \mathrm{e}^{-\mathrm{i}\omega\tau}\Gamma^{(1)}(\mathbf{r},\mathbf{r},\tau)\mathrm{d}\tau\mathrm{d}t_1 \\ &= \lim_{T\to\infty}\frac{1}{T}\int_{-T/2}^{+T/2}\tilde{\Gamma}^{(1)}(\mathbf{r},\mathbf{r},\omega)\mathrm{d}t_1 = \tilde{\Gamma}^{(1)}(\mathbf{r},\mathbf{r},\omega). \end{aligned} \tag{1.35}$$

- The spectral width (line width) is the width of the spectral density function $S(\omega)$ because $S(\omega)$ and $\Gamma^{(1)}(\tau)$ are FOURIER-transform pairs.
- The widths of $S(\omega)$ and $\Gamma^{(1)}(\tau)$ are inversely proportional to one another

$$\Delta\omega_{\mathrm{coh}} = \frac{\left(\int_0^\infty S(\omega)\mathrm{d}\omega\right)^2}{\int_0^\infty S^2(\omega)\mathrm{d}\omega} \propto \frac{1}{\tau_{\mathrm{coh}}}. \tag{1.36}$$

Source	$\Delta\nu_{\mathrm{coh}}$	$\tau_{\mathrm{coh}} = 1/\Delta\nu_{\mathrm{coh}}$	$L_{\mathrm{coh}} = c\tau_{\mathrm{coh}}$
Sunlight $400-800\,\mathrm{nm}$	$3.74\times10^{14}\,\mathrm{Hz}$	$2.67\,\mathrm{fs}$	$800\,\mathrm{nm}$
LED $\lambda_0 = 1\,\mu\mathrm{m}$	$1.5\times10^{13}\,\mathrm{Hz}$	$67\,\mathrm{fs}$	$20\,\mu\mathrm{m}$
Single-mode laser $\lambda_0 = 632\,\mathrm{nm}$	$1\times10^{6}\,\mathrm{MHz}$	$1\,\mu\mathrm{s}$	$300\,\mathrm{m}$

Table 1.2: Coherence properties for different light sources

- Nowadays, there exist lasers having sub-hertz linewidths, and hundreds of kilometers coherence lengths.

d) Polarization

- Since the wave equation is a linear differential equation, the supperposition principle holds. Consider a plane wave propagating in z-direction, then the cartesian

components of the electric field are

$$E_x(z,t) = |E_x|\cos(kz-\omega t+\varphi_x) \quad (1.37)$$
$$E_y(z,t) = |E_y|\cos(kz-\omega t+\varphi_y) \quad (1.38)$$
$$E_z(z,t) = 0. \quad (1.39)$$

- If $\varphi_x \neq \varphi_y$, the polarization is called *elliptic* and the field vector $\mathrm{Re}\,\mathbf{E}(\mathbf{r},t)$ rotates at $\mathbf{r}$ on an ellipse spanned by the unit vectors $\mathbf{e}_x$ and $\mathbf{e}_y$.
- If $\varphi_x = \varphi_y \pm \pi/2$ and $|E_x| = |E_y|$, the polarization is called *circular*.
- If $\varphi_x = \varphi_y + n\pi$ and $|E_x| = 0$ or $|E_y| = 0$, the polarization is called *linear*.
- At $z = 0$ the electric field components becomes

$$E_x(t) = |E_x|\cos(-\omega t+\varphi_x) \quad (1.40)$$
$$E_y(t) = |E_y|\cos(-\omega t+\varphi_y). \quad (1.41)$$

Therefore, an equation of ellipse derived from Eq.(1.40) and Eq.(1.41) reads

$$\left(\frac{E_x}{|E_x|}\right)^2 + \left(\frac{E_x}{|E_x|}\right)^2 - \frac{2E_xE_y}{|E_x||E_y|}\cos(\varphi_x-\varphi_y) = \sin^2(\varphi_x-\varphi_y). \quad (1.42)$$

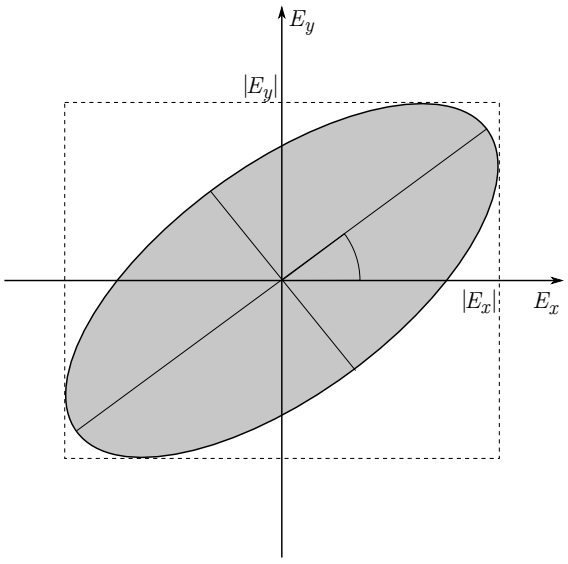

Fig. 1.6: Elliptic polarization

1.4 Einstein Coefficients and the Planck's Law of Radiation

- Assume an idealized material with two nondegenerate energy levels, 1 and 2, having populations N_1 and N_2, respectively. Moreover, let us consider that the total number of atoms in these two levels is constant

$$N_1 + N_2 = N. \tag{1.43}$$

- We can distinguish three forms of interaction between light and atoms (introduced in 1917 by A. Einstein):

  a) **Spontaneous emission**
  An excited atom emits a photon spontaneously (or induced via vacuum fluctuations) when the electron in the upper energy level E_2 jumps to the lower energy level E_1. The rate $\mathrm{d}N_2^{\mathrm{sp}}/\mathrm{d}t$ describing the depopulation of E_2 reads

$$\frac{\mathrm{d}N_2^{\mathrm{sp}}}{\mathrm{d}t} = -A_{21}N_2, \quad A_{21} = \frac{1}{\tau_{\mathrm{sp}}} \tag{1.44}$$

  where A_{21} is Einstein coefficient for spontaneous emission and τ_{sp} being the lifetime for spontaneous radiation in the upper energy level. The emitted photons are not coherent and the radiation is isotropic.

  b) **Stimulated emission**
  An incoming photon induces an excited atom to emit another one. The radiation is not isotropic (the emitted photons have the same direction and with the same phase). The corresponding rate equation reads

$$\frac{\mathrm{d}N_2^{\mathrm{st}}}{\mathrm{d}t} = -B_{21}N_2\rho(\nu), \tag{1.45}$$

  where B_{21} is Einstein coefficient for the stimulated emission and $\rho(\nu)$ is the spectral energy density.

  c) **Induced absorption**
  An incoming photon is absorbed by an electron in the lower energy level E_1, and subsequently the electron jumps into the upper energy level E_2:

$$\frac{\mathrm{d}N_1^{\mathrm{abs}}}{\mathrm{d}t} = -B_{12}N_1\rho(\nu), \tag{1.46}$$

  where B_{12} is Einstein coefficient for absorption.

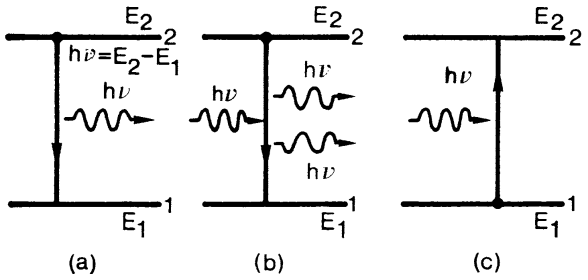

Fig. 1.7: Schematic illustration of the three processes: (a) spontaneous emission; (b) stimulated emission; (c) absorption.

- With A_{21}, B_{21} and B_{12} EINSTEIN was able to derive PLANCK's law for black-body radiation.
- Combining the three processes, the change of upper- and lower-level populations can be written as

$$\frac{\mathrm{d}N_1}{\mathrm{d}t} = -\frac{\mathrm{d}N_2}{\mathrm{d}t} = B_{21}N_2\rho(\nu) - B_{12}N_1\rho(\nu) + A_{21}N_2. \tag{1.47}$$

- The relation

$$\frac{\mathrm{d}N_2}{\mathrm{d}t} = -\frac{\mathrm{d}N_1}{\mathrm{d}t} \tag{1.48}$$

  can be easily derived from Eq.(1.43).

- Assumption: atoms are in thermal equilibrium with a reservoir of temperature T require equal numbers of "upward" and "downward" transitions such that

$$\frac{\mathrm{d}N_2}{\mathrm{d}t} = \frac{\mathrm{d}N_1}{\mathrm{d}t} = 0, \tag{1.49}$$

  and the population N_1 and N_2 are given by the BOLTZMANN distribution $N_1 \sim \mathrm{e}^{-E_1/k_\mathrm{B}T}$, $N_2 \sim \mathrm{e}^{-E_2/k_\mathrm{B}T}$ where $k_\mathrm{B} = 1.38 \times 10^{-23}\mathrm{J.K}^{-1}$ is the BOLTZMANN constant. Hence

$$\frac{N_2}{N_1} = \mathrm{e}^{-\frac{(E_2-E_1)}{k_\mathrm{B}T}} = \mathrm{e}^{-\frac{h\nu}{k_\mathrm{B}T}} \tag{1.50}$$

  where $E_2 - E_1 = h\nu$ is the photon energy.

- Equation (1.50) implies that $N_1 > N_2$, thus more absorption than stimulated emission.
- For high intense light, the spontaneous emission is negligible and, therefore, both levels are equally populated, i.e., $N_1 \approx N_2$.

- Equation (1.49) yields

$$B_{21}N_2\rho(\nu) - B_{12}N_1\rho(\nu) + A_{21}N_2 = 0,$$

so that

$$\frac{N_2}{N_1} = \frac{B_{12}\rho(\nu)}{B_{21}\rho(\nu) + A_{21}}. \tag{1.51}$$

Comparison Eq. (1.51) and (1.50) gives

$$\rho(\nu) = \frac{A_{21}}{B_{21}} \frac{1}{(\frac{B_{12}}{B_{21}} e^{\frac{h\nu}{k_B T}} - 1)} \tag{1.52}$$

- **Question 1:** What is the relation between coefficients A_{21}, B_{21} and B_{12}?
Answer: Following Einstein approach for $T \longrightarrow \infty \curvearrowright \rho(\nu) \longrightarrow \infty$:
Since $A_{21} < \infty$,

$$\begin{aligned} \lim_{T\longrightarrow\infty} \rho(\nu) &= \lim_{T\longrightarrow\infty} \frac{A_{21}}{B_{12} e^{\frac{h\nu}{k_B T}} - B_{21}} = \infty \\ &\Rightarrow \lim_{T\longrightarrow\infty} (B_{12} \underbrace{e^{\frac{h\nu}{k_B T}}}_{=1} - B_{21}) = 0 \\ &\Rightarrow \boxed{B_{12} = B_{21}.} \end{aligned} \tag{1.53}$$

Hence

$$\rho(\nu) = \frac{A_{21}}{B_{21}(e^{\frac{h\nu}{k_B T}} - 1)} \tag{1.54}$$

- Now we compare with the experimental results of Rayleigh-Jeans at low frequencies ($\nu \longrightarrow 0$)

$$\rho^{RJ}(\nu) = \frac{8\pi\nu^2}{c^3} k_B T \tag{1.55}$$

Taylor expansion around $\nu \longrightarrow 0$:

$$e^{\frac{h\nu}{k_B T}} = \sum_{\nu=0}^{\infty} \left(\frac{h\nu}{k_B T}\right)^{\nu} \frac{1}{\nu!} \approx 1 + \frac{h\nu}{k_B T} \tag{1.56}$$

thus

$$\lim_{\nu\longrightarrow 0} \rho(\nu) = \frac{A_{21}}{B_{21}(1 + \frac{h\nu}{kT} - 1)} = \frac{A_{21}}{B_{21}\frac{h\nu}{kT}} = \frac{A_{21}}{B_{21}} \frac{k_B T}{h\nu}. \tag{1.57}$$

Comparing Eq.(1.55) with (1.57) yields

$$\begin{aligned} \frac{A_{21}}{B_{21}} \frac{k_B T}{h\nu} &\stackrel{!}{=} \frac{8\pi\nu^2}{c^3} k_B T \\ \Rightarrow \frac{A_{21}}{B_{21}} &= \frac{8\pi h\nu^3}{c^3}. \end{aligned} \tag{1.58}$$

$$\boxed{\rho(\nu) = \frac{8\pi h\nu^3}{c^3}\frac{1}{\mathrm{e}^{\frac{h\nu}{k_\mathrm{B}T}} - 1}.} \tag{1.59}$$

which is PLANCK's law of black-body radiation.

- **Note:** The speed of light c is here the value in the medium $c = c_0/n$, where c_0 is the speed of light in vacuum and n is the index of refraction.
- EINSTEIN derivation was a strong indication that the concept of quanta with $E = h\nu$ is correct.
- PLANCK's law is universal since it is independent of the atoms that take part and the particular energy levels. The only condition is that the body is able to absorb photons of all frequencies.
- **Example:** Consider black-body radiation for a sphere filled with gas, in thermal equilibrium $T = 1000\,^\circ\mathrm{C}$. The ratio of spontaneous to stimulated emission is
  1. For visible light, $\frac{A_{21}}{B_{21}} = 10^{10}$.
  2. For radio frequencies, $\frac{A_{21}}{B_{21}} = 10^{8}$.
- **Question 2:** Write the rate equations for a degenerate two-level system (degeneracies g_1, g_2). Assume thermal equilibrium for the radiation field and upper- and lower-level populations, then derive the following relations for the Einstein coefficients:

$$\frac{g_1}{g_2}B_{12} = B_{21} = B, \tag{1.60}$$

$$\frac{A}{B} = \frac{8\pi h\nu^3}{c^3}, \tag{1.61}$$

$$\frac{A}{B\rho(\nu)} = \exp[h\nu/k_\mathrm{B}T] - 1. \tag{1.62}$$

- **Question 3:** Given your derivation in Question 2 why is X-ray laser particularly difficult to realize?

1.5 Line Shape and Line Broadening Mechanisms

- So far we considered the laser field as a plane wave. In reality lasers are not monochromatic and have certain distribution of spectrum implying line shape.
- Lines are broadened via various mechanisms:

- *Homogeneous broadening* is a particle property, the same for all atoms that take part.
- *Inhomogeneous broadening* is an ensemble property, only a selection of atoms participate.

a) **Natural broadening**

- Is a consequence of HEISENBERG's uncertainty principle.
- The shape and width of a transition between two energy levels $\hbar\omega = E_2 - E_1$ depends on the decay time τ of the excited state.
- The line shape function

$$g(\omega) = \frac{1}{2\pi} \frac{\gamma}{(\omega - \omega_0)^2 + (\gamma/2)^2} \tag{1.63}$$

  is Lorentzian "homegeneous mechanism".
- The full width at half maximum (FWHM): $\Delta\omega = \gamma = 1/\tau$ (inverse lifetime of the upper level), hence $\hbar\Delta\omega\tau = \Delta E\tau = \hbar$ is, indeed, an uncertainty relation.
- Defining of a quality factor "line fidelity" for characterizing the natural line width

$$Q = \frac{\omega_0}{\Delta\omega}. \tag{1.64}$$

- **Example:** For Calcium, the lifetime of an upper level, τ, is about $4.6\,\text{ns}$ for a transition wavelength $\lambda = 423\,\text{nm}$. The corresponding frequency is $\nu = c/\lambda = 7 \times 10^{14}\,\text{Hz}$. During τ, the electromagnetic wave oscillates $\nu\tau = 3 \times 10^6$ times until the intensity drops to $1/\text{e}$, therefore

$$Q = \frac{\omega_0}{\Delta\omega} \approx 4.4 \times 10^{15}\text{s}^{-1} \cdot 4.6 \times 10^{-9}\text{s} \approx 2 \times 10^7.$$

b) **Doppler broadening**

- If the atom moves with a velocity v_z relative to the observer, then the resonance frequencies are shifted due to DOPPLER effect

$$\omega = \omega_0 + \mathbf{k} \cdot \mathbf{v} = \omega_0 \left(1 + \frac{1}{2\pi\nu} \frac{2\pi}{\lambda} v_z\right) = \omega_0 \left(1 + \frac{v_z}{c}\right) \tag{1.65}$$

  where $\mathbf{k}$ is the wave vector.

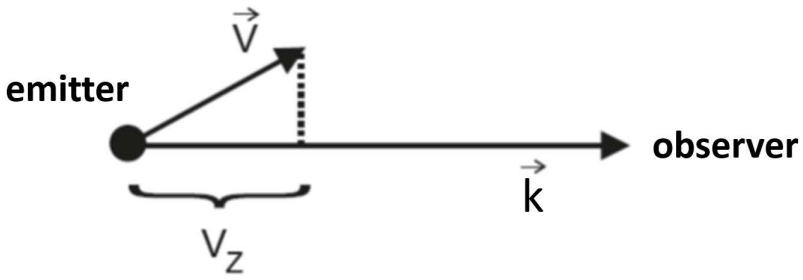

Fig. 1.8: Radiation emitters with a velocity component towards the observer.

- This is the case of an inhomogeneous broadening.

- If $\mathbf{k} \perp \mathbf{v} \Rightarrow \omega = \omega_0$.

- The angular frequency of the received radiation will be shifted (into the blue for positive v_z and into the red for negative v_z).

- A gas that absorb or emit light consists of atoms with mass M following, at thermal equilibrium, a statistical distribution that depends on T, namely Maxwell-Boltzmann distribution of velocities.

- The number of atoms dN whose velocities between v_z and $v_z + \mathrm{d}v_z$ is given by Maxwell's distribution

$$\mathrm{d}N = N\mathrm{e}^{-\frac{Mv_z^2(\omega)}{2k_\mathrm{B}T}}\mathrm{d}v_z. \tag{1.66}$$

  Using

$$\frac{\mathrm{d}\omega}{\mathrm{d}v_z} = \frac{\omega_0}{c}, \quad v_z = \frac{c(\omega-\omega_0)}{\omega_0} \tag{1.67}$$

  we obtain

$$\mathrm{d}N = N\mathrm{e}^{-\frac{Mc^2}{2k_\mathrm{B}T}\frac{(\omega-\omega_0)^2}{\omega_0^2}}\frac{c}{\omega_0}\mathrm{d}\omega. \tag{1.68}$$

- Given that the spectral intensity distribution $I(\omega)\mathrm{d}\omega \sim \mathrm{d}N$ and the intensity profile of the emitted line $I(\omega) = I(\omega_0)g(\omega)$, the line shape function $g(\omega)$ will follow as

$$g(\omega) = \frac{1}{\omega_0}\sqrt{\frac{Mc^2}{2\pi k_\mathrm{B}T}}\mathrm{e}^{-\frac{Mc^2}{2k_\mathrm{B}T}\frac{(\omega-\omega_0)^2}{\omega_0^2}}. \tag{1.69}$$

- The FWHM of this distribution is (left as an exercise)

$$\begin{aligned} \Delta\omega &= \frac{2\omega_0}{c}\sqrt{\frac{2k_B T}{M}\ln 2} \\ &= 7.16\times 10^{-7}\omega_0\sqrt{\frac{T}{M}} \end{aligned} \tag{1.70}$$

  T the temperature of the emitters in K, and M the atomic weight in atomic mass units (amu).

- Doppler broadening depends on the frequency ω_0 itself and produces a Gaussian profile.

- Doppler broadening increases with temperature and with the frequency of the line, and decreases as the atomic mass increases.

- The comparison between Gaussian and Lorentzian profiles reveals that the Gaussian decays faster, the wings of the line profile are still determined by the Lorentzian.

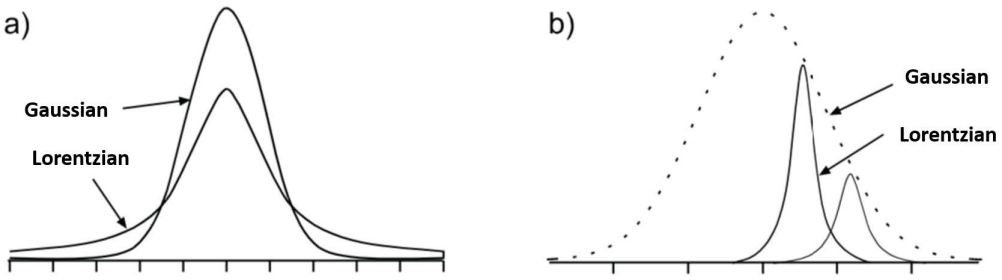

Fig. 1.9: a) Comparison between a Gaussian and a Lorentzian curve with the same half-width and area. b) Doppler broadening arises from the emission of many Doppler-shifted lines with natural line width.

- Doppler broadening is created by emission of many Doppler-shifted lines with a natural (Lorentzian) line width. The convolution of many Lorentzian distribution functions yields Gaussian distribution.

c) **Saturation broadening**

- If the intensity of the laser increases, a considerable part of the atom ensemble is excited (spontaneous emission cannot depopulate the upper levels sufficiently quick, hence absorption reduced). This is called *saturation* of a transition.

- Using rate equations

$$\frac{\mathrm{d}N_2}{\mathrm{d}t} = \underbrace{B_{12}N_1\rho(\nu)}_{\text{induced absorption}} - \underbrace{B_{21}N_2\rho(\nu)}_{\text{stimulated emission}} - \underbrace{A_{21}N_2}_{\text{spontaneous emission}} = -\frac{\mathrm{d}N_1}{\mathrm{d}t} = 0. \tag{1.71}$$

  Since $B_{21} = B_{12}$ we write

$$2B_{12}\rho(\nu)(N_2 - N_1) + 2A_{21}N_2 = 0$$

  or

$$2B_{12}\rho(\nu)(N_2 - N_1) + A_{21}(N_2 + N_1) + A_{21}(N_2 - N_1) = 0. \tag{1.72}$$

  Calling Eq. (1.43) gives

$$N_1 - N_2 = \frac{N}{1 + 2\frac{B_{12}\rho(\nu)}{A_{21}}} := \frac{N}{1 + \frac{I(\nu)}{I_\mathrm{s}}} \tag{1.73}$$

  with $I_\mathrm{s} = cA_{21}/2B_{12}$ is the saturation intensity.

- With the difference in population numbers, the absorption coefficient α (i.e., the material dependent cross-section for absorption, independent of the line function) also becomes a function of intensity

$$\alpha = \frac{\alpha_0}{1 + \frac{I}{I_\mathrm{s}}}. \tag{1.74}$$

- The impact on the line shapes depends on the type of broadening (homogeneous or inhomogeneous). Both cases are outlined in Figure 1.10.

- In the case of a homogeneous mechanism (if the Doppler shift is not considered). The Lorentzian line shape function is no longer normalized:

$$g(\omega) = \frac{C}{(\omega - \omega_0)^2 + (\gamma_\mathrm{s}/2)^2} \tag{1.75}$$

  with $\gamma_\mathrm{s} = \gamma\sqrt{1 + \frac{I}{I_\mathrm{s}}}$, thus $\gamma_\mathrm{s} > \gamma$. This means that the line shape is maintained but the line gets wider as the absorption in the center of the line is more reduced than in the wings.

- At the saturation intensity $I = I_\mathrm{s}$, according to Eq. (1.73), $N_2 = N/4$, meaning a quarter of all atoms are in the excited state, and the line width has increased by a factor of $\sqrt{2}$.

- In the case of inhomogeneous transitions, however, spectral selective saturation occurs. With sufficiently narrowband excitation, so-called *hole burning* occurs. For Doppler broadening, for example, each frequency component of the line profile can be assigned to a group of atoms with specific velocities. When light of a certain frequency is irradiated, interaction occurs only with atoms of matching velocity or frequency. The width of the resulting hole cannot be narrower than the natural line width.

- If Doppler effect is not removed, then the broadening is inhomogeneous (the effect is not the same for different velocities), hence selective spectral saturation or *spectral hole burning*.

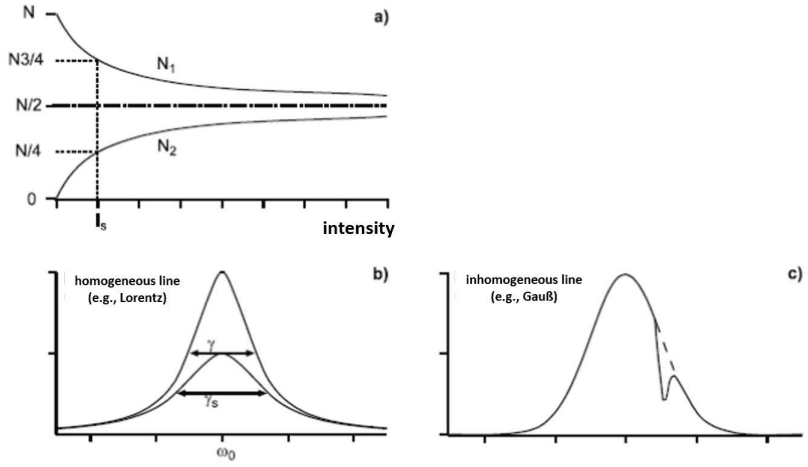

Fig. 1.10: a) Intensity dependence of the population numbers in the two-level atom. b) Saturation broadening of a homogeneous line. c) Spectral hole burning in an inhomogeneously broadened line profile.

d) **Pressure broadening**

- In the presence of collisions with other atoms the phase of the emitted photon is disturbed.

- The phase interrupts and thus shortens the emission process (increases energy uncertainty).

- The collisions can be interpreted as a decay taking into account that the rate has an additional decay channel.

- This leads to a LORENTZIAN line profile (homogeneous broadening)

$$g(\omega) = \frac{1}{2\pi} \frac{\gamma_{\text{tot}}}{(\omega - \omega_0)^2 + (\gamma_{\text{tot}}/2)^2} \tag{1.76}$$

with the FWHM

$$\Delta\omega = \gamma + 2\gamma_{\text{coll}}, \tag{1.77}$$

where

$$\gamma_{\text{coll}} = \sigma \rho v_{\text{rel}} \tag{1.78}$$

is the collision rate which is proportional to the scattering cross section σ and ρv_{rel} is the flux of atoms, i.e., the density times the relative velocity. For a gas in thermal equilibrium we use the MAXWELL-BOLTZMANN statistics to obtain $v_{\text{rel}} = 4\sqrt{k_{\text{B}}T/\pi M}$, and the ideal gas law yields $p = \rho k_{\text{B}} T$ for the pressure.

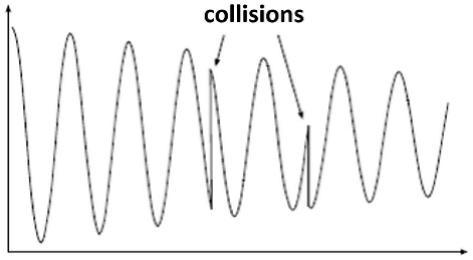

Fig. 1.11: Elastic collisions change the phase of the emitted wave of a damped harmonic oscillator.

- **Example:** For He-Ne laser, the half-width of collisional broadening at a pressure of $p = 0.5\,\text{mbar}$ is $\Delta\omega = 100\,\text{MHz}$.

e) **Time-of-flight broadening**

- This broadening mechanism results from the finite interaction time between the absorber material and the incident laser beam. This effect must be considered when the interaction time is short compared to the natural lifetime of the excited atom. In such cases, the line width of such a transition is not determined by the lifetime but by the flight time of an atom through a laser beam. The frequency profile of the radiation then depends on the intensity distribution of the laser beam and is typically an inhomogeneous mechanism as a result.

- **Example:** Calcium atoms from a $T = 1000\,^{\circ}\text{C}$ hot furnace have a root-mean-square velocity of $v_{\text{rms}} = \sqrt{3k_{\text{B}}T/M}$. The lifetime of an upper level $\tau_{21}(\lambda = 657\,\text{nm})$, is about $4.6\,\text{ns}$. When focussing the laser beam down to $4\,\mu\text{m}$, the time-of-flight broadening becomes relevant.

1.6 Important Solutions to Wave Equation

- We provide here important (approximate) solutions for the wave equation

$$\left(\nabla^2 - \frac{1}{c^2}\frac{\partial^2}{\partial t^2}\right)\mathbf{E}(\mathbf{r},t) = 0 \tag{1.79}$$

of the laser field in free space.
Monochromatic waves

$$\mathbf{E}(\mathbf{r},t) = \mathbf{E}(\mathbf{r})\mathrm{e}^{-\mathrm{i}\omega t}, \tag{1.80}$$

Plugging (1.80) into (1.79) yields

$$\boxed{(\Delta + k^2)\mathbf{E}(\mathbf{r}) = 0, \quad k = \frac{\omega}{c}} \tag{1.81}$$

which is called HELMHOLTZ *equation* for spatial modes.

- The solutions $\mathbf{e}_\sigma \mathrm{e}^{\mathrm{i}\mathbf{k}\cdot\mathbf{r}}$ are special solutions to the equation (1.81). If we concentrate on one polarization, the scalar HELMHOLTZ equation for the field amplitude reads

$$(\Delta + k^2)E_0(\mathbf{r}) = 0. \tag{1.82}$$

a) **Plane waves**
Writing the LAPLACIAN in cartesian coordinates yields

$$\mathbf{E}(\mathbf{r}) = \mathbf{E}_0 \mathrm{e}^{\mathrm{i}\mathbf{k}\cdot\mathbf{r}}. \tag{1.83}$$

b) **Spherical waves**

- In spherical coordinates the solution of Eq.(1.79) in one dimension reads

$$\mathbf{E}(\mathbf{r}) = A\frac{\mathrm{e}^{\mathrm{i}kr}}{r}. \tag{1.84}$$

with a constant A satisfying the scalar HELMHOLTZ equation in spherical coordinates. The wave fronts are spherical shells with a radial distance of $\lambda = 2\pi/k$, which propagate radially with the phase velocity c.

c) **Parabolic waves**

- The spherical waves can be simplified under certain circumstances. For example, we consider a spherical wave that propagates from the origin of coordinates at a location near the z-axis, so that the condition $\rho = \sqrt{x^2 + y^2} \ll z$ is fulfilled.

- Using the so-called FRESNEL *approximation*

$$r = \sqrt{\rho^2 + z^2} \approx z\left(1 + \frac{\rho^2}{2z^2}\right) = z + \frac{\rho^2}{2z} \tag{1.85}$$

and substituting in Eq (1.84) gives

$$\mathbf{E}(\mathbf{r}) = \frac{A}{z} e^{ikz} e^{ik\frac{\rho^2}{2z}}, \tag{1.86}$$

where we considered that $r \simeq z$ in the amplitude.

- The wave fronts are *paraboloids*. Moreover, if the distance z becomes much larger, the spherical wave turns into a plane wave.

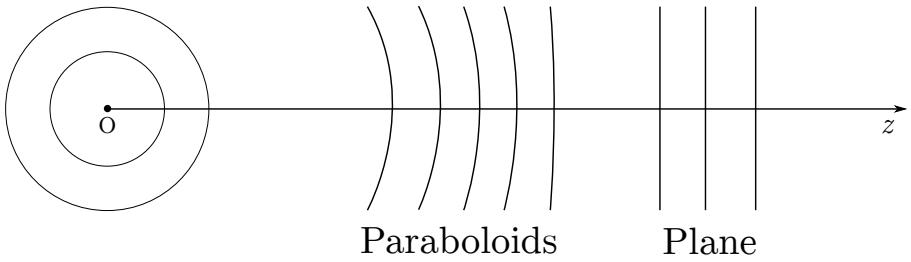

Fig. 1.12: Paraxial Helmholtz

- Other way: approximate wave equation, then find exact solutions.

1.6.1 Paraxial Helmholtz equation

- If the wave fronts change only slightly along z-direction, we may in good approximation consider it as a plane wave. We therefore start from a plane wave

$$\mathbf{E}_0(\mathbf{r}) = A(\mathbf{r}) e^{ikz} \tag{1.87}$$

with slowly varying amplitude $A(\mathbf{r})$ of the position.

- As a consequence the envelope $A(\mathbf{r})$ and its derivative with respect to z do not vary much within a wavelength $\lambda = 2\pi/k$ (this is the so-called *slowly varying envelope approximation*, or SVEA)

$$\frac{\partial A}{\partial z} \ll kA \quad \text{and} \quad \frac{\partial^2 A}{\partial z^2} \ll k^2 A. \tag{1.88}$$

- Inserting into HELMHOLTZ equation gives

$$\begin{aligned}\left(\nabla^2+k^2\right)A(\mathbf{r})\mathrm{e}^{\mathrm{i}kz} &= \nabla_{\mathrm{T}}^2 A(\mathbf{r})\mathrm{e}^{\mathrm{i}kz}+\left(\frac{\partial^2}{\partial z^2}+k^2\right)A(\mathbf{r})\mathrm{e}^{\mathrm{i}kz}\\ &= \nabla_{\mathrm{T}}^2 A(\mathbf{r})\mathrm{e}^{\mathrm{i}kz}+\left(\frac{\partial^2 A}{\partial z^2}-k^2A+2\mathrm{i}k\frac{\partial A}{\partial z}+k^2A\right)\mathrm{e}^{\mathrm{i}kz}\\ &\overset{\text{SVEA}}{\simeq} \nabla_{\mathrm{T}}^2 A(\mathbf{r})\mathrm{e}^{\mathrm{i}kz}+2\mathrm{i}k\frac{\partial A}{\partial z}\mathrm{e}^{\mathrm{i}kz}.\end{aligned}$$

- Thus we obtain the *paraxial* HELMHOLTZ equation

$$\boxed{\left(\frac{\partial^2}{\partial x^2}+\frac{\partial^2}{\partial y^2}\right)A(\mathbf{r})+2\mathrm{i}k\frac{\partial}{\partial z}A(\mathbf{r})=0.} \tag{1.89}$$

- It also possible to verify that the parabolic waves (1.86) are even exact solutions of paraxial HELMHOLTZ equation (1.89).

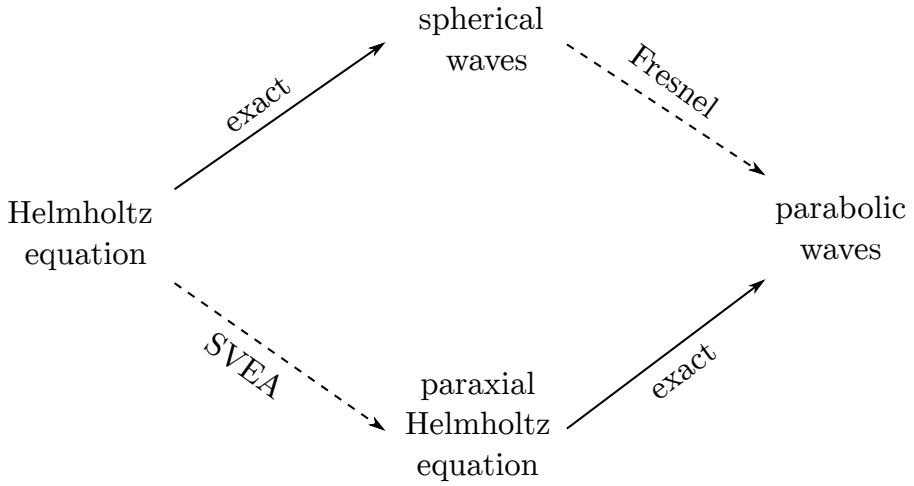

Fig. 1.13: Two different points of view for solving HELMHOLTZ equation.

1.6.2 Gaussian Beams

- Another class of solutions to the paraxial HELMHOLTZ equation is found by replacing $z \to q(z) = z - \mathrm{i}z_{\mathrm{R}}$, with a constant z_{R}, in the parabolic wave

$$\mathbf{E}(\mathbf{r}) = \frac{A}{q(z)}\mathrm{e}^{\mathrm{i}kz}\mathrm{e}^{\mathrm{i}k\frac{\rho^2}{2q(z)}}. \tag{1.90}$$

- The function $1/q(z)$ can be divided into real and imaginary parts

$$\frac{1}{q(z)} = \frac{1}{R(z)} + \mathrm{i}\frac{\lambda}{\pi W^2(z)}, \tag{1.91}$$

where

$$W(z) = W_0\sqrt{1+\left(\frac{z}{z_\mathrm{R}}\right)^2}, \quad W_0^2 = \frac{\lambda z_\mathrm{R}}{\pi}, \quad R(z) = z\left[1+\left(\frac{z_\mathrm{R}}{z}\right)^2\right]. \tag{1.92}$$

- Redefining the constant $A \longmapsto A/(\mathrm{i}z_\mathrm{R})$ and the GOUY phase $\zeta(z) = -\arctan\left(\frac{z}{z_\mathrm{R}}\right)$, we then find for the complex amplitude

$$\mathbf{E}(\mathbf{r}) = \frac{AW_0}{W(z)}\exp\left(-\frac{\rho^2}{W^2(z)}\right)\exp\left[\mathrm{i}kz + \mathrm{i}k\frac{\rho^2}{2R(z)} + \mathrm{i}\xi(z)\right], \tag{1.93}$$

so the intensity take the following form

$$I(\rho,z) = |A|^2\left(\frac{W_0}{W(z)}\right)^2\exp\left[-\frac{2\rho^2}{W^2(z)}\right] \tag{1.94}$$

which is GAUSSIAN function of ρ for every z.

- The width of the beam is determined by $W(z)$, where at $z=0$: $W(z=0)=W_0$ the beam is narrowest with waist radius W_0, or, the spot size of the beam is $2W_0$.

- The GAUSSIAN beam diverges during the propagation, where z_R is the RAYLEIGH length which characterizes the defocusing. The focal length at which the beam waist increases by a factor of $\sqrt{2}$ is twice the RAYLEIGH length, i.e.,

$$2z_\mathrm{R} = \frac{2\pi W_0^2}{\lambda}. \tag{1.95}$$

- The wave fronts of the GAUSSIAN beam are defined by the phase in (1.93), neglecting the z-dependence in $R(z)$ and $\zeta(z)$, then the wave fronts are given by the relation

$$z + \frac{\rho^2}{2R} \approx \text{const.} \tag{1.96}$$

This is an equation of a parabolic surface with radius of curvature R. The wave fronts are shown in Fig. 1.14.

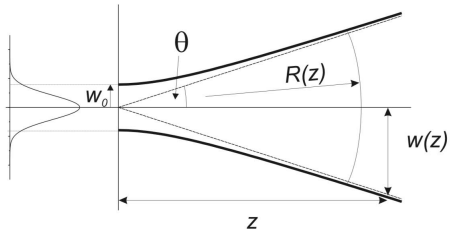

Fig. 1.14: Evolution of the beam radius of a GAUSSIAN beam.

1.6.3 Hermite-Gauß Modes

- The GAUSSIAN beams are not the only modes that satisfy the paraxial HELMHOLTZ equation (1.89).
- An important and interesting class of modes arises when the complex envelope $E_G(\mathbf{r})$ of GAUSSIAN beam is modified in such a way that

$$E(\mathbf{r}) = E_G(\mathbf{r}) f_x\left[\frac{\sqrt{2}x}{W(z)}\right] f_y\left[\frac{\sqrt{2}y}{W(z)}\right] \mathrm{e}^{\mathrm{i}f_z(z)} \tag{1.97}$$

  with real functions f_x,f_y and f_z.
- The phase of envelope given by $f_z(z)$ does not depend on x and y, and equals the phase of GAUSSIAN beam. This means that the wave fronts coincide with those of the GAUSSIAN beam. In particular, they have the same radius of curvature $R(z)$.
- These properties are ensured exactly when the envelope $E_0(\mathbf{r})$ (2.80) satisfies the paraxial HELMHOLTZ equation.
- Defining $u = \sqrt{2}x/W(z)$ and $v = \sqrt{2}y/W(z)$, we write

$$\frac{\partial f_x}{\partial x} = \frac{\sqrt{2}}{W(z)}\frac{\partial f_x}{\partial u}, \quad \frac{\partial f_x}{\partial z} = -\frac{u}{W(z)}\frac{\partial W(z)}{\partial z}\frac{\partial f_x}{\partial u} \tag{1.98}$$

  and

$$\frac{\partial}{\partial x}E_G(\mathbf{r}) = \mathrm{i}k\frac{x}{q(z)}E_G(\mathbf{r}) \tag{1.99}$$

$$\frac{1}{W(z)}\frac{\partial W(z)}{\partial z} = \frac{zW_0^2}{z_\mathrm{R}^2 W^2(z)} = \frac{1}{R(z)}. \tag{1.100}$$

- If we now use the relation $1/q(z) - 1/R(z) = 2\mathrm{i}/(kW^2(z))$, and since the GAUSSIAN envelope $E_G(\mathbf{r})$ satisfies the paraxial HELMHOLTZ equation, one obtains the differential equation

$$\frac{1}{f_x}\left(\frac{\partial^2 f_x}{\partial u^2} - 2u\frac{\partial f_x}{\partial u}\right) + \frac{1}{f_y}\left(\frac{\partial^2 f_y}{\partial v^2} - 2v\frac{\partial f_y}{\partial v}\right) - kW^2(z)\frac{\partial f_z}{\partial z} = 0 \tag{1.101}$$

- This equation consists of the sum of three terms, each depends only on one of the variables (u, v, z). We therefore solve this equation by separating the variables with two separation constants $-2m$ and $-2n$, so that

$$-\frac{1}{2}\frac{\partial^2 f_x}{\partial u^2} + u\frac{\partial f_x}{\partial u} = m f_x \tag{1.102}$$

$$-\frac{1}{2}\frac{\partial^2 f_y}{\partial v^2} + v\frac{\partial f_y}{\partial v} = n f_y \tag{1.103}$$

$$z_{\mathrm{R}}\left[1 + \left(\frac{z}{z_{\mathrm{R}}}\right)^2\right]\frac{\partial f_z}{\partial z} = -(m+n). \tag{1.104}$$

- The first two equations are eigenvalue equations for the differential operators on the left side with the eigenvalues m and n. Moreover, the eigenfunctions are precisely the HERMITE polynomials $H_m(u)$ and $H_n(v)$, thus

$$f_x(u) = H_m(u), \quad f_y(v) = H_n(v). \tag{1.105}$$

  Integrating the remaining equation yields

$$f_z(z) = -(m+n)\arctan\frac{z}{z_{\mathrm{R}}} = (m+n)\zeta(z). \tag{1.106}$$

- The complex amplitude thus becomes

$$\boxed{E_{m,n}(\mathbf{r}) = A_{m,n}\frac{W_0}{W(z)}h_m\left(\frac{\sqrt{2}x}{W(z)}\right)h_n\left(\frac{\sqrt{2}y}{W(z)}\right)\exp\left[\mathrm{i}kz + \mathrm{i}k\frac{\rho^2}{2R(z)} + \mathrm{i}(m+n+1)\zeta(z)\right],} \tag{1.107}$$

  where $h_l(u) = H_l(u)\mathrm{e}^{-u^2}$ represents the so-called HERMITE function.

- If $m = n = 0$, the amplitude is reduced to the usual GAUSSIAN beam.

- The intensity distributions of the lowest HERMITE-GAUSSIAN modes are shown in Fig.(1.15).

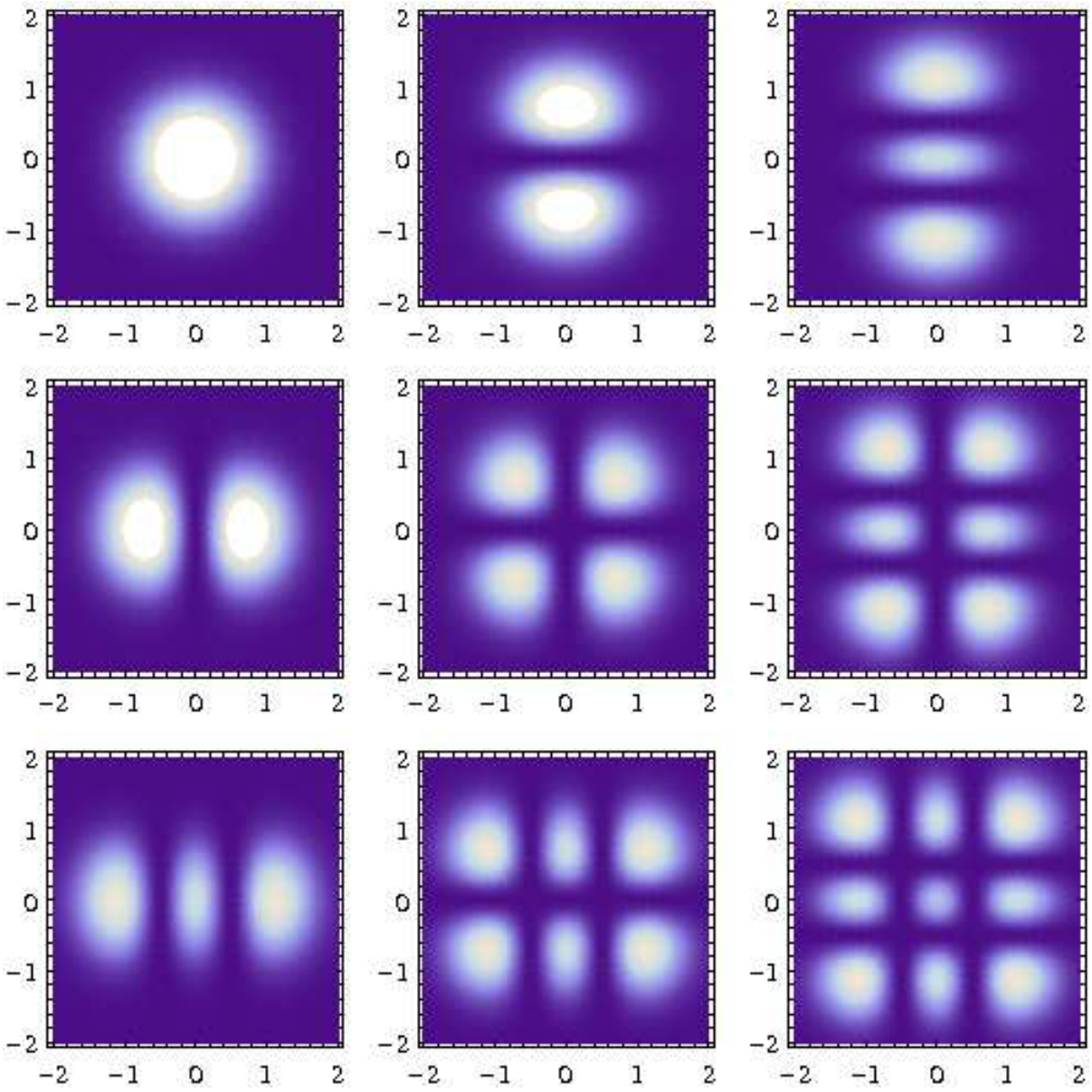

Fig. 1.15: Intensity distribution of the lowest Hermite–Gauss modes for $(m, n) = (0, 1, 2)$.

- These Hermite-Gauss modes are eigenmodes of confocal resonator that would fit exactly with these parabolic wave fronts. These modes are labeled as TEM_{mn}.

1.7 Optical Amplification

- An important consequence of the principle of stimulated emission is the ability to amplify light. A mechanism is needed to populate the upper laser level more strongly than the lower one, thus achieving *inversion*. Therefore one needs more electrons in E_2 than in E_1.

1.7.1 Two-level system

- We consider a medium of length $\mathrm{d}z = c\mathrm{d}t$. Once again, we use the rate equations (1.44), (1.45), and (1.46) for spontaneous emission, stimulated emission and induced absorption, with EINSTEIN coefficients A_{21}, B_{21} and B_{12}, respectively, and subtracting the numbers of photons created and annihilated per unit length yields

$$\begin{aligned}\frac{\mathrm{d}Q}{\mathrm{d}z} &= \frac{\text{number of created photons} - \text{number of destroyed photons}}{\mathrm{d}z} \\ &= \frac{B\rho(\nu)}{c}(N_2 - N_1) + \frac{A_{21}}{c}N_2, \end{aligned} \tag{1.108}$$

  where $B_{21} = B_{12} = B$ was used. The condition $N_2 > N_1$ is known as *population inversion*.

- In thermal equilibrium in two-level system ($\frac{\mathrm{d}Q}{\mathrm{d}z} = 0$):

$$B\rho(\nu)N_1 = B\rho(\nu)N_2 + A_{21}N_2, \tag{1.109}$$

  so that

$$\frac{N_2}{N_1} = \frac{B\rho(\nu)}{B\rho(\nu) + A_{21}} < 1, \tag{1.110}$$

  which means that there is *no amplification in two-level systems*. Mathematically speaking, the *optical gain* is not possible. While a two-level system does not allow laser activity, this is potentially possible in 3-level or 4-level schemes. In these schemes, the physical processes of excitation, decay, and laser transition are separated and can be entirely different in nature. The different schemes are outlined in Figure (1.16).

- Spontaneous emission acts as inversion, but it creates incoherent background or *noise*.

- Realistic lasers need at least three or four levels to reach population inversion.

- In three-level system half of atoms must be excited (pulsed operation mode), e.g., Ruby laser.
- In four-level system any pumping results a population inversion. Most of the lasers are four-level systems.

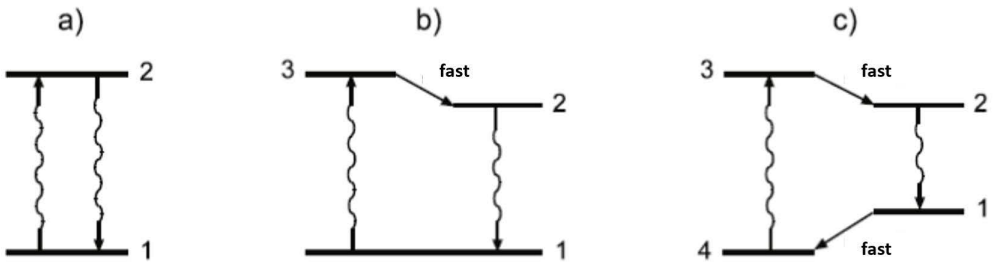

Fig. 1.16: (a) Two-Level, (b) Three-level and (c) Four-level laser schemes.

1.7.2 Three-level system

- Inversion of the levels 2 and 1 involved in laser activity can be achieved when excitation from pumped level 3 to the upper laser level 2 is much faster than the spontaneous decay of the pumped level 3 back to the ground state, and when the population rate of the upper laser level 2 is much greater than the spontaneous decay rate from level 2 to level 1.
- The full rate equations read as

$$\begin{aligned}
\frac{\mathrm{d}N_1}{\mathrm{d}t} &= N_2A_{21} + N_3A_{31} + (N_2 - N_1)B_{21}\rho(\nu_{12}) + (N_3 - N_1)B_{31}\rho(\nu_{13}) \\
\frac{\mathrm{d}N_2}{\mathrm{d}t} &= N_3A_{32} - N_2A_{21} - (N_2 - N_1)B_{21}\rho(\nu_{12}) + (N_3 - N_2)B_{32}\rho(\nu_{23}) \\
\frac{\mathrm{d}N_3}{\mathrm{d}t} &= -N_3A_{32} - N_3A_{31} - (N_3 - N_1)B_{31}\rho(\nu_{13}) - (N_3 - N_2)B_{32}\rho(\nu_{23})
\end{aligned} \tag{1.111}$$

- By adding up those equations one finds the natural condition

$$N = N_1 + N_2 + N_3 = \text{const.} \quad \Rightarrow \quad \frac{\mathrm{d}N}{\mathrm{d}t} = 0. \tag{1.112}$$

- With the pump frequency $\nu_\mathrm{P} = \nu_{13}$, emission at $\nu_\mathrm{L} = \nu_{12}$ is desired, and we don't expect any intensity at ν_{23}, thus we can consider $\rho(\nu_{23}) = 0$. Furthermore,

we want to focus on the steady state condition. Since N is constant (implicitly assumed in the formulation of the system of equations), the three equations are not linearly independent. Therefore, it is sufficient to consider the second and the third equations:

$$0 = N_3 A_{32} - N_2 A_{21} - (N_2 - N_1) B_{21} \rho(\nu_L) \quad (1.113)$$
$$0 = -N_3 (A_{32} + A_{31}) - (N_3 - N_1) B_{31} \rho(\nu_P). \quad (1.114)$$

- With $N_3 = N - N_1 - N_2$, it becomes a linear system of equations for N_1 and N_2 with the solutions:

$$N_1 = \frac{A_{21}A_{32} + A_{21}A_{31} + A_{21}u_P + A_{31}u_L + A_{32}u_L + u_L u_P}{X} \quad (1.115)$$
$$N_2 = \frac{A_{32}u_P + A_{31}u_L + A_{32}u_L + u_L u_P}{X}, \quad (1.116)$$

where we used $u_P = B_{31}\rho(\nu_P)$, $u_L = B_{21}\rho(\nu_L)$, and

$$X = A_{21}(A_{32} + A_{31}) + A_{32}u_P + 2A_{21}u_P + 2A_{31}u_L + 2A_{32}u_L + 3u_L u_P$$

.

- Forming the difference results in

$$N_2 - N_1 = \frac{(A_{32} - A_{21})u_P - A_{21}(A_{32} + A_{31})}{X}. \quad (1.117)$$

- To ensure a positive difference, meaning achieving inversion, one evidently needs $A_{21} < A_{32}$, ideally $A_{21} \ll A_{32}$. Additionally, it is favorable for a low pump power if $A_{31} \ll A_{32}$. Instead of EINSTEIN coefficients, the typical time constants for the transitions are usually provided, where $\tau_{21} \gg \tau_{32}$ and $\tau_{31} \gg \tau_{32}$.

- **Example 1.1**: For ruby lasers, $\tau_{21} = 3 \times 10^{-3}\,\mathrm{s}$, $\tau_{31} = 10^{-6}\,\mathrm{s}$, and $\tau_{32} = 10^{-8}\,\mathrm{s}$. The above condition is thus excellently fulfilled for ruby lasers.

1.7.3 Four-level system

- In a 3-level system, population inversion occurs only when at least half of all atoms are excited. In contrast, in a 4-level system, inversion is possible immediately after pumping begins if level 1 is depopulated continuously by a very fast process. Due to this advantage, most lasers follow a 4-level scheme.

- To fully describe a four-level system, one would need to add another rate equation to the rate equations of the three-level system and expand the equations to account for all transitions between the four levels.
- For most laser-suitable systems, simplifying assumptions can be made that drastically simplify the mathematical treatment:
  - The lower laser level E_1 is rapidly depopulated, i.e., $N_1 \simeq 0$.
  - Consequently, inversion $N_2 > N_1$ is obtained as soon as pumping occurs even slightly.
  - Typically, high pump power is not needed, i.e., the population of the ground level E_4 hardly changes ($N_4 = \text{const.}$)
- For efficient systems, a few additional conditions should be met:
  - Pump power should efficiently populate the upper laser level, i.e., τ_{34}, $\tau_{31} \gg \tau_{32}$.
  - The time constant (lifetime) of the upper laser level (τ_{21}, τ_{24}) should be as large as possible to minimize competition from spontaneous emission and non-radiative energy loss.
  - Other potential competitive processes should be negligible (transitions from the upper pump or upper laser level to further states).
- **Example 1.2**: For Nd:YAG lasers, $\tau_{21} = 2.3 \times 10^{-4}\,\text{s}$, $\tau_{31} = 10^{-6}\,\text{s}$, $\tau_{32} = 10^{-8}\,\text{s}$ and $\tau_{14} = 10^{-7}\,\text{s}$. The above condition is thus excellently fulfilled for Nd:YAG lasers.

1.7.4 Characteristics of the inversion

- To calculate the amplification coefficient, consider that the gain intensity is governed by
$$\frac{\mathrm{d}I}{\mathrm{d}z} = \frac{h\nu B g(\nu)}{c}(N_2 - N_1)I := \gamma(\nu)I \tag{1.118}$$
where $g(\nu)$ is the normalized line shape function of the laser transition, i.e., $\int_{-\infty}^{+\infty} g(\nu)\mathrm{d}\nu = 1$. Therefore
$$I(z) = I(0)\mathrm{e}^{\gamma(\nu)z} \tag{1.119}$$
with $\gamma(\nu) = h\nu B\, g(\nu)(N_2 - N_1)/c$ is the gain coefficient that is independent of z and t for very short z.

- Since $A_{21} = \frac{1}{\tau_{\rm sp}} = \frac{8\pi h\nu^3}{c^3}B$, we write

$$\gamma(\nu) = \frac{\lambda_0^2}{8\pi n^2} A_{21}\, g(\nu)(N_2 - N_1) = \sigma(\nu)(N_2 - N_1), \tag{1.120}$$

  where $\sigma(\nu)$ is the cross section for the stimulated emission and n is the refraction index of the medium.

- Assume a four-level system as shown in Fig.(1.16). Consider that the lower laser level is depleted ($N_1 \longrightarrow 0$) and the upper laser level is pumped with rate P_2. The decay rates are
  - from 2 to 1 is τ_{21}
  - from 2 to 4 is τ_{24}.

- The lifetime of the upper laser level is given by

$$\frac{1}{\tau_2} = \frac{1}{\tau_{24}} + \frac{1}{\tau_{21}} \tag{1.121}$$

- The rate equations are

$$\frac{{\rm d}N_2}{{\rm d}t} = P_2 - \frac{N_2}{\tau_2} - \frac{\sigma I}{h\nu}(N_2 - N_1) \tag{1.122}$$

$$\frac{{\rm d}N_1}{{\rm d}t} = \frac{N_2}{\tau_{21}} - \frac{N_1}{\tau_1} + \frac{\sigma I}{h\nu}(N_2 - N_1) \tag{1.123}$$

- Suppose that the lower laser level is energetically empty, hence use the approximation $N_2 - N_1 \approx N_2$, i.e., instantaneous depopulation of level 1, we obtain

$$\frac{{\rm d}N_2}{{\rm d}t} = P_2 - \frac{N_2}{\tau_2}\left(1 + \frac{\sigma\tau_2 I}{h\nu}\right) \tag{1.124}$$

  whose solution reads

$$N_2(t) = \frac{P_2\tau_2}{1 + \sigma\tau_2 I/h\nu}\left(1 + {\rm e}^{-\frac{t}{\tau_2}(1+\sigma\tau_2 I/h\nu)}\right) \tag{1.125}$$

$$= \frac{P_2\tau_2}{1 + I/I_{\rm s}}\left(1 + {\rm e}^{-\frac{t}{\tau_2}(1+I/I_{\rm s})}\right) \tag{1.126}$$

  where $I_{\rm s} = h\nu/\sigma\tau_2$ is the saturation intensity.

- The condition $N_2(0) = 0$ implies that the pumping rate P_2 is switched on at $t = 0$.

- The evolution of inversion follows an exponential law. The maximum gain and inversion growth rate scale with $1 + I/I_s$, since at finite intensity $I \approx$ const, stimulated emission reduces the population in the upper laser level. For saturation amplification, we can now write

$$\gamma \approx \sigma N_2 = \frac{\sigma P_2 \tau_2}{1 + \frac{I}{I_s}} = \frac{\gamma_0}{1 + \frac{I}{I_s}}. \tag{1.127}$$

1.7.5 Laser Mode Competition

- So far we discussed the amplification of one line. However, in reality several laser modes exhibit different gains, and will compete for the existing population inversion in the laser.
- A laser medium yields gain over a certain spectral bandwidth determined by the line shape function.
- The mechanism of mode competition can limit the number of modes in self-organized manner.
- For homogeneous broadening all modes are feed by the same atoms and molecules. This results mode competition, i.e., strong fluctuation of the individual laser modes (see argon-ion laser).
- In the case of homogeneous gain medium, the whole gain profile is equally affected by the saturation. The modes situated far from the peak of the gain profile will exhibit losses and die out. However, the modes located close to the peak are enhanced at the expense of others, until reaching saturation. At the end, a single mode survives, and the laser oscillates monochromatically.
- For inhomogeneous broadening the modes get gain from different molecules and atoms, and thus independently amplified. Each mode burns a spectral hole independent of the others that do not compete for the same gain (see helium-neon laser) and lead to stable multi-mode operation.

1.7.6 Pumping Processes

a) **Optical Pumping**

- Shining a laser medium (solid or liquid) with a short-pulse flash lamp yields a fairly short pulses. Flash lamp pulses as short as $\sim 1\,\mu s$ exist.

- Unfortunately, this yields a pulse as long as the *excited-state lifetime* of the laser medium, which can be considerably longer than the pump pulse.
- Since solid-state laser media have lifetimes in the microsecond scale, it produces pulses *microseconds* to *milliseconds* long.

b) **Electrical Pumping**

- In gas lasers, the population inversion is achieved by using *avalanche electrons* in a high voltage discharge.
- As the electrons move in the discharge, they speed up and thus gain kinetic energy. The inelastic collision of an electron with an atom in the ground state leads to an energy transfer of a part this kinetic energy. As a result, the atom is excited and the electron moves with lower kinetic energy.

c) **Chemical Pumping**

- In some chemical reactions, the product is formed in an excited state, hence the condition of population inversion is established via creation of excited molecules.
- In reality, rare halide molecules exist solely in an excited state, therefore, population inversion is achievable. Lasers operating on such principle are known as *excimer laser*.

1.8 Phonomenological Laser Model

- To model a laser, one needs to consider
  - An active medium to amplify light.
  - A pumping mechanism to create population inversion.
  - A part of the amplified light has to be coupled back into the medium with the correct phase.

  We aim to describe the functioning of a laser using a very simplified model, as depicted in Figure 1.17, in a phenomenological manner. The active medium has a gain coefficient γ and length L_{m}. Feedback occurs through reflection from two mirrors with reflectivity coefficients R_1 and R_2, with no additional losses beyond that.

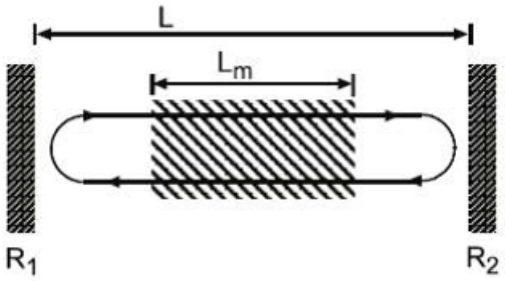

Fig. 1.17: Laser model. A gain medium of length L_m is situated within a resonator of length L, formed by mirrors with reflectivities R_1 and R_2.

- To keep the laser working, the amplitude of the electromagnetic wave needs to be stationary (temporally constant).
- The losses by mirrors (the out-coupled light) has to be compensated by the amplification caused by the pumping.
- The part of the wave that is reflected (not coupled out) has to be coupled back with the same phase.
- In each plane perpendicular to the laser axis the field $\mathbf{E}$ at time t has to exactly match the field $\mathbf{E}$ at time $t+\tau$ with τ is the round-trip time

$$\mathbf{E}(t) \stackrel{!}{=} \mathbf{E}(t+\tau). \tag{1.128}$$

- A continuous wave (cw) laser has a pulse length longer than the round-trip time.
- During propagation through the medium the field gets amplified with the factor $\mathrm{e}^{\gamma L_\mathrm{m}/2}$ and it gets damped to the mirrors with factors $\sqrt{R_1}$ and $\sqrt{R_2}$, respectively. Thus

$$\begin{aligned} \mathbf{E}(t) &= E_0 \mathrm{e}^{\mathrm{i}(kz-\omega t)} \\ &\stackrel{!}{=} E_0 \mathrm{e}^{\mathrm{i}(kz-\omega(t+\tau))} \mathrm{e}^{\gamma L_\mathrm{m}} \sqrt{R_1}\sqrt{R_2} \end{aligned}$$

- It follows that

$$\sqrt{R_1 R_2}\mathrm{e}^{-\mathrm{i}\omega\tau}\mathrm{e}^{\gamma L_\mathrm{m}} \stackrel{!}{=} 1 \tag{1.129}$$

  which is the heuristic laser model.
- Introducing the refractive index n the round-trip time τ reads

$$\tau = 2\frac{nL_\mathrm{m}}{c} + 2\frac{L-L_\mathrm{m}}{c} = 2\frac{L'}{c}, \tag{1.130}$$

  where $L' = L + L_\mathrm{m}(n-1)$ is the optical length.

- In order to fulfill the condition (1.128), the amplitude as well as the phase in Eq. (1.129) have to equal 1 independently, i.e.,

$$\boxed{\mathrm{e}^{-\mathrm{i}2\omega L'/c} = 1.} \quad \text{"phase condition"} \tag{1.131}$$

Hence

$$\frac{2\omega L'}{c} \stackrel{!}{=} 2q\pi, \quad q \in \mathbb{N}, \tag{1.132}$$

i.e., discrete values for the frequencies of the amplified and emitted light

$$\boxed{\omega_q = q\frac{\pi c}{L'}} \quad \text{or} \quad \boxed{\nu_q = q\frac{c}{2L'}.} \tag{1.133}$$

The arrangement of the two mirrors forms a *resonator* or *oscillator* with discrete resonance frequencies ν_q. The corresponding fields are called *longitudinal* modes of the resonator, and the frequency spacing is known as the *free spectral range* (FSR).

- **Example:** Typical length of a resonator for He-Ne laser is $L' = 50\,\mathrm{cm}$ at $\lambda = 633\,\mathrm{nm}$, thus the $q = 2.6 \times 10^6$-th longitudinal mode is excited, meaning that the corresponding standing wave has the same number of antinodes.

- The amplitude condition yields

$$\sqrt{R_1 R_2}\mathrm{e}^{\gamma L_\mathrm{m}} = 1, \tag{1.134}$$

which reads in logarithmic form as

$$\gamma = \frac{1}{L_\mathrm{m}} \ln\left(\frac{1}{\sqrt{R_1 R_2}}\right). \tag{1.135}$$

- The relationship between the required gain γL_m and the coupling losses due to the incomplete reflectivity $R_1 R_2 \leq 1$ of the two mirrors gives the conditions in the laser, ensured by saturation of the gain (see equation (1.127))

$$\mathrm{e}^{\gamma L_\mathrm{m}} = \frac{1}{\sqrt{R_1 R_2}} = \mathrm{e}^{\frac{\gamma_0 L_\mathrm{m}}{1+I/I_\mathrm{s}}}, \tag{1.136}$$

we obtain

$$1 + \frac{I}{I_\mathrm{s}} = \frac{\gamma_0 L_\mathrm{m}}{\ln\left(\frac{1}{\sqrt{R_1 R_2}}\right)}. \tag{1.137}$$

- In the limit $I \longrightarrow 0$ ($I \ll I_s$), and using $\ln\left(\frac{1}{\sqrt{R_1 R_2}}\right) \approx 1 - \sqrt{R_1 R_2}$ yields *the threshold for lasing*

$$\boxed{\gamma_0 L_m = 1 - \sqrt{R_1 R_2},} \quad \text{or} \quad \boxed{\sqrt{R_1 R_2} = 1 - \gamma_0 L_m}. \tag{1.138}$$

Hence, for a given reflectivity $R = \sqrt{R_1 R_2}$, the gain $\gamma_0 L_m$ has to exceed a certain value (depending on the gain coefficient and the length of the gain medium) for the lasing process to start. Vice versa, for a given gain $\gamma_0 L_m$, the reflectivity $R = \sqrt{R_1 R_2}$ has a lower bound for laser operation. The gain coefficient is spectrally limited. In only a few cases is its spectral width smaller than the free spectral range of the resonator, so that normally multiple modes are amplified. However, the number of active modes, as described the threshold condition, is also a function of the resonator losses, as only the modes for which the gain compensates for the coupling losses can oscillate. This is illustrated in Figure 1.18.

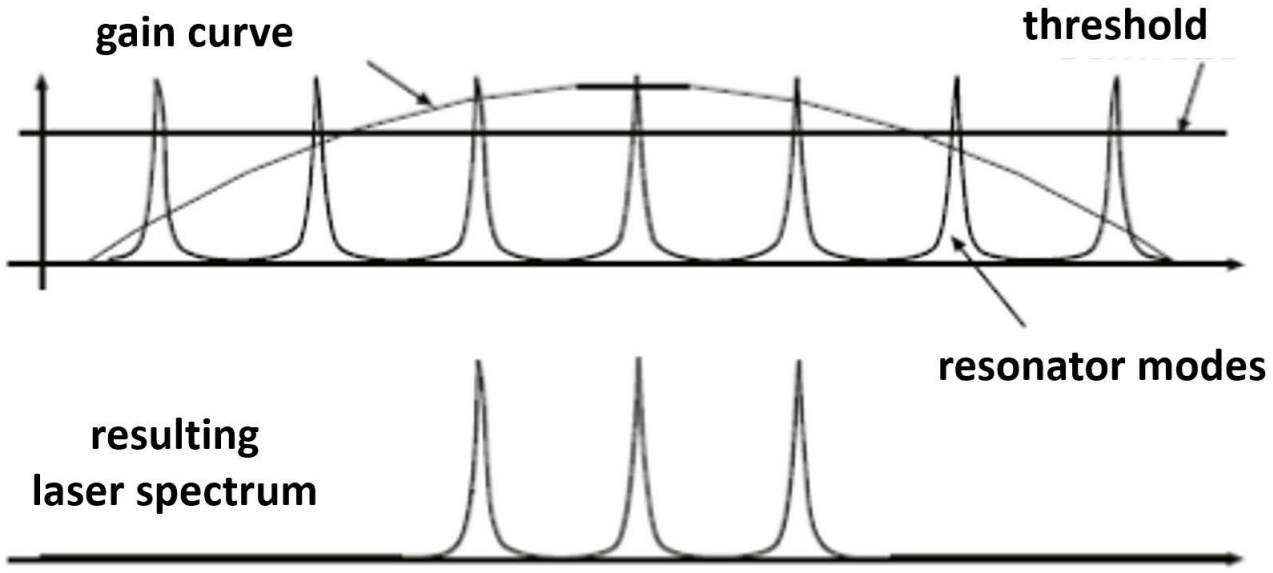

Fig. 1.18: Gain curve, lasing threshold, resonator modes, and the resulting active modes of a laser.

Alternative Derivation Using Rate Equations

- Let us consider N_2 the population of the upper level and $N_2 \gg N_1$

$$\frac{\mathrm{d}N_2}{\mathrm{d}t} = P_2 - \frac{N_2}{\tau_2} - \frac{\sigma}{h\nu} I N_2 \tag{1.139}$$

- Moreover, we define $\frac{I}{\tau_\mathrm{R}}$ as losses due to finite lifetime of photon in resonator

$$\frac{1}{\tau_\mathrm{R}} \approx (1-R)\frac{c}{L_\mathrm{m}}, \tag{1.140}$$

where $R = \sqrt{R_1 R_2}$ and the above approximation holds if $R_1 \approx R_2 \approx 1$.
The rate equation for the intensity I of light reads

$$\frac{\mathrm{d}I}{\mathrm{d}t} = c\sigma N_2 I - \frac{I}{\tau_\mathrm{R}}. \tag{1.141}$$

- In equilibrium ($\mathrm{d}I/dt = 0$), we obtain that

$$c\sigma N_2 I - \frac{1}{\tau_\mathrm{R}} I = 0, \tag{1.142}$$

hence

$$N_2 = \frac{1}{c\sigma\tau_\mathrm{R}} \tag{1.143}$$

which is independent on I.

- Assuming $I > 0$, the equilibrium condition ($\mathrm{d}N_2/dt = 0$) yields

$$P_2 - \frac{N_2}{\tau_2} - \frac{\sigma}{h\nu} I N_2 = 0, \tag{1.144}$$

therefore

$$I = P_2 h\nu c\tau_\mathrm{R} - \frac{h\nu}{\sigma\tau_2}. \tag{1.145}$$

- At the threshold where $I \longrightarrow 0$, we find

$$\begin{aligned} P_\mathrm{th} &= \frac{1}{c\sigma\tau_2\tau_\mathrm{R}} \\ &= \frac{1-R}{\sigma\tau_2 L_\mathrm{m}} \end{aligned} \tag{1.146}$$

where we have used the relation (1.140).

- Thanks to the relation

$$\gamma_0 = \sigma N_2 = \sigma P_2 \tau_2,$$

we find the threshold condition for lasing

$$\boxed{\gamma_0 L_m = 1 - R.} \tag{1.147}$$

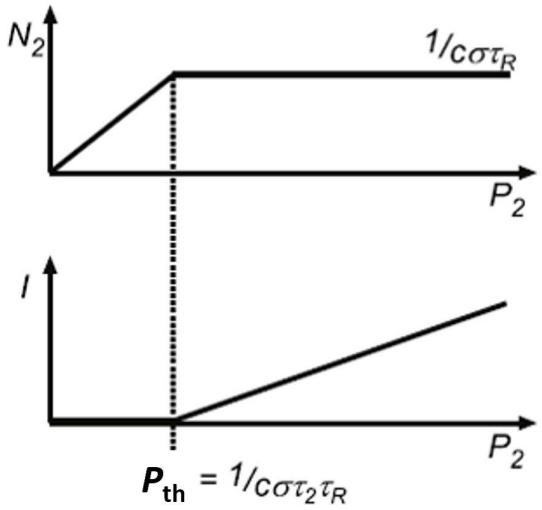

Fig. 1.19: The population of the upper laser level N_2 and the intensity I as a function of the pumping rate P_2.

E We discussed in the lecture the Wiener-Khinchin theorem, stating that the spectral power density $S(\nu)$ is proportional to the Fourier transform of the first order temporal correlation function $\Gamma^{(1)}(\tau)$. Here, we calculate the coherence length of a source with Gaussian spectral density power following the standard way and using the Wiener-Khinchin theorem. We start with the standard way where we analyse the field via a Michelson interferometer since the measured visibility is identical to $g^{(1)}(\tau)$.

1. Sketch the Michelson interferometer with incoming and outgoing fields, a 50:50 beam spliter, and one movable mirror (adjustable path length Δl). Show that for one frequency component the outgoing field is

$$E_{out}(\nu) = \frac{1}{2} E_{in}(\nu)\left(e^{i2\pi\frac{\nu}{c}l} + e^{i2\pi\frac{\nu}{c}(l+\Delta l)}\right).$$

Show that the outgoing spectral power density is given by

$$S_{out}(\nu) = \frac{1}{2} S_{in}(\nu)\left(1 + \cos\left(2\pi\frac{\nu}{c}\Delta l\right)\right).$$

Use this result to calculate the total detected intensity

$$I_{\mathrm{det}}(\nu) = \int_0^\infty S_{\mathrm{out}}(\nu)\mathrm{d}\nu.$$

2. Now consider a GAUSSIAN spectral power density for the incoming field, i.e.,

$$S_{\mathrm{in}}(\nu) = S_0 \exp\left[-4\ln(2)\left(\frac{\nu-\nu_0}{\Delta\nu}\right)^2\right]$$

with central frequency ν_0 and full-width at half-maximum $\Delta\nu$. Calculate an approximate expression for I_{det} by extending the lower integral border from 0 to $-\infty$. Give an explanation why this mathematical trick is good for $\nu_0 \gg \Delta\nu$. To compare, the result reads

$$I_{\mathrm{det}} = \frac{I_0}{4}\Delta\nu\sqrt{\frac{\pi}{\ln 2}}\left(1+\exp\left[-\frac{1}{\ln 2}\left(\frac{\pi\Delta\nu\Delta l}{2c}\right)^2\right]\cos\left(2\pi\frac{\nu_0}{c}\Delta l\right)\right).$$

Hint: I_{det} consists of two integrals which you can address independently. The first is solved with a substitution and the GAUSSIAN integral $\int_{-\infty}^{+\infty}\exp(-u^2)du = \sqrt{\pi}$. The second contains a cos-term. Rewrite it with exponentials and use the same techniques as for the first term. A quadratic expansion might also be helpful.

3. Using your result for I_{det} calculate the measured visibility $V(\Delta l)$ in the case $\nu_0 \gg \Delta\nu$ and check that the coherence length L_{coh} fulfilling $V(L_{\mathrm{coh}}) = \mathrm{e}^{-1}$ is obtained as

$$L_{\mathrm{coh}} = \frac{2\sqrt{\ln 2}}{\pi}\frac{c}{\Delta\nu}.$$

4. Using the WIENER-KHINCHIN theorem, calculate $g^{(1)}(\tau)$ apart from a proportionality factor, i.e.,

$$S_{\mathrm{in}}(\nu) \propto \int_{-\infty}^{\infty} g^{(1)}(\tau)\mathrm{e}^{-\mathrm{i}2\pi\nu\tau}\mathrm{d}\tau.$$

Determine the coherence length L_{coh} by calculating the coherence time τ_{coh}.

E Under what circumstances and temperature will the transition rate of the thermal background ($\propto$ photon density times the EINSTEIN coefficient B) equal the spontaneous transition rate ($\propto$ the EINSTEIN coefficient A) in a 2-level system without degeneracy?

E Write the rate equations for a degenerate two-level system (degeneracies g_1, g_2). Assume thermal equilibrium for the radiation field and upper- and lower-level populations, then derive the following relations for the EINSTEIN coefficients:

$$\begin{aligned} \frac{g_1}{g_2} B_{12} &= B_{21} = B, \\ \frac{A}{B} &= \frac{8\pi h\nu^3}{c^3}, \\ \frac{A}{B\rho(\nu)} &= \exp[h\nu/k_{\mathrm{B}}T] - 1. \end{aligned} \tag{1.148}$$

E Given your derivation in (1.148) why is X-ray laser particularly difficult to realize?

E Assuming an ensemble of atoms with mass M to follow a MAXWELL velocity distribution. Then the intensity profile of the emitted line will follow as

$$\begin{aligned} I(\omega) &= I(\omega_0) \exp\left(-\frac{Mv^2(\omega)}{2k_{\mathrm{B}}T} \right) \\ &= I(\omega_0) \exp\left(-\frac{Mc^2}{2k_{\mathrm{B}}T} \left[\frac{\omega - \omega_0}{\omega_0} \right]^2 \right). \end{aligned}$$

Show that the FWHM of this distribution reads

$$\begin{aligned} \Delta\omega &= \frac{2\omega_0}{c} \sqrt{\frac{2k_{\mathrm{B}}T}{M} \ln 2} \\ &= 7.16 \times 10^{-7} \omega_0 \sqrt{\frac{T}{M}} \end{aligned}$$

where T is the temperature of the emitters in K, and M is the atomic weight in atomic mass units (amu).

Chapter 2

Laser Radiation and Resonators

2.1 Laser Radiation

- Until now, we have considered plane waves which are unphysical since they carry infinite amount of power. Moreover, plane waves was only good for longitudinal structure of light field.
- From now on, consider also the transverse structure of the field containing finite energy.
- For transverse-limited beams, one has to compensate for diffraction. In a laser resonator that means a beam decays during the round trip if the beam is not focused.
- Due to diffraction, the transverse distribution of the electric field is a function of x, y and z

$$E(x,y,z,t) = \tilde{E}(x,y,z)\mathrm{e}^{\mathrm{i}(kz-\omega t)}, \quad \tilde{E}(x,y,z) \in \mathbb{C}, \tag{2.1}$$

  where $\tilde{E}(x,y,z)$ is a complex scalar wave amplitude.
- Any physical field has to fulfill the Helmholtz wave equation

$$\left[\nabla^2 - \frac{1}{c^2}\frac{\partial^2}{\partial t^2}\right] E(x,y,z,t) = \left[\nabla^2 - \frac{1}{c^2}\frac{\partial^2}{\partial t^2}\right] \tilde{E}(x,y,z)\mathrm{e}^{\mathrm{i}(kz-\omega t)} = 0 \tag{2.2}$$

- Splitting of time dependence gives

$$[\nabla^2 + k^2]\tilde{E}(x,y,z)\mathrm{e}^{\mathrm{i}kz} = 0 \tag{2.3}$$

  or

$$\frac{\partial^2 \tilde{E}}{\partial x^2} + \frac{\partial^2 \tilde{E}}{\partial y^2} + \frac{\partial^2 \tilde{E}}{\partial z^2} + 2\mathrm{i}k\frac{\partial \tilde{E}}{\partial z} = 0 \tag{2.4}$$

- Using paraxial approximation which states that the transverse momentum of light is small, i.e., $\frac{\partial^2 \tilde{E}}{\partial z^2} \ll 2ik\frac{\partial \tilde{E}}{\partial z}$ (slowly varying envelope approximation SVEA), we obtain the paraxial wave equation

$$\frac{\partial^2 \tilde{E}}{\partial x^2} + \frac{\partial^2 \tilde{E}}{\partial y^2} + 2ik\frac{\partial \tilde{E}}{\partial z} \overset{\text{SVEA}}{\simeq} 0. \tag{2.5}$$

- Possible solution for Eq. (2.5) takes the form

$$\tilde{E}(x,y,z) = A(z)\mathrm{e}^{ik\frac{x^2+y^2}{2\tilde{q}(z)}}. \tag{2.6}$$

- Substituting in Eq. (2.5) yields an equation

$$\left[\left(\frac{k}{\tilde{q}}\right)^2\left\{\frac{\mathrm{d}\tilde{q}}{\mathrm{d}z} - 1\right\}(x^2+y^2) + \frac{2ik}{\tilde{q}}\left\{\frac{\tilde{q}}{A}\frac{\mathrm{d}A}{\mathrm{d}z} + 1\right\}\right]A(z) = 0 \tag{2.7}$$

that must be valid for any x and y values. Consequently, this is valid only when both braces in Eq. (2.7) individually vanish, i.e.,

$$\frac{\mathrm{d}\tilde{q}}{\mathrm{d}z} - 1 = 0, \tag{2.8}$$

$$\frac{\mathrm{d}A(z)}{\mathrm{d}z} = -\frac{A(z)}{\tilde{q}}. \tag{2.9}$$

- The solution of Eq. (2.8),

$$\tilde{q}(z) = \tilde{q}_0 + z - z_0, \tag{2.10}$$

governs the evolution of the complex beam parameter.

- The solution of Eq. (2.9) reads

$$\frac{A(z)}{A_0} = \frac{\tilde{q}_0}{\tilde{q}(z)}. \tag{2.11}$$

It determines the evolution of the amplitude distribution.

- To seek for the meaning of $\tilde{q}(z)$, let us write

$$\frac{1}{\tilde{q}(z)} = \frac{1}{\tilde{q}_{\mathrm{re}}(z)} + \mathrm{i}\frac{1}{\tilde{q}_{\mathrm{im}}(z)}, \tag{2.12}$$

then plugging into Eq.(2.6) yields

$$\tilde{E}(x,y,z) = A_0\frac{\tilde{q}_0}{\tilde{q}(z)}\exp\left\{ik\frac{x^2+y^2}{2\tilde{q}_{\mathrm{re}}(z)} - k\frac{x^2+y^2}{2\tilde{q}_{\mathrm{im}}(z)}\right\}, \tag{2.13}$$

hence the real and imaginary parts of the electric field amplitude are

$$\mathrm{Re}\,\tilde{E} \sim \mathrm{e}^{-k\frac{x^2+y^2}{2\tilde{q}_{\mathrm{im}}(z)}} = \mathrm{e}^{-\frac{x^2+y^2}{W^2(z)}} \tag{2.14}$$

$$\mathrm{Im}\,\tilde{E} \sim \mathrm{e}^{\mathrm{i}k\frac{x^2+y^2}{2\tilde{q}_{\mathrm{re}}(z)}} = \mathrm{e}^{\mathrm{i}k\frac{x^2+y^2}{2R(z)}}, \tag{2.15}$$

where $W(z)$ is the beam width at position z (indicates where the intensity $I(x,y)$ decays to $1/e^2$ of its initial value), and $R(z)$ denotes the radius of curvature of the wave front.

- The equation (2.12) can be, therefore, written as

$$\boxed{\frac{1}{\tilde{q}(z)} = \frac{1}{R(z)} + \mathrm{i}\frac{\lambda}{\pi W^2(z)},} \quad \text{with} \quad k = \frac{2\pi}{\lambda}. \tag{2.16}$$

  This relation contains all the physics of the Gaussian beam.

- At $z = z_0$ (in focus), the radius of curvature is by construction $R(z = z_0) = \infty$, i.e., the beam is a plane wave. It follows that

$$\frac{1}{\tilde{q}(z = z_0)} = \frac{1}{\tilde{q}_0} = \mathrm{i}\frac{1}{\tilde{q}_{\mathrm{im}}(z = z_0)} = \mathrm{i}\frac{\lambda}{\pi W_0^2}, \tag{2.17}$$

  hence

$$\boxed{\tilde{q}_0 = -\mathrm{i}\frac{\pi W_0^2}{\lambda},} \tag{2.18}$$

  where $W_0 = W(z)\big|_{z=0}$.

- The equation (2.10) becomes

$$\tilde{q}(z) = -\mathrm{i}\frac{\pi W_0^2}{\lambda} + z - z_0, \tag{2.19}$$

  which is the beam waist of the Gaussian wave (width of the beam in focus).

- Without loss of generality, we can set $z_0 = 0$.

- Defining the Rayleigh length as $z_{\mathrm{R}} = \pi W_0^2/\lambda$, the equation (2.10) can be written as

$$\tilde{q}(z) = -\mathrm{i}z_{\mathrm{R}} + z. \tag{2.20}$$

- Substituting in Eq. (2.12) and comparing the imaginary and real parts, respectively, gives

$$W(z) = W_0\sqrt{1+\left(\frac{z}{z_\mathrm{R}}\right)^2} \tag{2.21}$$

$$R(z) = z+\frac{z_\mathrm{R}^2}{z}. \tag{2.22}$$

- Plugging into the original ansatz (2.6), we obtain the general expression

$$\tilde{E}(x,y,z,t) = \underbrace{E_0\frac{W_0}{W(z)}\mathrm{e}^{-(x^2+y^2)/W^2(z)}}_{\text{a}}\underbrace{\mathrm{e}^{\mathrm{i}(kz-\arctan(z/z_\mathrm{R}))}}_{\text{b}}\underbrace{\mathrm{e}^{\mathrm{i}k(x^2+y^2)/2R(z)}}_{\text{c}}\underbrace{\mathrm{e}^{-\mathrm{i}\omega t}}_{\text{d}}, \tag{2.23}$$

  where

  a) $E_0\frac{W_0}{W(z)}\mathrm{e}^{-(x^2+y^2)/W^2(z)}$ is the amplitude,

  b) $\mathrm{e}^{\mathrm{i}(kz-\arctan(z/z_\mathrm{R}))}$ is the longitudinal phase with $-\arctan(z/z_\mathrm{R})$ being the Gouy phase,

  c) $\mathrm{e}^{\mathrm{i}k(x^2+y^2)/2R(z)}$ is the radial phase,

  d) $\mathrm{e}^{-\mathrm{i}\omega t}$ is the temporal phase.

- A wave with Gaussian transverse profile stays a Gaussian during the propagation.

- Rayleigh length z_R is the distance where the beam broadens by the factor $\sqrt{2}$, i.e., $W(z_\mathrm{R}) = \sqrt{2}W_0$.

- At $z = z_\mathrm{R} = \pi W_0^2/\lambda$ (Rayleigh length), the radius of curvature is minimal.

- At $z > z_\mathrm{R}$, the radius of curvature decreases steadily.

- The length $2z_\mathrm{R}$ is called *confocal parameter*.

- For $z \gg z_\mathrm{R}$, the second term in the square brackets of Eq. (2.21) dominates, so that the beam radius is approximated as $W(z) \approx \lambda z/\pi W_0$.

- The asymptotic angle $\theta \approx \tan\theta \approx W(z)/z$ (paraxial approximation) is called *divergence angle*, thus we obtain $\theta = \lambda/\pi W_0$, i.e., the smaller the waist W_0, the more the beam diverges. As a consequence of diffraction-induced beam divergence, transmitting laser light over long distances in free space requires focusing lenses at suitable distances.

$z_R = \frac{\pi W_0^2}{\lambda}$	Rayleigh length
$W(z) = W_0\sqrt{1+\left(\frac{z}{z_R}\right)^2}$	Beam radius
$R(z) = z + \frac{z_R^2}{z}$	Wave front radius
$\theta = \frac{W_0}{z_R}$	Divergence angle

Table 2.1: Beam parameters of the Gaussian fundamental mode.

- Focusing a GAUSSIAN beam with lens has *diffraction limited spot size* (Figure 2.1) because the focused spot also has a GAUSSIAN energy distribution.

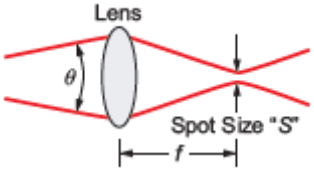

Fig. 2.1: Focussing a laser beam

- **Example:** The radius of He-Ne laser beam at $\lambda = 633\,\text{nm}$, which should not diffract by more than a factor of 2 over a distance of 10 m. Under these conditions the width should be at least 1 mm, i.e., $W_0 \geq 1\,\text{mm}$.
- A detector accounts only for the average power. Using $<\cos^2(\omega t)>= 1/2$, the field amplitude reads

$$E(x,y,z) = E(\rho,z) = E_0\frac{W_0}{W(z)}\mathrm{e}^{-\frac{\rho^2}{W^2(z)}}. \tag{2.24}$$

- The intensity $I(\rho,z)$ is obtained via averaging over one period

$$I(\rho,z) = \frac{1}{2}c\epsilon_0 E^2(\rho,z) = \frac{1}{2}c\epsilon_0 E_0^2\left(\frac{W_0}{W(z)}\right)^2\mathrm{e}^{-\frac{2\rho^2}{W^2(z)}}. \tag{2.25}$$

- The power P contained in GAUSSIAN beam is

$$\begin{aligned} P &= \int_0^\infty\int_0^{2\pi} I(\rho,z)\rho\mathrm{d}\rho\mathrm{d}\varphi \\ &= \frac{1}{2}c\epsilon_0 E_0^2\left(\frac{W_0}{W(z)}\right)^2\int_0^\infty\int_0^{2\pi}\mathrm{e}^{-\frac{2\rho^2}{W^2(z)}}\rho\mathrm{d}\rho\mathrm{d}\varphi \\ &= \frac{1}{4}c\epsilon_0\pi W_0^2 E_0^2. \end{aligned} \tag{2.26}$$

- The ground state is only one possible solution of the paraxial wave equation. Moreover, there exist three complete family of higher-order solutions in cartesian and cylindrical coordinates:

a) **Cartesian coordinates**
A general solution is

$$\tilde{E}(x,y,z) = A(z)H_m\left(\frac{x}{x_0}\right)H_n\left(\frac{y}{y_0}\right)\mathrm{e}^{\mathrm{i}k\frac{x^2+y^2}{2\tilde{q}(z)}}, \tag{2.27}$$

where $H_m(u) = (-1)^m \mathrm{e}^{u^2}\frac{\mathrm{d}^m \mathrm{e}^{-u^2}}{\mathrm{d}u^m}$ are HERMITE polynomials. $H_0(u) = 1$ recovers the case of GAUSSIAN beam that we discussed earlier. Higher orders begins from the term $H_1(u) = 2u$ and defines HERMITE-GAUSSS modes. The distributions are called Transverse Electromagnetic Modes (TEM_{mn}) where TEM_{00} has a GAUSSIAN shape and others has in general GAUSS-HERMITE modes (see Figure (2.2)).

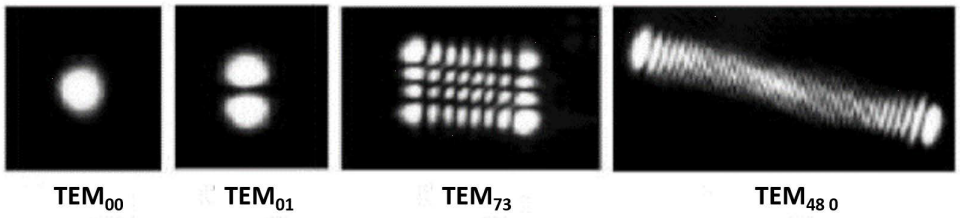

Fig. 2.2: TEM modes, captured using a titanium sapphire laser.

b) **Cylindrical coordinates**
Using ρ, φ (radius and azimuthal angle) and LAGUERRE polynomials $L_n(\rho, \varphi)$, one can define LAGUERRE-GAUSS modes. Different modes have zeros of the amplitude distribution in radial and azimuthal directions.

- When using polar coordinates ρ and φ instead of cartesian coordinates x and y, the modes are described by a product of LAGUERRE and GAUSSIAN functions, with the notation LG_{mp}. This is particularly useful when there is genuine cylindrical symmetry in the optical resonator.

- Both the HERMITE-GAUSSIAN and LAGUERRE-GAUSSIAN polynomials form a complete system of eigenfunctions, making a unique conversion always possible.

- Figure (a) depicts the representation of a HERMITE-GAUSSIAN mode (in cartesian coordinates with one zero in the x-direction and four zeros in the y-direction) through three LAGUERRE-GAUSSIAN modes.

- The Laguerre-Gaussian modes are characterized by different numbers of zeros in the radial (ρ) and azimuthal (φ) directions. The three Laguerre-Gaussian modes in Fig. (a) have 0 and 5, 1 and 3, 2 and 1 zeros in the ρ- and φ-directions, respectively.
- Figure (b) illustrates the conversion of a Laguerre-Gaussian mode into three Hermite-Gaussian modes.

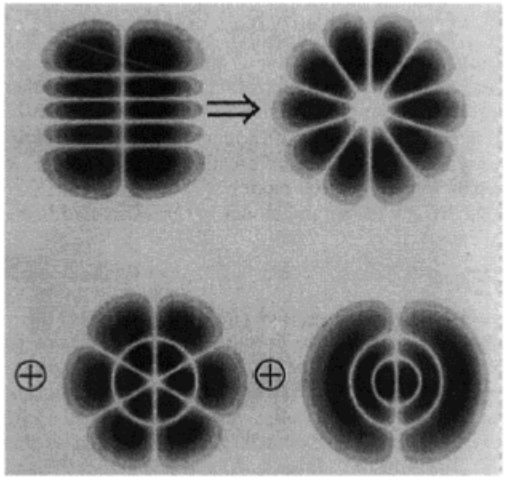

(a) The representation of a TEM_{14} Hermite-Gaussian mode using three Laguerre-Gaussian modes LG_{05}, LG_{13}, and LG_{21}.

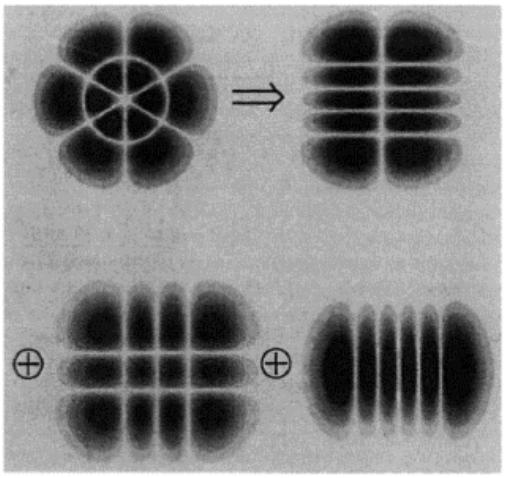

(b) The representation of an LG_{13} Laguerre-Gaussian mode from three Hermite-Gaussian modes TEM_{14}, TEM_{32}, and TEM_{50}.

2.2 Resonators

- Optical resonators are devices in which the electromagnetic field is enclosed between highly reflective mirrors that define the mode structure.
- When deriving the mode of electromagnetic field in vacuum, we took advantage of the fact that we could use any complete set of orthonormal basis functions of the Helmholtz operator to represent the electromagnetic field.
- In particular, we did not care about the coordinate system used for derivation. In a resonator, it is the geometry of mirrors that determines a specific choice of modes. Therefore, it is immediately clear that optical resonators are suitable for selecting special modes.

2.2.1 Planar Resonators

- We first consider two plane-parallel, infinitely extended plates, which are not completely reflecting, but rather have transmission coefficients T_1, T_2 and reflection coefficients R_1, R_2, respectively (Fig. 2.4). In this FABRY–PEROT interferrometer (FPI) of length L, a monochromatic plane electromagnetic wave entering at an angle θ has the form

$$\mathbf{E}(z,t) = E_0 \mathbf{e}_\sigma \mathrm{e}^{\mathrm{i}(\mathbf{k}\cdot\mathbf{r}-\omega t)}. \tag{2.28}$$

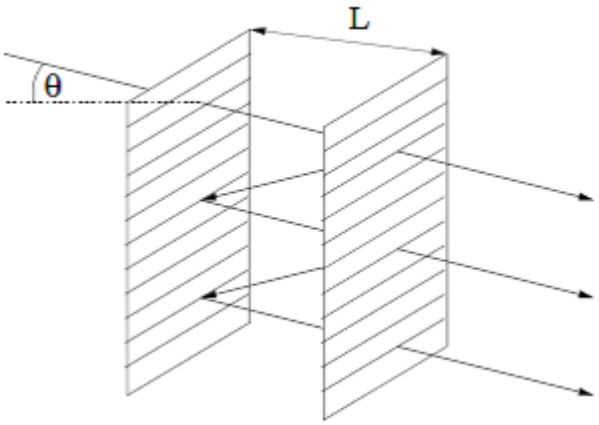

Fig. 2.4: FABRY–PEROT interferrometer consists of two plane-parallel mirrors with transmission coefficients T_1, T_2 and reflection coefficients R_1, R_2, respectively.

- The amplitude E_0' of the electromagnetic field behind the FABRY–PEROT resonator is then given as a superposition of all partial waves that are reflected many times inside the resonator.
- The reflection take place at inner sides of both mirrors, hence the phase jumps of π at the optically dense medium.
- The phase factor $\mathrm{e}^{\mathrm{i}(\mathbf{k}\cdot\mathbf{r}-\omega t)}$ is chosen such that is unity in the mirror plane.
- The transmitted complex amplitude reads

$$\begin{aligned} E_0' &= \sum_{i=1}^{\infty} E_{\mathrm{T}_i} \\ &= E_0 T_1 T_2 \underbrace{\mathrm{e}^{-\mathrm{i}\omega\frac{L}{c}\cos\theta}}_{(1)} + E_0 T_1 T_2 R_1 R_2 \underbrace{\mathrm{e}^{\mathrm{i}2\pi}}_{(2)} \underbrace{\mathrm{e}^{-\mathrm{i}\omega\frac{3L}{c}\cos\theta}}_{(3)} + E_0 T_1 T_2 R_1^2 R_2^2 \mathrm{e}^{\mathrm{i}4\pi} \mathrm{e}^{-\mathrm{i}\omega\frac{5L}{c}\cos\theta} + \cdots \\ &= E_0 T_1 T_2 \mathrm{e}^{-\mathrm{i}\omega\frac{L}{c}\cos\theta} (1 + R_1 R_2 \mathrm{e}^{-\mathrm{i}\omega\frac{2L}{c}\cos\theta} + R_1^2 R_2^2 \mathrm{e}^{-\mathrm{i}\omega\frac{4L}{c}\cos\theta} + \cdots) \end{aligned} \tag{2.29}$$

(1) : is the dynamic phase due to resonator length.
(2) : 2 times reflection at optically dense medium, i.e., $\left(e^{i\pi}\right)\left(e^{i\pi}\right) = e^{2i\pi}$.
(3) : is the dynamic phase due to 3 passes through the resonator.

$$\frac{E_0'}{E_0} = Te^{-i\frac{\delta}{2}}\left(1 + Re^{-i\delta} + R^2e^{-2i\delta} + \dots\right), \tag{2.30}$$

where we have assumed $T_1 = T_2 = \sqrt{T}$, $R_2 = R_1 = \sqrt{R}$ and defined the phase shift

$$\delta = \frac{\omega}{c}(2L)cos\theta \tag{2.31}$$

arising from the difference in travel between two adjacent partial waves.

- The infinite geometric series is evaluated using $\sum_{n=0}^{\infty} q^n = \frac{1}{1-q}$ with $q = Re^{-i\delta}$:

$$\frac{E_0'}{E_0} = \frac{Te^{-i\frac{\delta}{2}}}{1 - Re^{-i\delta}}. \tag{2.32}$$

- The transmission function of the resonator can be expressed as

$$T_{\mathrm{FP}} = \left|\frac{E_0'}{E_0}\right|^2 = \frac{T^2}{1 - 2R\cos\delta + R^2}. \tag{2.33}$$

Using $\cos\delta = 1 - 2\sin^2(\delta/2)$, the denominator of this expression can be cast in the form

$$1 - 2R\cos\delta + R^2 = (1-R)^2\left[1 + \frac{4R}{(1-R)^2}\sin^2\frac{\delta}{2}\right], \tag{2.34}$$

so that we obtain

$$\boxed{T_{\mathrm{FP}} = \left|\frac{E_0'}{E_0}\right|^2 = \left(\frac{T}{1-R}\right)^2\left[1 + \frac{4R}{(1-R)^2}\sin^2\frac{\delta}{2}\right]^{-1}.} \tag{2.35}$$

Equation (2.35) is known as the Airy function. It is depicted in in Fig. 3.8 as a function of the phase shift $\delta/2\pi$.

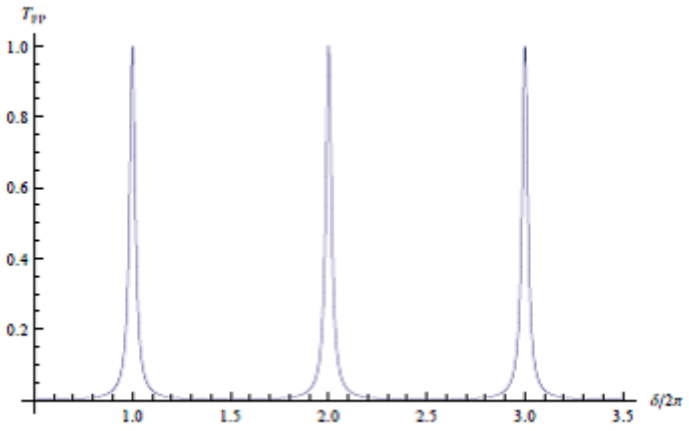

Fig. 2.5: Transmission of a FABRY–PEROT resonator.

- The maxima of the transmission function are reached at phase shifts $\delta = 2\pi m$ ($m \in \mathbb{N}_0$), i.e., with constructive interference of the partial waves. The maxima in the frequency space reads

$$\nu_m = \frac{\omega_m}{2\pi} = m\frac{c}{2L\cos\theta}, \tag{2.36}$$

hence the distance between two maxima

$$\delta\nu = \nu_{m+1} - \nu_m = \frac{c}{2L\cos\theta} \tag{2.37}$$

is called the dispersion region or the *free spectral range* (FSR).

- To compute the line width of the interference structure assume $\delta \ll 2\pi$ (very close to resonances), hence

$$T_{\mathrm{FP}} = \frac{T^2}{(1-R)^2 + 4R\sin^2(\frac{\omega}{c}L\cos\theta)} \simeq \frac{T^2}{(1-R)^2 + 4R\frac{\omega^2}{c^2}L^2\cos^2\theta} \tag{2.38}$$

which is a LORENTZIAN curve with a half-width $\omega_{1/2}$

$$\omega_{1/2}^2 = \frac{c^2(1-R)^2}{4RL^2\cos^2\theta} \tag{2.39}$$

corresponding to a linewidth (FWHM)

$$\Delta\nu = \frac{2\omega_{1/2}}{2\pi}, \tag{2.40}$$

or

$$\Delta\nu = \frac{c}{2L\cos\theta}\frac{1-R}{\pi\sqrt{R}}. \tag{2.41}$$

- The ratio of FSR to FWHM

$$\boxed{F = \frac{\delta\nu}{\Delta\nu} = \frac{\pi\sqrt{R}}{1-R}} \tag{2.42}$$

defines the *finesse* of the resonator.

- **Example:** A FABRY-PEROT interferometer (FPI) with a length of $L = 30\,\text{cm}$ and a mirror reflectivity $R = 99\%$. The finesse is $F = \pi\sqrt{0.99}/0.01 \simeq 314$. For normal incidence, the free spectral range is calculated as $\delta\nu = c/2L \simeq 500\,\text{MHz}$ and hence $\Delta\nu = \delta\nu/F \simeq 1.6\,\text{MHz}$.

- An intuition behind the connection between the lifetime of photons in the resonator and the finesse is based on the following considerations:

  - The larger R, the more round trips the photons experience in the resonator, so a storage time τ has to be taken into account.

  - If one would abruptly block the flow of photons into the resonator, the transmitted intensity decays exponentially.

- Therefore, the spectrum is a LORENTZ curve with line width $\Delta\nu = \frac{\Delta\omega}{2\pi} = \frac{1}{2\pi\tau}$ and the finesse reads

$$F = \frac{c}{2L\cos\theta}\frac{1}{\Delta\nu} = \frac{c}{2L\cos\theta}2\pi\tau = \frac{c\pi\tau}{L\cos\theta}. \tag{2.43}$$

Replacing τ by NT, where N is the average of round trips in the resonator and $T = 2L\cos\theta/c$ is the time for one round trip, yields

$$F = \frac{c}{2L\cos\theta}2\pi NT = \frac{c}{2L\cos\theta}2\pi N\frac{2L\cos\theta}{c} = 2\pi N. \tag{2.44}$$

Thus, the finesse roughly indicates the average number of round trips of the photon in the resonator.

2.2.2 Spherical Resonators

- Planar resonators have a crucial disadvantage that they have to be adjusted extremely precisely so that an incident beam (typically with a finite transverse extent) is superimposed to the reflected partial waves. This is the reason behind the usefulness of spherical resonators in practical applications.

- The eigenmodes of spherical resonators are the GAUSSIAN modes. The reason is that their wave fronts are curved and, therefore, adapted to the curvature of mirrors. A GAUSSIAN beam impinging on a spherical mirror is reflected into itself if its curvature matches with the beam. So we get a spherical resonator if we place mirrors with appropriate curvatures in the right places on the Gaussian profile in Fig. (1.14).

- We have seen that HERMITE–GAUSSIAN modes are also solutions for paraxial HELMHOLTZ equation having the same wave fronts as GAUSSIAN beams. This implies that HERMITE-GAUSS modes are also eigenmodes for spherical resonators. The corresponding phase whose indices (m, n) on the beam axis at $\rho = 0$ reads

$$\varphi(0, z) = kz + (m + n + 1)\zeta(z) \tag{2.45}$$

- To observe constructive interference, the phase shift of the wave after a complete trip through the resonator of length L must be a multiple of 2π,

$$2kL\cos\theta + 2(m + n + 1)\Delta\zeta = 2\pi q, \quad q \in \mathbb{Z}, \tag{2.46}$$

  where $\Delta\zeta = \zeta(z_2) - \zeta(z_1)$ represents the difference of the GOUY phases at the mirror positions. Setting $k = 2\pi\nu/c$ the resonance frequencies of these resonator modes are

$$\nu_{m,n,q} = q\delta\nu + (m + n + 1)\frac{\Delta\zeta}{\pi}\delta\nu, \tag{2.47}$$

  where $\delta\nu$ is the distance between two resonance frequencies

$$\delta\nu = \frac{c}{2L\cos\theta}. \tag{2.48}$$

  The three indices (m, n, q) are explained as follows: modes with different q but the same (m, n) have the same transverse intensity distributions are called *longitudinal* modes. The indices (m, n) describe the different *transverse* modes.

- From (2.47) one can deduce that all transverse modes with the sum index $m + n$ have the same resonance frequency. Two transverse modes with the same longitudinal index q have the frequency separation

$$\nu_{m,n,q} - \nu_{m',n',q} = \big[(m + n) - (m' + n')\big]\frac{\Delta\zeta}{\pi}\delta\nu, \tag{2.49}$$

  which characterizes the frequency shift between the groups of longitudinal modes.

2.2.3 Stability of Resonators

- Instead of fitting the two mirrors to a given GAUSSIAN beam, we look for a GAUSSIAN beam that match both curved mirrors M_1 and M_2 with radii of curvature R_1 and R_2 and spacing L.
- The curvature at z_1 and z_2 should match mirrors, thus we obtain three equations

$$R(z_1) = z_1 + \frac{z_R^2}{z_1} = -R_1 \tag{2.50}$$

$$R(z_2) = z_2 + \frac{z_R^2}{z_2} = +R_2 \tag{2.51}$$

and

$$L = z_2 - z_1. \tag{2.52}$$

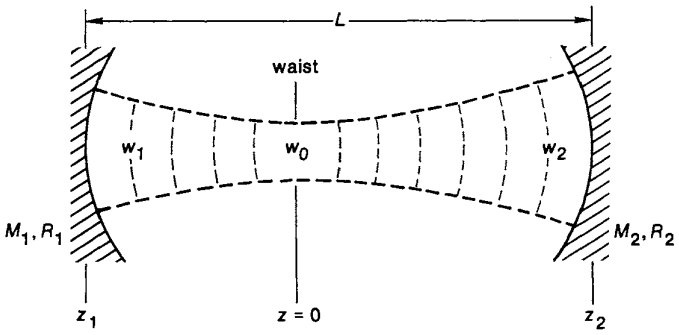

Fig. 2.6: Model for investigating stability analysis of the resonator.

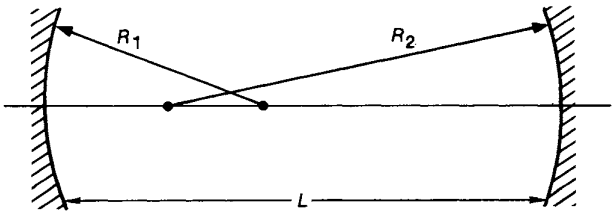

Fig. 2.7: The resonator g-factors.

- Let us define g-factors as

$$g_1 = 1 - \frac{L}{R_1} \quad \text{and} \quad g_2 = 1 - \frac{L}{R_2}. \tag{2.53}$$

- Therefore, the Rayleigh length of the mode is given by

$$z_R^2 = \frac{g_1 g_2 (1 - g_1 g_2)}{(g_1 + g_2 - 2 g_1 g_2)^2} L^2, \tag{2.54}$$

and the positions of the two mirrors with respect to beam waist are

$$z_1 = \frac{g_2 (1 - g_1)}{g_1 + g_2 - 2 g_1 g_2} L \quad \text{and} \quad z_2 = \frac{g_1 (1 - g_2)}{g_1 + g_2 - 2 g_1 g_2} L. \tag{2.55}$$

- Moreover, the mode sizes can be written as follows

  - Waist spot size:

$$W_0^2 = \frac{L\lambda}{\pi} \sqrt{\frac{g_1 g_2 (1 - g_1 g_2)}{(g_1 + g_2 - 2 g_1 g_2)^2}}. \tag{2.56}$$

  - Spot size at first mirror:

$$W_1^2 = \frac{L\lambda}{\pi} \sqrt{\frac{g_2}{g_1 (1 - g_1 g_2)}}. \tag{2.57}$$

  - Spot size at second mirror:

$$W_2^2 = \frac{L\lambda}{\pi} \sqrt{\frac{g_1}{g_2 (1 - g_1 g_2)}}. \tag{2.58}$$

- Real and finite solutions W_0, W_1 and W_2 can exist only if g-factors fulfills the stability condition for the resonator

$$\boxed{0 \leq g_1 g_2 < 1.} \tag{2.59}$$

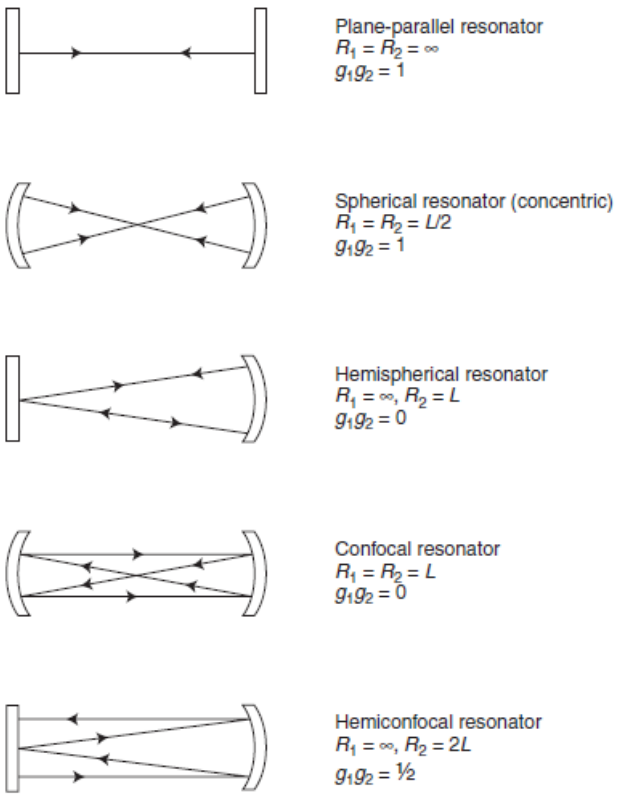

Fig. 2.8: Examples of stable resonators.

– Plane-parallel resonator: $g_1 = g_2 = 1$.

– Spherical (concentric) resonator: $g_1 = g_2 = -1$.

– Hemispherical resonator: $g_1 = 1$, $g_2 = 0$.

– Confocal resonator: $g_1 = g_2 = 0$.

– Hemiconfcal resonator: $g_1 = 1$, $g_2 = 1/2$.

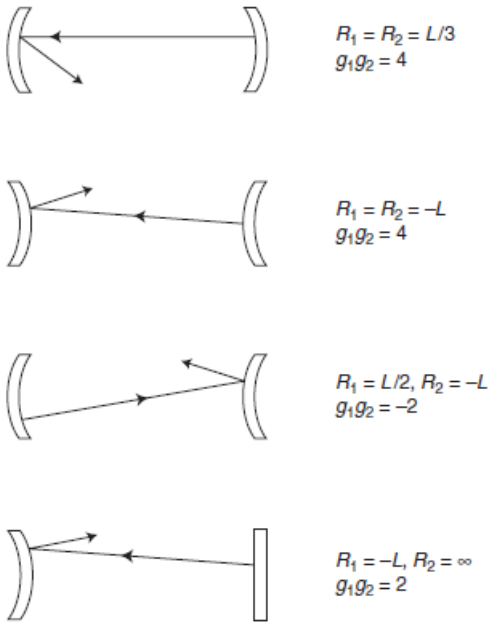

Fig. 2.9: Examples of unstable resonators.

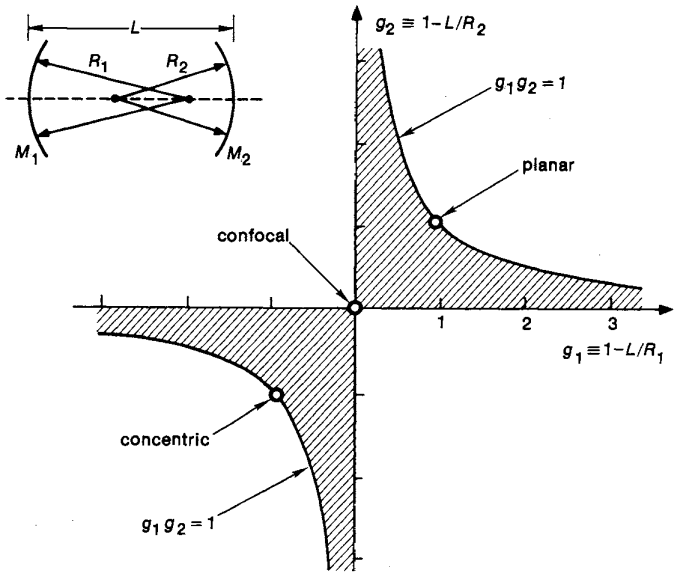

Fig. 2.10: Stability diagram for a two-mirror optical resonator.

- Semi-confocal is more stable because it is not on edge of stability region.
- The products of g-factors of the confocal, concentric, and hemispheric resonators reside exactly at the boundaries of stability region. Therefore, usually their parameters are slightly detuned to move inside the stability region.

- **Example:** Concentric resonator $L = 2R$, hence $g = -1$. Decreasing length by ΔL yields $L_{\text{new}} = 2R - \Delta L$, and $g_{\text{new}} = 1 - \frac{\Delta L}{R}$.

- Choosing a particular resonator due to certain requirements concerning mode volume, beam width, etc.

- Plane-parallel resonator has a large mode volume in its entire length, but very hard to adjust. Not often used in laser resonators.

- Confocal resonator has a very small mode volume, low diffraction losses, and easier to adjust.

- Hemispherical resonator is often used but has small beam waist. Having a good mode size at active medium, can change mode size by translating mirrors, and can change beam position by radially translating mirrors.

- Mode sizes for symmetric resonators ($g_1 = g_2 = g$)

$$W_0^2 = \frac{L\lambda}{\pi}\sqrt{\frac{1+g}{4(1-g)}}, \quad W_{1,2}^2 = \frac{L\lambda}{\pi}\sqrt{\frac{1}{1-g^2}}. \tag{2.60}$$

- All these resonators lie along the diagonal passing through the origin in the g-plane (see Fig. (2.10)).

- The curvature of mirrors can be steadily increased for a fixed spacing length L (see Fig. (2.11)).

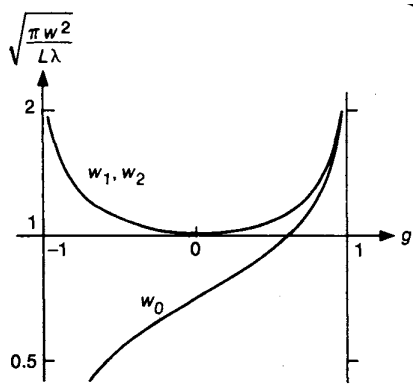

Fig. 2.11: Mode radii W_0 at the beam waist and $W_{1,2}$ at the mirrors of a symmetric resonator as a function of the g-parameter.

2.2.4 Applications

a) **Scanning FPI**

- Periodically changing the resonator length L due to piezoelectric elements.

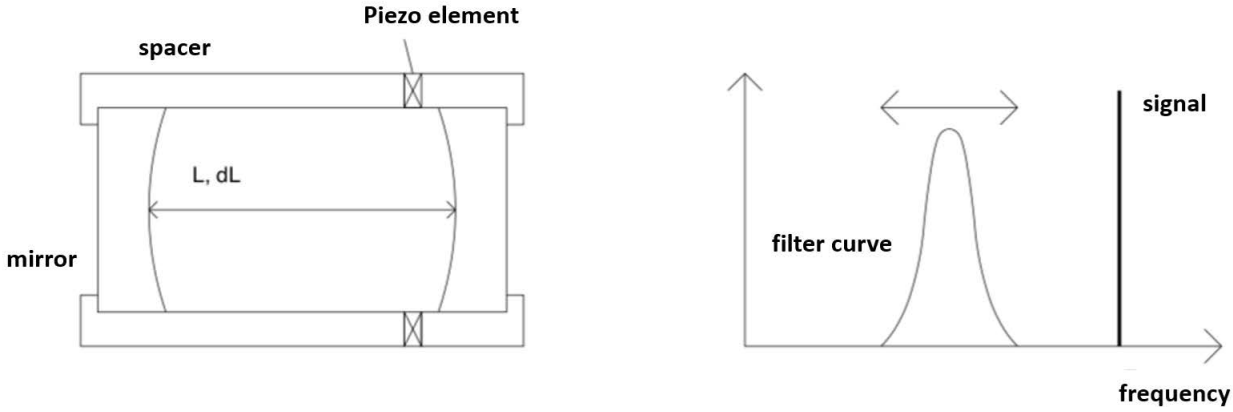

Fig. 2.12: Left: The principle of the scanning FABRY-PEROT interferometer, as used as a spectrum analyzer for laser radiation. Right: By changing the resonator length, the resonance frequencies shift. Thus, the corresponding filter curves can be tuned (scanned) over the wavelength of an incident laser beam.

- Change the transmission of FPI for different wavelengths.
- Visualize signal versus L with an oscilloscope.
- The transmission condition for the m-th mode in the FABRY-PEROT interferometer of length L is

$$L = m\frac{\lambda}{2} \quad \text{or} \quad \nu = m\frac{c}{2L}. \tag{2.61}$$

Hence

$$\frac{\delta\nu}{\delta L} = -\frac{1}{L^2}\frac{mc}{2} = -\frac{\nu}{L} \Rightarrow \frac{\delta\nu}{\nu} = -\frac{\delta L}{L}. \tag{2.62}$$

To cover at least the free spectral range FSR, one needs a piezo displacement ΔL of at least

$$|\delta\nu| = \left|\delta L\frac{\nu}{L}\right| \overset{!}{>} \text{FSR} = \frac{c}{2L}, \tag{2.63}$$

Thus

$$\delta L > \frac{c}{2\nu} = \frac{\lambda}{2}. \tag{2.64}$$

b) **Etalons**

- Made of low-loss slab (glass) with refractive index n having two parallel sides coated with a metal or dielectric mirror coating.

Fig. 2.13: Types of Etalon constructions.

- Etalons of interference filters are equivalent to FPI. Usually the length varies from mm to cm. Commonly used to limit modes in the laser cavity.
- **Example:** For an etalon with thickness $L = 0.5\,\text{cm}$ and reflectivity $R = 90\%$, the finesse is $F = 30$ where the free spectral range is $\delta\nu = 30\,\text{GHz}$ and the linewidth being $\Delta\nu = 1\,\text{GHz}$.

c) **Dichroic Filters**

- Same principle as etalons but different names in specific applications.
- Dichroic filters are also interference filters having passbands down to few hundreds of nanometers. They are manufactured by coating a substrate with multi-layered thin film to achieve specific range of transmitted wavelengths and higher reflectivities.

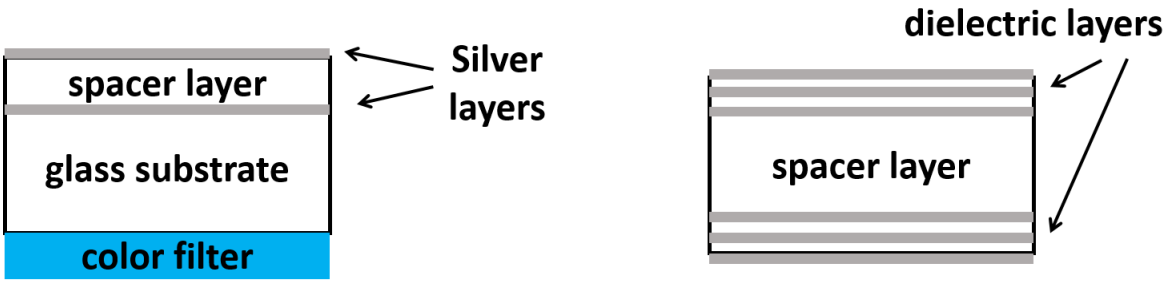

Fig. 2.14: Types of interference filters.

- Thin films, e.g., silver and aluminium are used for this purpose. The reflectivity at an interface

$$R_{\perp} = \left(\frac{n_1 - n_2}{n_1 + n_2}\right)^2 \tag{2.65}$$

is known as Fresnel equation. A higher reflectivity could be achieved by increasing the refraction index contrast, but Kramers-Kronig relations predicts high absorption for high index of refraction.

- To outcome this problem, multi-layers with small refractive index contrast are used. The operation is illustrated in Fig. 2.15 for a two-layer reflective layer sequence on a substrate.

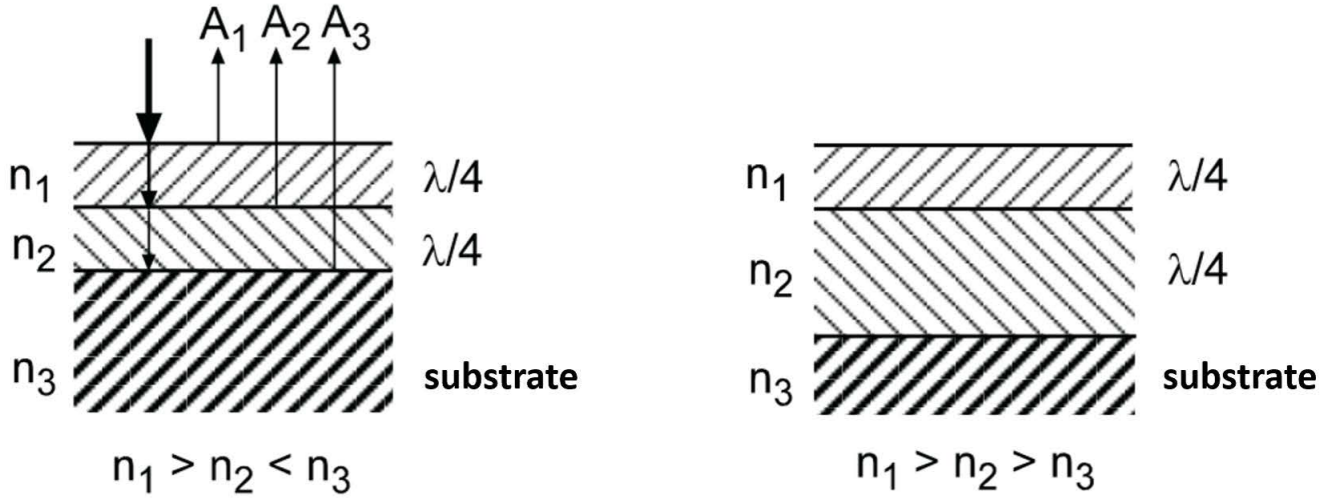

Fig. 2.15: Reflective dual coating on a substrate.

- Choose a stack of alternating layers thicknesses of high and low index $n_{\mathrm{h,l}}$ of refraction such that reflected waves of the individual contributions add up constructively. A phase difference is accumulated from the delay between forward and backward propagating waves, and the phase jump of 0 or π depending the refraction index contrast given in the equation (2.65). As a consequence, the maximum reflectance happens for a layer thickness of $\lambda/4$.

- Other problems are caused by the wavelength dependence of refractive indices $n = n(\lambda)$ and thermal expansion of film materials.

λ	SiO_2	Ta_2O_5	MgF_5
488 nm	1.463	2.188	1.379
633 nm	1.457	2.152	1.378
1064 nm	1.450	2.117	1.376

Table 2.2: Refractive indices of some film materials varies with wavelength.

2.3 ABCD Formalism

- We want to describe the action of an optical element via matrix formalism. Consider a light ray in paraxial approximation travelling in z-direction at distance $y(z)$ from the optical axis till $y'(z)$, i.e., $y'(z) = \frac{dy}{dz} = \tan\Theta \simeq \Theta$.
- In geometrical optics, a ray is characterized by its distance from the axis and its slope.

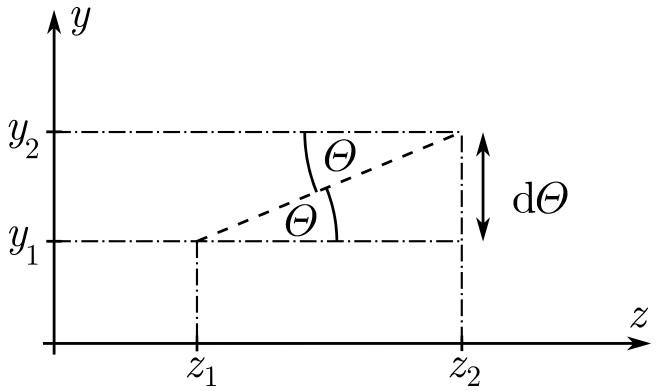

Fig. 2.16: The quantities y_1 and y_2 are distances of the ray from the optical axis before and after the optical element, Θ is the direction angle, and $z_2 - z_1 = d$.

- For the translation from z_1 to z_2 in vacuum:

$$y(z_2) = y(z_1) + y'(z_1)(z_2 - z_1) \tag{2.66}$$
$$y'(z_2) = y'(z_1) \quad \text{(free space)} \tag{2.67}$$

  Skipping the arguments, we rewrite both equations as

$$y_2 = y_1 + y_1'(z_2 - z_1) \tag{2.68}$$
$$y_2' = y_1' \tag{2.69}$$

- In matrix notation, the latter is equivalent to

$$\begin{pmatrix} y_2 \\ y_2' \end{pmatrix} = \begin{pmatrix} A & B \\ C & D \end{pmatrix} \begin{pmatrix} y_1 \\ y_1' \end{pmatrix} \Leftrightarrow \begin{array}{l} y_2 = Ay_1 + By_1' \\ y_2' = Cy_1 + Dy_1' \end{array} \tag{2.70}$$

- Free space

$$\begin{pmatrix} A & B \\ C & D \end{pmatrix} = \begin{pmatrix} 1 & z_2 - z_1 \\ 0 & 1 \end{pmatrix} \tag{2.71}$$

  which is ABCD matrix for free space.

- Thin lens

$$\frac{1}{d_1}-\frac{1}{d_2}=\frac{1}{f} \quad \Rightarrow \frac{y_1}{d_1}-\frac{y_1}{d_2}=\frac{y_1}{f} \quad \Rightarrow y_2'=y_1'-\frac{y_1}{f} \quad \text{and} \quad y_2=y_1. \tag{2.72}$$

Thus

$$\begin{pmatrix} y_2 \\ y_2' \end{pmatrix} = \begin{pmatrix} 1 & 0 \\ -\frac{1}{f} & 1 \end{pmatrix} \begin{pmatrix} y_1 \\ y_1' \end{pmatrix} = \begin{pmatrix} y_1 \\ -\frac{y_1}{f}+y_1', \end{pmatrix} \tag{2.73}$$

i.e. the lens changes the direction of the ray.

- In general, within ABCD formalism we can combine optical elements.

- **Example:** Ray passes through a lens with focal length f, then through free space d:

$$\begin{pmatrix} A & B \\ C & D \end{pmatrix} = \begin{pmatrix} 1 & d \\ 0 & 1 \end{pmatrix} \begin{pmatrix} 1 & 0 \\ -\frac{1}{f} & 1 \end{pmatrix} = \begin{pmatrix} 1-\frac{d}{f} & d \\ -\frac{1}{f} & 1 \end{pmatrix}. \tag{2.74}$$

- **Summary of different ABCD matrices**

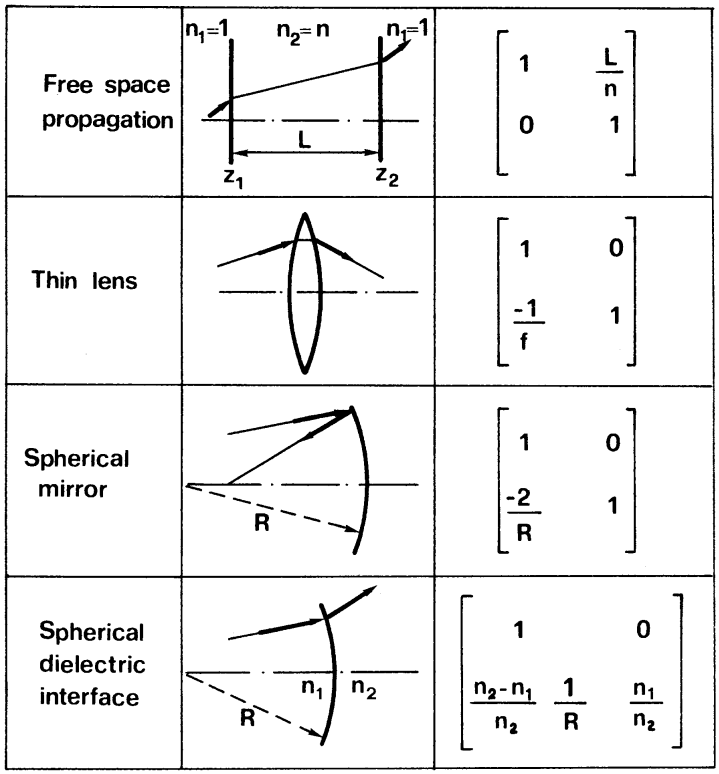

Fig. 2.17: ABCD matrices for some common cases.

- In the the case of gradient index lens or GRIN-lens of arbirary thickness L, where the refraction index profile reads

$$n(r) = n_0 - \frac{1}{2} n_2 r^2, \tag{2.75}$$

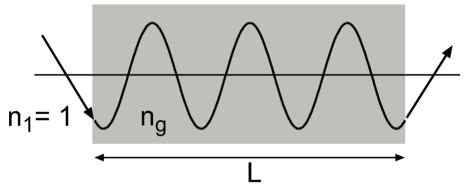

we have

$$\begin{pmatrix} A & B \\ C & D \end{pmatrix} = \begin{pmatrix} \cos\left(L\sqrt{\frac{n_2}{n_0}}\right) & \frac{1}{\sqrt{n_0 n_2}} \sin\left(L\sqrt{\frac{n_2}{n_0}}\right) \\ \sqrt{n_0 n_2} \sin\left(L\sqrt{\frac{n_2}{n_0}}\right) & \cos\left(L\sqrt{\frac{n_2}{n_0}}\right) \end{pmatrix} \tag{2.76}$$

- For a GAUSSIAN aperture with the transmission profile

$$T(r) = T_0 \mathrm{e}^{-r^2/a^2} \tag{2.77}$$

the ABCD matrix is

$$\begin{pmatrix} 1 & 0 \\ -\frac{\mathrm{i}\lambda}{\pi a} & 1 \end{pmatrix}, \tag{2.78}$$

where λ is the wavelength.

E Consider the field component,

$$E(\rho, z, t) = \frac{A_0}{1 + \mathrm{i}\frac{z}{z_0}} \exp\left[- \frac{\rho^2}{W_0^2 (1 + \mathrm{i}\frac{z}{z_0})} \right] \mathrm{e}^{\mathrm{i}k(z - ct)} \tag{2.79}$$

with $\rho = \sqrt{x^2 + y^2}$, $A_0 \in \mathbb{C}$ and $k, z_0 \in \mathbb{R}$.

1. Derive the paraxial HELMHOLTZ equation in cylindrical coordinates from the wave equation using the separation $E(\mathbf{r},t) = A(\mathbf{r})\mathrm{e}^{\mathrm{i}k(z-ct)}$. Verify that the given field E fulfills this equation.
   Hint: Use $\partial_z^2 A(\boldsymbol{r}) \approx 0$ *and* $z_0 = kW_0^2/2$.

2. Show that the GAUSSIAN beam (2.79) can also be written in the form

$$E(\rho,z,t) = A_0 \frac{W_0}{W(z)} \exp\left[-\frac{\rho^2}{W^2(z)}\right] \exp\left[\mathrm{i}\left(kz + k\frac{\rho^2}{2R(z)} - \psi(z)\right)\right] \exp(-\mathrm{i}\omega t).$$

   Determine the functions $W(z)$, $R(z)$ and $\psi(z)$ and discuss their meaning. Which geometry is described by a constant phase surface in the limits $z/z_0 \longrightarrow 0$ and $z_0/z \longrightarrow 0$?

3. You saw in the lecture that the function,

$$E_{m,n}(\rho,z,t) = E(\rho,z,t) H_m\left(\frac{\sqrt{2}x}{W(z)}\right) H_n\left(\frac{\sqrt{2}y}{W(z)}\right) \mathrm{e}^{\mathrm{i}f_z(z)} \tag{2.80}$$

   where $H_m(u)$ and $H_n(v)$ are Hermite polynomials and $f_z(z) = -(m+n)\arctan z/z_0$, is also a solution to the paraxial Helmholtz equation. Show that these solutions are L^2-orthogonal with respect to x and y (i.e., for fixed z).
   Hint: First look up the orthogonality relation for Hermite polynomials.

4. Compute $|E_{0,0}(\rho,z,t)|^2$ and plot this intensity profile for $t = z = 0$. What happens with the intensity for $z > 0$?

Chapter 3

Ultrashort Laser Pulses

- Ultrafast laser pulses are laser bursts with durations in the femtosecond (10^{-15} s) to picosecond (10^{-12} s) range, making them the shortest controlled events in nature.

- The combination of ultrashort temporal duration and broad spectral bandwidth enables the study and manipulation of dynamic processes at atomic, molecular, and material scales.

- These pulses are central to understanding and controlling fast physical, chemical, and biological processes, such as electron motion, molecular vibrations, and chemical reactions.

- The field of ultrafast optics underpins transformative technologies, including femtochemistry, precision micromachining, and nonlinear optical phenomena.

- With high peak intensities, ultrafast pulses drive nonlinear effects like self-phase modulation, supercontinuum generation, and high-harmonic generation. Their applications span scientific research, material processing, optical communication, and medicine, providing unprecedented spatial and temporal resolution.

- This chapter explores the fundamental principles of ultrafast laser pulses, their propagation in linear and nonlinear media.

3.1 Basics

3.1.1 Phase Velocity

- The phase of a plane wave reads

$$\varphi(\mathbf{r},t) = \mathbf{k}\cdot\mathbf{r} - \omega t - \varphi_0. \tag{3.1}$$

- The phase velocity is defined as $\frac{\mathrm{d}\varphi}{\mathrm{d}t} \stackrel{!}{=} 0$, hence

$$\mathbf{k}\cdot\mathbf{v}_\mathrm{p} - \omega = 0 \Rightarrow \boxed{v_\mathrm{p} = \frac{\omega}{|\mathbf{k}|}.} \tag{3.2}$$

- The phase velocity in free space is the speed of light

$$v_\mathrm{p} = \frac{\omega}{|\mathbf{k}|} = \frac{|\mathbf{k}|c}{|\mathbf{k}|} = c. \tag{3.3}$$

3.1.2 Superposition Principle

- The wave equation is linear, thus the superposition principle holds, i.e.,

$$\Delta\psi_1 = \frac{1}{c^2}\frac{\partial^2}{\partial t^2}\psi_1, \quad \Delta\psi_2 = \frac{1}{c^2}\frac{\partial^2}{\partial t^2}\psi_2 \Rightarrow \Delta(a_1\psi_1 + a_2\psi_2) = \frac{1}{c^2}\frac{\partial^2}{\partial t^2}(a_1\psi_1 + a_2\psi_2).$$

- Consider discrete superposition in one dimension

$$\psi(x,0) = \sum_j f_{k_j}(x,0) = \sum_j A_{k_j}\mathrm{e}^{\mathrm{i}k_j x}. \tag{3.4}$$

This superposition propagates as follows

$$\begin{aligned}
\psi(x,t) &= \sum_j A_{k_j}\mathrm{e}^{\mathrm{i}(k_j x - \omega_j t)} \\
&= \sum_j A_{k_j}\mathrm{e}^{\mathrm{i}k_j(x - v_j t)} \\
&\stackrel{\text{in free space}}{=} \sum_j A_{k_j}\mathrm{e}^{\mathrm{i}k_j(x - ct)} \\
&= \psi(x - ct, 0).
\end{aligned} \tag{3.5}$$

Thus the discrete superposition $\psi(x,t)$ travels without change of envelope in free space.

3.1.3 Group Velocity

- Consider a wavepacket in one dimension

$$E(x,0) = \int_{-\infty}^{\infty} \mathrm{d}k \tilde{E}(k) \mathrm{e}^{\mathrm{i}kx} \tag{3.6}$$

propagating as

$$E(x,t) = \int_{-\infty}^{\infty} \mathrm{d}k \tilde{E}(k) \mathrm{e}^{\mathrm{i}(kx-\omega t)}, \tag{3.7}$$

where $\tilde{E}(k)$ are FOURIER components.

- Suppose that $\tilde{E}(k)$ is sharply peaked around k_0. TAYLOR expansion yields

$$\omega(k) \simeq \omega(k_0) + \left.\frac{\partial\omega}{\partial k}\right|_{k=k_0} (k-k_0) + \ldots \tag{3.8}$$

Plugging (3.8) into (3.7) yields

$$E(x,t) = \underbrace{\mathrm{e}^{\mathrm{i}(k_0 x - \omega(k_0)t)}}_{(1)} \int_{-\infty}^{\infty} \mathrm{d}k \underbrace{\tilde{E}(k) \mathrm{e}^{\mathrm{i}(k-k_0)\left(x - \left.\frac{\partial\omega}{\partial k}\right|_{k=k_0} t\right)}}_{(2)}, \tag{3.9}$$

(1) : is a monochromatic plane wave which propagates with phase velocity $\omega(k_0)/k_0$ within the envelope of the wave packet.
(2) : is an envelope function traveling with velocity $\left.\frac{\partial\omega}{\partial k}\right|_{k=k_0}$.

- The group velocity is defined as

$$\boxed{v_\mathrm{g} = \frac{\partial\omega}{\partial k}.} \tag{3.10}$$

- The group velocity in free space is the speed of light

$$v_\mathrm{g} = \frac{\partial\omega}{\partial k} = \frac{\partial(kc)}{\partial k} = c. \tag{3.11}$$

- In media: $n = \frac{c}{v_\mathrm{p}} \Rightarrow \omega = \frac{kc}{n(\omega)}$ ($v_\mathrm{p} = \frac{\omega}{k}$), then

$$\begin{aligned} \frac{\partial k}{\partial\omega} &= \frac{1}{c}\frac{\partial}{\partial\omega}(\omega n(\omega)) \\ &= \frac{1}{c}\left(n(\omega) + \omega\frac{\partial}{\partial\omega}n(\omega)\right). \end{aligned} \tag{3.12}$$

Consequently, we find that

$$v_g = \frac{\partial \omega}{\partial k} = \frac{c}{n(\omega) + \omega \frac{\partial n(\omega)}{\partial \omega}}. \tag{3.13}$$

which could be greater than c, for instance, if $\frac{\partial n}{\partial \omega} < 0$ (strong anomalous dispersion). However, in accordance with KRAMERS-KRONIG relation, this will never exceed c due to strong absorption in this region.

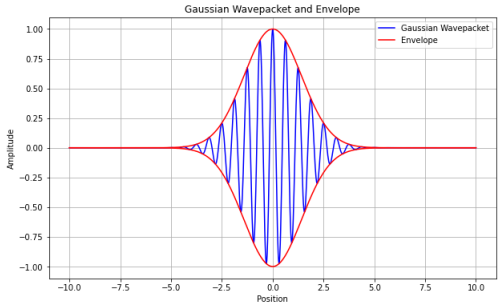

Fig. 3.1: GAUSSIAN wavepacket. The red colored "envelope" travels at the group velocity v_g while the blue colored ripples travel at the phase velocity v_p.

3.1.4 Signal Velocity

- Consider a signal that evolves from

$$\psi(x = 0, t) = \Theta(t) e^{i\omega t}, \tag{3.14}$$

with Θ is the HEAVISIDE step function, to

$$\psi(x, t) = \int_{-\infty}^{\infty} dt' G(x, t - t') \psi(x = 0, t') \tag{3.15}$$

with the GREEN's function

$$G(x, \tau) = \frac{1}{2\pi} \int_{-\infty}^{\infty} d\omega e^{i\omega(n(\omega)\frac{x}{c} - \tau)}. \tag{3.16}$$

- KRAMERS-KRONIG relations stipulate that $n(\omega)$ is an analytic function in upper complex plane ω-plane, $n(\omega) \xrightarrow[|\omega| \to \infty]{} 1$. Therefore

$$\oint_C d\omega e^{i\omega(n(\omega)\frac{x}{c} - \tau)} = 0. \tag{3.17}$$

$$\int_{-\infty}^{\infty} d\omega e^{i\omega(n(\omega)\frac{x}{c} - \tau)} + \int_{\curvearrowleft} d\omega e^{i\omega(n(\omega)\frac{x}{c} - \tau)} = 0 \tag{3.18}$$

- For large semicircle, the condition $|\omega| \to \infty$, $n(\omega) = 1$ is fulfilled, so

$$\int_{\curvearrowleft} \mathrm{d}\omega \mathrm{e}^{\mathrm{i}\omega(n(\omega)\frac{x}{c}-\tau)} = \int_{\curvearrowleft} \mathrm{d}\omega \mathrm{e}^{\mathrm{i}\omega(\frac{x}{c}-\tau)} \underset{x>c\tau}{=} 0 \tag{3.19}$$

Thus

$$\boxed{G(x,\tau) = 0 \Leftrightarrow x > c\tau,} \tag{3.20}$$

i.e., there is no *superluminal signalling*.

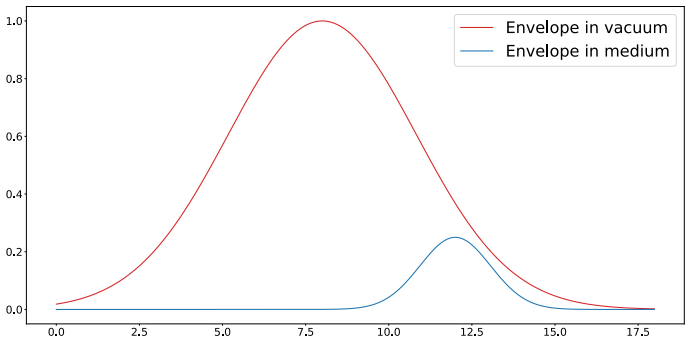

Fig. 3.2: Comparison of two wave packets in vacuum and in medium.

3.2 Propagation of Light in Linear Media

- The Maxwell equations reads

$$\begin{aligned} \nabla \cdot \mathbf{D}(\mathbf{r},t) &= \rho(\mathbf{r},t), & (3.21)\\ \nabla \cdot \mathbf{B}(\mathbf{r},t) &= 0, & (3.22)\\ \nabla \times \mathbf{E}(\mathbf{r},t) &= -\dot{\mathbf{B}}(\mathbf{r},t), & (3.23)\\ \nabla \times \mathbf{H}(\mathbf{r},t) &= \mathbf{j}(\mathbf{r},t) + \dot{\mathbf{D}}(\mathbf{r},t), & (3.24) \end{aligned}$$

where $\mathbf{B}(\mathbf{r},t)$ represents the magnetic induction, $\mathbf{E}(\mathbf{r},t)$ is the electric field, $\mathbf{D}(\mathbf{r},t)$ denotes the displacement field, $\mathbf{H}(\mathbf{r},t)$ is the magnetic field, $\rho(\mathbf{r},t)$ is the charge density, and $\mathbf{j}(\mathbf{r},t)$ corresponds to the current density.

- The Maxwell equations can be grouped in two distinct ways

1. *Physical regrouping*:
   - Equations (3.22) and (3.23) describe the electric field $\mathbf{E}(\mathbf{r},t)$ and the magnetic induction $\mathbf{B}(\mathbf{r},t)$, which are considered as *microscopic* fields.

  - Equations (3.21) and (3.24) involve the displacement field $\mathbf{D}(\mathbf{r},t)$ and the magnetic field $\mathbf{H}(\mathbf{r},t)$, which are viewed as *macroscopic* fields.

2. *Mathematical regrouping*:
  - Equations (3.21) and (3.22) represent divergence relations, associated with Gauß theorem.
  - Equations (3.23) and (3.24) correspond to curl relations, as described by Stokes' theorem.

- When an electromagnetic field encounters a medium composed of usually bound distributions of charges, these charges will undergo a displacement in response to the field. This displacement results in the generation of an induced polarization field (and, in the case of a magnetic medium, magnetization as well).

- In general, we can write the constitutive equations as

$$\mathbf{D}(\mathbf{r},t) = \epsilon_0\mathbf{E}(\mathbf{r},t) + \mathbf{P}[\mathbf{E}(\mathbf{r},t)] \tag{3.25}$$

$$\mathbf{H}(\mathbf{r},t) = \frac{1}{\mu_0}\mathbf{B}(\mathbf{r},t) + \mathbf{M}[\mathbf{B}(\mathbf{r},t)], \tag{3.26}$$

  which implies that the polarization, denoted as $\mathbf{P}$, and the magnetization, denoted as $\mathbf{M}$, are functionals of the fields $\mathbf{E}$ and $\mathbf{B}$, respectively. While, in electro-optics and magneto-optics, $\mathbf{P}$ and $\mathbf{M}$ may also be functionals of $\mathbf{B}$ and $\mathbf{E}$ respectively, such considerations are beyond the scope of this lecture. The specific nature of this dependence must still be determined based on the properties of the medium in question.

- In linear media, it is reasonable to assume a linear proportionality between the applied electric field and the polarization, as well as between the magnetization and the magnetic induction, i.e.,

$$\mathbf{P}(\mathbf{r},t) = \epsilon_0(\epsilon-1)\mathbf{E}(\mathbf{r},t) \tag{3.27}$$

$$\mathbf{M}(\mathbf{r},t) = \frac{1}{\mu_0}\left(\frac{1}{\mu}-1\right)\mathbf{B}(\mathbf{r},t), \tag{3.28}$$

  hence

$$\mathbf{D}(\mathbf{r},t) = \epsilon_0\epsilon\mathbf{E}(\mathbf{r},t) \tag{3.29}$$

$$\mathbf{H}(\mathbf{r},t) = \frac{1}{\mu_0}\frac{1}{\mu}\mathbf{B}(\mathbf{r},t), \tag{3.30}$$

  where ϵ and μ represent the permittivity and the permeability of the medium, respectively. This results in the wave equation for the electric field, expressed as

$$-\Delta\mathbf{E}(\mathbf{r},t) + \epsilon_0\mu_0\epsilon\mu\ddot{\mathbf{E}}(\mathbf{r},t) = 0. \tag{3.31}$$

- Comparing it with the wave equation in a vacuum,

$$-\Delta\mathbf{E}(\mathbf{r},t)+\frac{1}{c^2}\ddot{\mathbf{E}}(\mathbf{r},t)=0,\quad c=\frac{1}{\sqrt{\epsilon_0\mu_0}} \tag{3.32}$$

we can establish a relation between the expression $\epsilon_0\mu_0\epsilon\mu$ and the speed of light in the medium, such that

$$\epsilon_0\mu_0\epsilon\mu=\frac{1}{v^2}\Rightarrow v=\frac{1}{\sqrt{\epsilon_0\mu_0\epsilon\mu}}. \tag{3.33}$$

Therefore the ratio

$$\frac{c}{v}=\sqrt{\epsilon\mu}=n \tag{3.34}$$

is the index of refraction n of the medium.

- For most natural materials, the magnetic properties can be neglected, hence $\mu\approx 1$ and $n=\sqrt{\epsilon}$.

- In practice, assuming a constant response to the externally applied field across all frequencies is not meaningful, as it oversimplifies the material response by neglecting important details. Specifically, it presupposes that the medium maintains the same refractive index even at very high frequencies, such as X-rays or gamma rays. This assumption contradicts the observed phenomenon that materials become perfectly transparent at such extreme frequencies, where the refractive index n approaches 1.

3.2.1 Dispersion and Absorption

- Now, our aim is to establish a more realistic model for the linear response of a medium, which as we shall see later, related to the polarization of a dipole or an ensemble of dipoles.

- For simplicity, let's initially assume that the medium is non-magnetic, allowing the magnetic material equation in a vacuum, $\mathbf{H}=\frac{1}{\mu_0}\mathbf{B}$ remains valid. Indeed, in the majority of ordinary media, magnetic effects play a negligible role in the propagation of light.

- The linear relation between polarization and electric field can be expressed as

$$\mathbf{P}(\mathbf{r},t)=\epsilon_0\int \mathrm{d}^3r'\int_{-\infty}^{t}dt'\bar{\chi}^{(1)}(\mathbf{r},\mathbf{r}',t-t')\cdot\mathbf{E}(\mathbf{r}',t'), \tag{3.35}$$

where $\bar{\chi}^{(1)}(\mathbf{r},\mathbf{r}',t-t')$ represents the tensorial linear susceptibility.

- The structure of (3.35) reflects a temporal causal response of polarization to an external electric field. The justification for causality lies in the fact that only electric fields at times preceding t contribute to the polarization. Furthermore, the formulation also allows for the prospect that the material's response occurs at a different point than the excitation (spatial dispersion). Typically, this effect can be disregarded as a general rule. Moreover, in (3.35), the tensorial description is necessary if the material to be *birefringent*.

- Our focus here is on a simplified description in which the influences of anisotropy and spatial dispersion are overlooked. Henceforth, we will employ the linear susceptibility

$$\chi_{ij}^{(1)}(\mathbf{r},\mathbf{r}',t) = \chi^{(1)}(\mathbf{r},t)\delta_{ij}\delta(\mathbf{r}-\mathbf{r}') \tag{3.36}$$

  of an isotropic medium, where the polarization is

$$\begin{aligned}\mathbf{P}(\mathbf{r},t) &= \epsilon_0 \int_{-\infty}^{t} \mathrm{d}t' \chi^{(1)}(\mathbf{r},t-t')\mathbf{E}(\mathbf{r},t') \\ &= \epsilon_0 \int_{0}^{\infty} \mathrm{d}t' \chi^{(1)}(\mathbf{r},t')\mathbf{E}(\mathbf{r},t-t').\end{aligned} \tag{3.37}$$

- The equation (3.37) exhibits the mathematical structure of a *convolution*. Therefore, applying a Fourier transform to the equation results in the following expression

$$\mathbf{P}(\mathbf{r},\omega) = \epsilon_0 \chi^{(1)}(\mathbf{r},\omega)\mathbf{E}(\mathbf{r},\omega) \tag{3.38}$$

  in the frequency domain, accompanied by the relation

$$\chi^{(1)}(\mathbf{r},\omega) = \chi^{(1)^*}(\mathbf{r},-\omega^*), \tag{3.39}$$

  indicating that the frequency components of the susceptibility are indeed complex quantities.

3.2.2 Kramers-Kronig Relations

- The Fourier components $\chi^{(1)}(\mathbf{r},\omega)$ of the linear susceptibility fulfill an important integral relation that we seek to derive. To achieve this, we return to equation (3.37) and emphasize that this constitutes a one-sided Fourier transformation.

- To extend the integration across the entire time axis and simultaneously account for the causality of the dielectric response, we necessitate the condition that the susceptibility vanishes at negative times. This can be accomplished by defining

$$\chi^{(1)}(t) = \Theta(t)\chi^{(1)}(t), \tag{3.40}$$

where $\Theta(t)$ is the HEAVISIDE step function

$$\Theta(t) = \begin{cases} 1, & t \geq 0 \\ 0, & t < 0 \end{cases} \tag{3.41}$$

- Now, let us transform both sides of equation (3.40) using the relations

$$\chi^{(1)}(\omega) = \int_{-\infty}^{\infty} \mathrm{d}t\, \mathrm{e}^{\mathrm{i}\omega t}\chi^{(1)}(t), \quad \chi^{(1)}(t) = \frac{1}{2\pi}\int_{-\infty}^{\infty} \mathrm{d}\omega\, \mathrm{e}^{-\mathrm{i}\omega t}\chi^{(1)}(\omega) \tag{3.42}$$

to obtain

$$\begin{aligned}
\chi^{(1)}(\omega) &= \int_{-\infty}^{\infty} \mathrm{d}t\, \mathrm{e}^{\mathrm{i}\omega t}\Theta(t)\chi^{(1)}(t) \\
&= \int_{-\infty}^{\infty} \mathrm{d}t\, \mathrm{e}^{\mathrm{i}\omega t}\Theta(t)\frac{1}{2\pi}\int_{-\infty}^{\infty} \mathrm{d}\omega'\, \mathrm{e}^{-\mathrm{i}\omega' t}\chi^{(1)}(\omega') \\
&= \frac{1}{2\pi}\int_{-\infty}^{\infty} \mathrm{d}t \int_{-\infty}^{\infty} \mathrm{d}\omega'\, \mathrm{e}^{\mathrm{i}(\omega-\omega')t}\Theta(t)\chi^{(1)}(\omega') \\
&\overset{\text{Fubini}}{=} \frac{1}{2\pi}\int_{-\infty}^{\infty} \mathrm{d}\omega'\chi^{(1)}(\omega') \int_{-\infty}^{\infty} \mathrm{d}t\, \mathrm{e}^{\mathrm{i}(\omega-\omega')t}\Theta(t) \\
&= \frac{1}{2\pi}\int_{-\infty}^{\infty} \mathrm{d}\omega'\, \chi^{(1)}(\omega') \int_{0}^{\infty} \mathrm{d}t\, \mathrm{e}^{\mathrm{i}(\omega-\omega')t} \\
&= \frac{1}{2\pi\mathrm{i}}\int_{-\infty}^{\infty} \mathrm{d}\omega'\, \chi^{(1)}(\omega') \left[\mathrm{i}\pi\delta(\omega-\omega') - \mathrm{P}\frac{1}{\omega-\omega'}\right] \\
&= \frac{1}{2}\chi^{(1)}(\omega') - \frac{1}{2\pi\mathrm{i}}\mathrm{P}\int_{-\infty}^{\infty} \mathrm{d}\omega'\frac{\chi^{(1)}(\omega')}{\omega-\omega'}.
\end{aligned} \tag{3.43}$$

Here P is the principal value.

- For the proof

$$\int_{0}^{\infty} \mathrm{d}t\, \mathrm{e}^{\mathrm{i}(\omega-\omega')t} = \pi\delta(\omega-\omega') + \mathrm{i}\mathrm{P}\frac{1}{\omega-\omega'}, \tag{3.44}$$

consider

$$\begin{aligned}
\lim_{T\to\infty}\int_{0}^{T} \mathrm{d}t\, \mathrm{e}^{\mathrm{i}(\omega-\omega')t} &= \lim_{T\to\infty}\left[\frac{\mathrm{e}^{\mathrm{i}(\omega-\omega')T}-1}{\mathrm{i}(\omega-\omega')}\right] \\
&= \lim_{T\to\infty}\left[\frac{\sin(\omega-\omega')T}{\omega-\omega'} + \mathrm{i}\frac{1-\cos(\omega-\omega')T}{\omega-\omega'}\right] \\
&\longrightarrow \pi\delta(\omega-\omega') + \mathrm{i}\mathrm{P}\frac{1}{\omega-\omega'}.
\end{aligned}$$

- Ultimately, the expression for the linear susceptibility is given by

$$\chi^{(1)}(\omega) = -\frac{1}{\mathrm{i}\pi}\mathrm{P}\int_{-\infty}^{\infty} d\omega' \frac{\chi^{(1)}(\omega')}{\omega - \omega'}.$$

  Indeed, yielding a complex function that incorporates both real and imaginary components

$$\boxed{\mathrm{Re}\,\chi^{(1)}(\omega) = -\frac{1}{\pi}\mathrm{P}\int_{-\infty}^{+\infty} \mathrm{d}\omega' \frac{\mathrm{Im}\,\chi^{(1)}(\omega')}{\omega - \omega'}, \quad \mathrm{Im}\,\chi^{(1)}(\omega) = \frac{1}{\pi}\mathrm{P}\int_{-\infty}^{+\infty} \mathrm{d}\omega' \frac{\mathrm{Re}\,\chi^{(1)}(\omega')}{\omega - \omega'}.} \tag{3.45}$$

- The equations given in (3.45) are known as Kramers-Kronig *relations*. As evident from (3.45), it is clear that generating a purely real susceptibility in the frequency domain is impossible.

- The implications of the Kramers-Kronig relations become particularly evident when calculating the energy dissipated in the medium. To do this, it is crucial to recall that the source term for the electromagnetic field energy is $-\mathbf{j}\cdot\mathbf{E}$.

- Now we interpret the current density $\mathbf{j}$ as the current density induced by the electric field in the medium

$$\mathbf{j}_{\mathrm{ind}} = -\dot{\mathbf{P}}(\mathbf{r},t) + \nabla\times\mathbf{M}(\mathbf{r},t) \tag{3.46}$$

  and compute the total energy supplied to the electromagnetic field as

$$\begin{aligned} W &= -\int \mathrm{d}t \int \mathrm{d}^3 r\, \mathbf{j}_{\mathrm{ind}}(\mathbf{r},t)\cdot\mathbf{E}(\mathbf{r},t) \\ &= -\int \mathrm{d}\omega \int \frac{\mathrm{d}^3 k}{(2\pi)^3}\mathrm{Re}\left[\mathbf{j}_{\mathrm{ind}}(\mathbf{k},\omega)\cdot\mathbf{E}^*(\mathbf{k},\omega)\right] \\ &= -\int \mathrm{d}\omega \int \frac{\mathrm{d}^3 k}{(2\pi)^3}\frac{1}{2}\left[\mathbf{j}_{\mathrm{ind}}(\mathbf{k},\omega)\cdot\mathbf{E}^*(\mathbf{k},\omega) + \mathbf{j}^*_{\mathrm{ind}}(\mathbf{k},\omega)\cdot\mathbf{E}(\mathbf{k},\omega)\right] \\ &= -\int \mathrm{d}\omega \int \frac{\mathrm{d}^3 k}{(2\pi)^3}\omega\mathrm{Im}\,\chi^{(1)}(\omega)\left|\mathbf{E}(\mathbf{k},\omega)\right|^2. \end{aligned} \tag{3.47}$$

  Here, we substituted the Fourier transform of the induced current density via the polarization, and subsequently employed the relation (3.38).

- The equation (3.47) ensures that the total energy of the electromagnetic field decreases with respect to the imaginary part of the susceptibility. Consequently, the imaginary part characterizes the dissipative aspect of the medium, while the real part signifies its dispersive character.

- KRAMERS-KRONIG relations (3.45) reveal a direct connection between both parts. Any medium responding to an external electromagnetic field must inevitably absorb radiation. However, one can conceive of materials in which absorption in specific frequency intervals is negligibly small (e.g., glass). Still, this does not hold true outside these regions (e.g., ultraviolet frequencies), as glass is not particularly transparent in those cases and must absorb electromagnetic radiation.

3.2.3 Dipole Model for Linear Polarization

- In the dipole model, the polarization of a material is influenced by the polarizability of individual atoms or molecules within the material, along with the intensity of the applied electric field. While the dipole model offers a simplified representation of real materials, it serves as a valuable framework for comprehending the behavior of linear materials under the influence of electric fields.

- This model is extensively employed for investigating matter polarization due to its clarity and simplicity. We will utilize this model to derive the susceptibility formula or response function for the external electric field acting on matter.

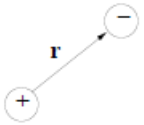

Fig. 3.3: Electric dipole model

- To construct a straightforward model encompassing the fundamental characteristics of linear susceptibility, we consider a dipole consisting of two elementary charges $\pm e$ separated with distance $\mathbf{r}$. NEWTON's equations of motion for point masses with charge q_i and position $\mathbf{r}_i$ have the form

$$m_i \ddot{\mathbf{r}}_i = q_i \left[\mathbf{E}(\mathbf{r}_i, t) + \dot{\mathbf{r}}_i \times \mathbf{B}(\mathbf{r}_i, t)\right] + \mathbf{F}_{\text{diss}} + \sum_j \mathbf{F}_{ij}, \tag{3.48}$$

  where the individual forces include the LORENTZ force, potential dissipative (friction) forces, and conservative binding forces between the charges.

- Let $q_i = \pm e$ and the electric field is polarized along the x direction (dipole direction), i.e., $\mathbf{E}(t) = E(t)\mathbf{e}_x$. The equation of motion reads

$$m\ddot{x} = F_{\text{driv}} + F_{\text{diss}} + F_{\text{cons}}. \tag{3.49}$$

Plugging $F_{\text{driv}} = eE(t), F_{\text{diss}} = -m\gamma\dot{x}, \text{and} \quad F_{\text{cons}} = -m\omega_0^2 x$ into (3.49) yields the equation of driven damped harmonic oscillator

$$m\ddot{x} + m\gamma\dot{x} + m\omega_0^2 x = F_{\text{driv}}, \tag{3.50}$$

where γ is the coefficient of friction and ω_0 is the natural frequency arising from the conservative binding force.

- Let us consider a driving electric field

$$E(t) = E_0 \mathrm{e}^{-\mathrm{i}\omega t} \tag{3.51}$$

and with the ansatz

$$x(t) = x_0 \mathrm{e}^{-\mathrm{i}\omega t} \tag{3.52}$$

we get the solution

$$(-\omega^2 - \mathrm{i}\gamma\omega + \omega_0^2)x(t) = \frac{e}{m}E_0 \mathrm{e}^{-\mathrm{i}\omega t}, \tag{3.53}$$

hence

$$x(t) = \frac{\frac{e}{m}E(t)}{\omega_0^2 - \omega^2 - \mathrm{i}\gamma\omega}. \tag{3.54}$$

- Moreover, the induced dipole moment is

$$d(t) = ex(t) = \alpha(\omega)E(t) \tag{3.55}$$

where $\alpha(\omega)$ is the polarizability, representing how effectively this dipole interacts with the electromagnetic field. From Eq.(3.54) we obtain that

$$\alpha(\omega) = \frac{e^2/m}{\omega_0^2 - \omega^2 - \mathrm{i}\gamma\omega}. \tag{3.56}$$

Defining the number density n, the linear susceptibility reads

$$\begin{aligned} \chi^{(1)}(\omega) &= n\alpha(\omega) \\ &= \frac{ne^2/m}{\omega_0^2 - \omega^2 - \mathrm{i}\gamma\omega} \end{aligned} \tag{3.57}$$

which is a complex function. Dividing the linear susceptibility into real and imaginary parts gives

$$\mathrm{Re}\,\chi^{(1)}(\omega) = \frac{ne^2}{m}\frac{(\omega_0^2 - \omega^2)}{(\omega_0^2 - \omega^2)^2 + \gamma^2\omega^2} \tag{3.58}$$

$$\mathrm{Im}\,\chi^{(1)}(\omega) = \frac{ne^2}{m}\frac{\gamma\omega}{(\omega_0^2 - \omega^2)^2 + \omega^2\gamma^2} \geq 0. \tag{3.59}$$

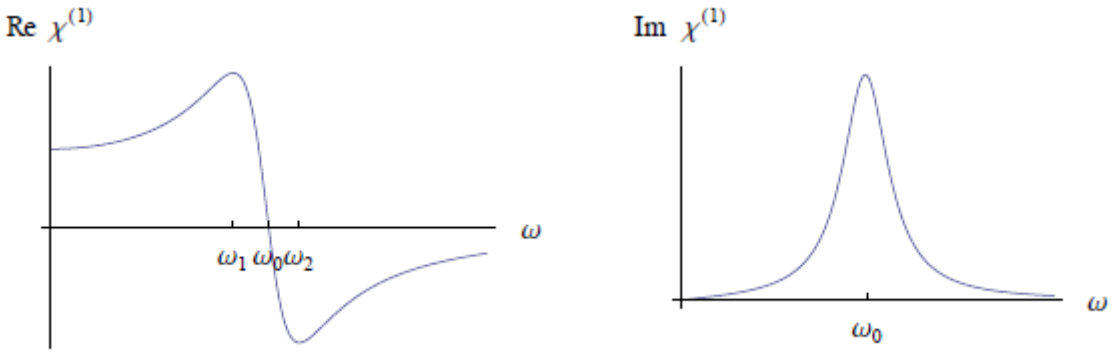

Fig. 3.4: Real and imaginary parts of linear susceptibility.

- Both functions are depicted schematically in Fig. 3.4. In the intervals of $\omega < \omega_1$ and $\omega > \omega_2$, light undergoes increased refraction with rising frequency (normal dispersion). Conversely, in the interval $\omega_1 < \omega < \omega_2$ anomalous dispersion occurs. The imaginary part reaches its maximum at the resonance frequency ω_0. Additionally, it is evident that absorption takes place across the entire frequency range. One can explicitly verify that the susceptibility obtained in this manner indeed satisfies the Kramers–Kronig relations.

- In general, a medium comprises numerous oscillators with diverse resonance frequencies and oscillator strengths. Even within an atom, there is a variety of dipole transitions, and their transition matrix elements are derived quantum mechanically. Thus, we can model a more general medium using a susceptibility

$$\chi^{(1)}(\omega) = \frac{ne^2}{m} \sum_k \frac{f_k}{\omega^2 - \omega_k^2 - \mathrm{i}\gamma_k \omega}, \tag{3.60}$$

  where the sum is taken over all possible dipole transitions with oscillator strengths f_k, resonance frequencies ω_k and damping γ_k.

- Equation (3.60) represents the Drude–Lorentz model for dielectric media, which is suitable for describing propagation of light at low intensities or energy densities. Additionally, the absorption spectra can be fitted to the imaginary part of equation (3.60) where peaks occur at frequencies ω_k. The maxima are determined by oscillator strengths f_k and the widths are determined by the damping parameters γ_k.

3.2.4 Dispersion and Optical Pulses

- Dispersion implies that the refractive index depends on frequency through the electric susceptibility. This has a direct influence on the propagation of electromagnetic waves through dielectric media. The refractive index is now frequency-dependent, as indicated by the following formula:

$$n(\omega) = \sqrt{1 + \chi^{(1)}(\omega)} \tag{3.61}$$

- Assuming a linearly polarized light propagating in the z-direction, it can be described by an electric field wave

$$E(z,t) = \frac{1}{2}\left[E_0(z,t)\mathrm{e}^{-\mathrm{i}\omega_0 t} + \text{c.c.}\right] \tag{3.62}$$

- The envelope $E_0(z,t)$ at $z = 0$ position can be given by the Gaussian profile

$$E_0(0,t) = A\mathrm{e}^{-t^2/(2t_0^2)}. \tag{3.63}$$

- Fourier transforming $E(0,t)$ gives

$$\begin{aligned} E_0(0,\omega) &= \int_{-\infty}^{+\infty} \mathrm{d}t\, \mathrm{e}^{\mathrm{i}(\omega-\omega_0)t} E_0(0,t) \\ &= \sqrt{2\pi} A t_0 \mathrm{e}^{-(\omega-\omega_0)t_0^2/2} \end{aligned} \tag{3.64}$$

  which is also a Gaussian function. This field at location z is now determined via $E_0(z,\omega) = E_0(0,\omega)\mathrm{e}^{\mathrm{i}k(\omega)z}$. Let us expand the wave number $k(\omega)$ in a Taylor series around the carrier frequency ω_0

$$k(\omega) \simeq k(\omega_0) + \beta_1(\omega-\omega_0) + \frac{1}{2}\beta_2(\omega-\omega_0)^2 + \cdots. \tag{3.65}$$

  Here

$$\beta_1 = \left.\frac{\partial k}{\partial \omega}\right|_{\omega=\omega_0} = \frac{1}{v_\mathrm{g}} = \frac{\tau_\mathrm{g}}{z}, \quad \beta_2 = \left.\frac{\partial^2 k}{\partial \omega^2}\right|_{\omega=\omega_0} = \frac{1}{z}\frac{\partial \tau_\mathrm{g}}{\partial \omega} = \frac{1}{z}\frac{\partial \tau_\mathrm{g}}{\partial \lambda}\frac{\partial \lambda}{\partial \omega} \tag{3.66}$$

  where v_g is the group velocity and τ_g being the group time delay.

- In a dispersive medium, the wave number depends on the refractive index through the relation $k = \frac{2\pi n}{\lambda}$, therefore

$$\frac{\partial k}{\partial \lambda} = \frac{2\pi}{\lambda^2}\left(\lambda\frac{\partial n}{\partial \lambda} - n\right) \tag{3.67}$$

$$\frac{\partial \lambda}{\partial \omega} = \frac{\partial}{\partial \omega}\left(\frac{2\pi c}{\omega}\right) = -\frac{2\pi c}{\omega^2}. \tag{3.68}$$

This enables us to write τ_g as

$$\tau_g = \frac{z}{c}\left(n - \lambda\frac{\partial n}{\partial \lambda}\right) \tag{3.69}$$

$$\frac{\partial \tau_g}{\partial \lambda} = -\frac{z}{c}\lambda\frac{\partial^2 n}{\partial \lambda^2} = D_\lambda z \tag{3.70}$$

where D_λ is the dispersion parameter. Through this analysis, we can derive the formula for β_2 as follows:

$$\beta_2 = -\frac{D_\lambda \lambda^2}{2\pi c}. \tag{3.71}$$

- We thus find that the TAYLOR expansion of the wave number $k(\omega)$ around $\omega = \omega_0$ up to second order can be expressed as

$$k(\omega) = k(\omega_0) + \frac{\tau_g}{z}(\omega - \omega_0) - \frac{D_\lambda \lambda^2}{4\pi c}(\omega - \omega_0)^2 \tag{3.72}$$

Transforming back into the time domain we obtain

$$E_0(z,t)\mathrm{e}^{-\mathrm{i}\omega_0 t} = \underbrace{\frac{A}{\sqrt{1+\mathrm{i}\xi}}}_{(a)}\underbrace{\mathrm{e}^{-\mathrm{i}\omega_0(t-z/v_p)}}_{(b)}\underbrace{\exp\left(-\frac{(t-\tau_g)^2}{2t_0^2(1+\xi^2)}\right)}_{(c)}\underbrace{\exp\left(-\mathrm{i}\frac{\xi(t-\tau_g)^2}{2t_0^2(1+\xi^2)}\right)}_{(d)}, \tag{3.73}$$

where $v_p = \omega_0/k(\omega_0)$ is the phase velocity, and $\xi = \beta_2 z/t_0^2$ is the normalized propagation length.

- Equation (3.73) reveals the following properties of the pulse propagation:
  - (b): the carrier wave propagates with phase velocity v_p.
  - (c): the envelope moves with group velocity v_g.
  - (c): the pulse is broadened by a factor $\sqrt{1+\xi^2}$.
  - (a): the peak intensity of the pulse reduced by the factor $1+\xi^2$.
  - (d): the carrier frequency changes inside the pulse (chirp).

- From Equation (3.64), we infer that the spectral bandwidth of the pulse

$$\Delta\nu = \frac{1}{\Delta t_0}\frac{2\ln 2}{\pi}, \quad \Delta t_0 = t_0\sqrt{4\ln 2} \tag{3.74}$$

where Δt_0 is the full width at half maximum (FWHM) of the original GAUSSIAN pulse. After propagation through the medium, according to (3.73), the full width at half maximum (FWHM) of the pulse pulse has broadened to

$$\Delta t = \Delta t_0\sqrt{1+\xi^2} \tag{3.75}$$

The time-bandwidth product is thus given by

$$\Delta\nu\Delta t = 0.441\sqrt{1+\xi^2} \tag{3.76}$$

which is a special case of the time-bandwidth theorem

$$\Delta\nu\Delta t \geq K, \tag{3.77}$$

where K is a number on the order of unity and depends on the pulse shape.

- When a pulse reaches the minimum of the time-bandwidth product (here for $\xi = 0$), it is referred to as a bandwidth-limited pulse or transform-limited pulse.

- The frequency chirp is obtained from the last term in equation (3.73), which we write as $e^{i\psi(t)}$ and remember that $d\psi/dt$ represents the carrier frequency shift. The chirp, or the frequency shift, is

$$\frac{d\omega}{dt} = \frac{d^2\psi(t)}{dt^2} = \frac{\xi}{t_0^2(1+\xi^2)} \overset{|\xi|\gg 1}{\approx} \frac{1}{t_0^2\xi} = \frac{1}{\beta_2 z} \tag{3.78}$$

  - If β_2 is positive, that is, the group time delay increases with frequency, then the chirp is also positive (down-chirp). As a result, lower frequencies arrive before higher (local) frequencies.

  - If β_2 is negative, the group time delay decreases with frequency, hence the chirp is also negative (up-chirp). Therefore, higher (local) frequencies arrive before lower frequencies.

  - In both cases the temporal width of the pulse increases and the peak intensity is lowered.

- This behavior is shown in Fig.(3.5), which shows the electric field of an originally Gaussian pulse before and after propagation through a linear dispersive medium with positive dispersion.

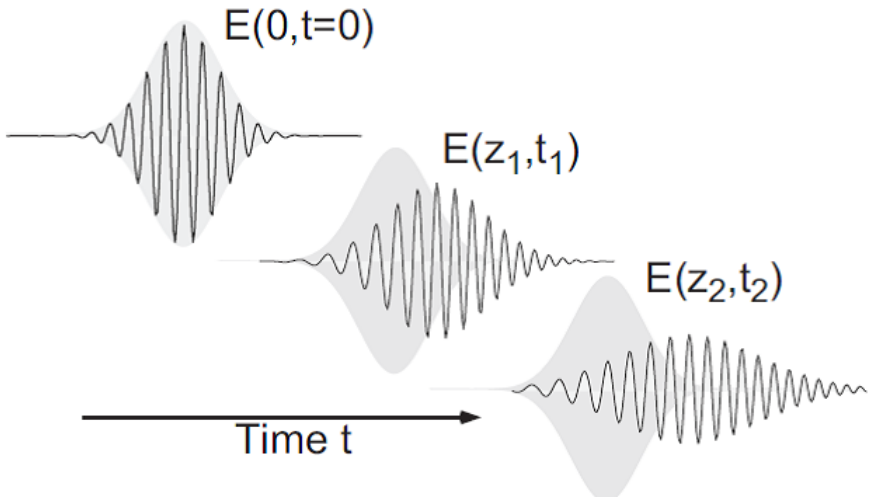

Fig. 3.5: A GAUSSIAN pulse before and after propagation through a linear medium with positive dispersion.

3.3 Nonlinear Optics

- In general, the optical response can often be described by expressing the polarization as a TAYLOR expansion in the field strength as

$$P_i = \epsilon_0 \left[\chi_{ij}^{(1)} E_j + \chi_{ijk}^{(2)} E_j E_k + \chi_{ijkl}^{(3)} E_j E_k E_l + \cdots \right]. \tag{3.79}$$

  Here $\chi_{ijk}^{(2)}$ and $\chi_{ijkl}^{(3)}$ are second and third order nonlinear susceptibilities, where $\chi^{(3)}$ is tensor of rank 4 that has 81 components and $\chi^{(2)}$ is tensor of rank 3 which has 27 components. The number of independent components depends strongly on the symmetry of crystals, e.g, for centrosymmetric materials $\chi_{ijk}^{(2)} = 0$.

- The expansion (3.79) also shows that nonlinear effects in polarization only become visible with larger field strengths.

- To see how such nonlinearities can occur, let us go back to our dipole model of a dielectric medium, in which we write the equation of motion of the dipole in a harmonic approximation as

$$m(\ddot{x} + \gamma\dot{x} + \omega_0^2 x) = eE. \tag{3.80}$$

  Here, we assumed that the conservative binding force is linear in the displacement (HOOKE's Law). Accordingly, the corresponding potential must be quadratic

(harmonic). This is certainly only accurate in a first approximation. Consider, for example, the potential of an electron as it moves around the atomic nucleus. The effective potential consists of the COULOMB potential and the centrifugal barrier (KEPLER problem in classical mechanics, see Fig. (3.6))

$$V_{\text{eff}}(r) = -\frac{e^2}{4\pi\epsilon_0 r} + \frac{L^2}{2mr^2}$$

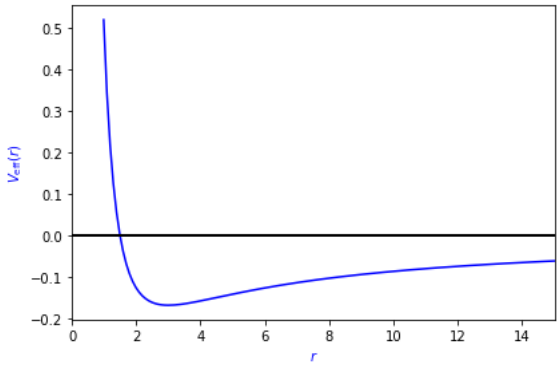

Fig. 3.6: The Effective potential of an electron moving in the vicinity of atomic nucleus.

- The potential can only be approximated by a parabola for very small displacements from the equilibrium position x_0. Now let us write TAYLOR expansion close to x_0

$$V(x) = V(x_0) + \frac{1}{2!}V''(x_0)(x-x_0)^2 + \frac{1}{3!}V'''(x_0)(x-x_0)^3 + \cdots \tag{3.81}$$

- To obtain the first nonlinear order, substitute the third term in Eq. (3.81) and solve for the resulting expression

$$m(\ddot{x} + \gamma\dot{x} + \omega_0^2 x) = eE - \frac{1}{2}V'''x^2. \tag{3.82}$$

- This is a nonlinear differential equation which can be solved according to this ansatz

$$x(t) = x_1(t) + x_2(t) + \cdots = \tilde{x}_1 \mathrm{e}^{-\mathrm{i}\omega t} + \tilde{x}_2 \mathrm{e}^{-2\mathrm{i}\omega t} + \cdots \tag{3.83}$$

and the electric field as a monochromatic wave $E(t) = E_0 \mathrm{e}^{-\mathrm{i}\omega t}$.

- Substituting in Eq.(3.82) yields two different equations for FOURIER coefficients $\mathrm{e}^{-\mathrm{i}\omega t}$ and $\mathrm{e}^{-2\mathrm{i}\omega t}$, respectively,

$$m(\ddot{x}_1 + \gamma\dot{x}_1 + \omega_0^2 x_1) = eE_0 \mathrm{e}^{-\mathrm{i}\omega t} \tag{3.84}$$

$$m(\ddot{x}_2 + \gamma\dot{x}_2 + \omega_0^2 x_2) = -\frac{1}{2}V'''x_1^2. \tag{3.85}$$

- The solution x_1 of Eq. (3.84) can be obtained in similar way to the linear theory

$$x_1(t) = \frac{\frac{e}{m}E_0}{\omega_0^2 - \omega^2 - \mathrm{i}\gamma\omega}\mathrm{e}^{-\mathrm{i}\omega t}. \tag{3.86}$$

- Substituting this solution into Equation 3.85, we find that

$$m(\ddot{x}_2 + \gamma\dot{x}_2 + \omega_0^2 x_2) = -\frac{V'''}{2m}\frac{\left(\frac{e}{m}E_0\right)^2}{(\omega_0^2 - \omega^2 - \mathrm{i}\gamma\omega)^2}\mathrm{e}^{-2\mathrm{i}\omega t}. \tag{3.87}$$

  This is in agreement with the hypothesis that $x_2(t) \propto \mathrm{e}^{-2\mathrm{i}\omega t}$. Finally, the solution to nonlinear differential equation 3.82 reads

$$x_2(t) = -\frac{V'''}{2m}\left(\frac{e}{m}\right)^2 E_0^2 \frac{1}{\left[\omega_0^2 - \omega^2 - \mathrm{i}\gamma\omega\right]^2\left[\omega_0^2 - (2\omega)^2 - 2\mathrm{i}\gamma\omega\right]}\mathrm{e}^{-2\mathrm{i}\omega t}. \tag{3.88}$$

- In addition to the already known resonance denominator (which appears squared here), a new resonance denominator with the resonance frequency $\propto 2\omega$ appears here. The frequency dependence of this part of the solution is $\mathrm{e}^{-2\mathrm{i}\omega t}$, although it was only irradiated with an electric field of frequency $\mathrm{e}^{-\mathrm{i}\omega t}$. As expected, the amplitude of the electric field appears square as E_0^2. Therefore, we can write the electric dipole moment in the following form

$$d(t) = ex_1(t) + ex_2(t) = \alpha^{(1)}(\omega)E(t) + \alpha^{(2)}(\omega)E^2(t). \tag{3.89}$$

  Here, $\alpha^{(1)}(\omega)$ and $\alpha^{(2)}(\omega)$ represent the linear and nonlinear polarizabilities, respectively,

$$\alpha^{(1)}(\omega) = \frac{e^2}{m}\frac{1}{\omega_0^2 - \omega^2 - \mathrm{i}\gamma\omega} \tag{3.90}$$

$$\alpha^{(2)}(\omega) = -\frac{V'''e^3}{2m^3}\frac{1}{\left[\omega_0^2 - \omega^2 - \mathrm{i}\gamma\omega\right]^2\left[\omega_0^2 - (2\omega)^2 - 2\mathrm{i}\gamma\omega\right]}. \tag{3.91}$$

- The wave equation in a dielectric medium can be written as

$$\begin{aligned}\nabla^2\mathbf{E}(\mathbf{r},t) - \frac{1}{c^2}\ddot{\mathbf{E}}(\mathbf{r},t) &= \mu_0\ddot{\mathbf{P}}(\mathbf{r},t) \\ &= \mu_0\ddot{\mathbf{P}}_{\mathrm{L}}(\mathbf{r},t) + \mu_0\ddot{\mathbf{P}}_{\mathrm{NL}}(\mathbf{r},t),\end{aligned} \tag{3.92}$$

  where $\ddot{\mathbf{P}}_{\mathrm{L}}$ and $\ddot{\mathbf{P}}_{\mathrm{NL}}$ are the linear and nonlinear driving fields of polarization.

- In frequency space, the equation (3.92) transforms to the Helmholtz equation

$$\nabla^2\mathbf{E}(\mathbf{r},\omega) + \frac{\omega^2}{c^2}\mathbf{E}(\mathbf{r},\omega) = -\mu_0\omega^2\mathbf{P}_{\mathrm{L}}(\mathbf{r},\omega) - \mu_0\omega^2\mathbf{P}_{\mathrm{NL}}(\mathbf{r},\omega). \tag{3.93}$$

- Introducing the linear polarization $\mathbf{P}_{\mathrm{L}}(\mathbf{r},\omega) = \epsilon_0\chi^{(1)}(\omega)\mathbf{E}(\mathbf{r},\omega)$, the equation (3.93) becomes

$$\boxed{\nabla^2\mathbf{E}(\mathbf{r},\omega) + \frac{\omega^2}{c^2}\epsilon(\omega)\mathbf{E}(\mathbf{r},\omega) = -\mu_0\omega^2\mathbf{P}_{\mathrm{NL}}(\mathbf{r},\omega),} \tag{3.94}$$

  where $\epsilon(\omega) = 1 + \chi^{(1)}(\omega)$ is the dielectric permittivity.

- The wave equation (3.94) governs light propagation in arbitrary media.

- The right hand side of the equation (3.94) serves as a source term of the electric field applied to the linear medium. Until now it is unclear how the frequency components of nonlinear polarization look like. Later on we will concentrate on second and third order of the optical responses.

3.3.1 Second-order Nonlinearities

- We have seen that every linear response can be written as a time convolution integral over the susceptibility, which reflects the causality principle (3.35). Any nonlinear response can be written in the same way. If we limit ourselves to homogeneous media, we can omit the location arguments for the sake of simplicity

$$\mathbf{P}^{(2)}_{\mathrm{NL}}(t) = \epsilon_0\int_0^\infty \mathrm{d}\tau_1\int_0^\infty \mathrm{d}\tau_2\bar{\bar{\chi}}^{(2)}(\tau_1,\tau_2) : \mathbf{E}(t-\tau_1)\mathbf{E}(t-\tau_2) \tag{3.95}$$

  or, in index notation,

$$P^{(2)}_{\mathrm{NL},i}(t) = \epsilon_0\int_0^\infty \mathrm{d}\tau_1\int_0^\infty \mathrm{d}\tau_2\chi^{(2)}_{ijk}(\tau_1,\tau_2)E_j(t-\tau_1)E_k(t-\tau_2) \tag{3.96}$$

- The Fourier transform reduces the number of integrals by one, but a convolution remains,

$$P^{(2)}_{\mathrm{NL},i}(\omega) = \epsilon_0\int_{-\infty}^\infty \mathrm{d}\omega'\chi^{(2)}_{ijk}(\omega;\omega',\omega-\omega')E_j(\omega')E_k(\omega-\omega') \tag{3.97}$$

- We now suppose that the electric fields are monochromatic fields with discrete frequencies. This approximation is permissible when it comes to stationary fields in narrow frequency bands. Let's assume the electric field can be as

$$\mathbf{E}(t) = \tilde{\mathbf{E}}(\omega_1)\mathrm{e}^{-\mathrm{i}\omega_1 t} + \tilde{\mathbf{E}}(\omega_2)\mathrm{e}^{-\mathrm{i}\omega_2 t} + \tilde{\mathbf{E}}^*(\omega_1)\mathrm{e}^{\mathrm{i}\omega_1 t} + \tilde{\mathbf{E}}^*(\omega_2)\mathrm{e}^{\mathrm{i}\omega_2 t} \tag{3.98}$$

- In the frequency space we get

$$\mathbf{E}(\omega) = \tilde{\mathbf{E}}(\omega_1)\delta(\omega-\omega_1) + \tilde{\mathbf{E}}(\omega_2)\delta(\omega-\omega_2) + \tilde{\mathbf{E}}^*(\omega_1)\delta(\omega+\omega_1) + \tilde{\mathbf{E}}^*(\omega_2)\delta(\omega+\omega_2). \tag{3.99}$$

- Multiplying the two fields $E_j(\omega')E_k(\omega-\omega')$ and integrating over ω' then yields the nonlinear polarization (3.97).

3.3.1.1 Frequency Doubling

- As an example, let's look at the term

$$E_j(\omega')E_k(\omega-\omega') = \tilde{E}_j(\omega_1)\tilde{E}_k(\omega_1)\delta(\omega'-\omega_1)\delta(\omega-\omega'-\omega_1) + 15\,\text{terms}. \tag{3.100}$$

  The product of the delta functions is equivalent to

$$\delta(\omega'-\omega_1)\delta(\omega-\omega'-\omega_1) = \delta(\omega'-\omega_1)\delta(\omega-2\omega_1), \tag{3.101}$$

  thus

$$E_j(\omega')E_k(\omega-\omega') = \tilde{E}_j(\omega_1)\tilde{E}_k(\omega_1)\delta(\omega'-\omega_1)\delta(\omega-2\omega_1) \tag{3.102}$$

- Substituting this result into $P^{(2)}_{NL,i}(\omega)$ leads to

$$P^{(2)}_{\mathrm{NL},i}(\omega) = \epsilon_0\chi^{(2)}_{ijk}(\omega;\omega_1,\omega_1)\tilde{E}_j(\omega_1)\tilde{E}_k(\omega_1)\delta(\omega-2\omega_1) + \cdots \tag{3.103}$$

  or

$$P^{(2)}_{\mathrm{NL},i}(2\omega_1) = \epsilon_0\chi^{(2)}_{ijk}(2\omega_1;\omega_1,\omega_1)\tilde{E}_j(\omega_1)\tilde{E}_k(\omega_1)\delta(\omega-2\omega_1) + \cdots \tag{3.104}$$

- The nonlinear polarization here only has a component at twice the frequency of one of the monochromatic field modes, $\omega = 2\omega_1$. This contribution is linked to frequency doubling (second-harmonic generation, SHG). The term $P^{(2)}_{\mathrm{NL},i}(2\omega_1)$ drives a wave of frequency $2\omega_1$ in the wave equation (3.92). Analogously, there is of course another term $P^{(2)}_{\mathrm{NL},i}(2\omega_2)$ that drives a wave at frequency $2\omega_2$.

3.3.1.2 Optical Rectification

- Further processes can be obtained by multiplying out the nonlinear polarization. This is how you find, for example

$$E_j(\omega')E_k(\omega-\omega') = \tilde{E}_j(\omega_1)\tilde{E}^*_k(\omega_1)\delta(\omega'-\omega_1)\delta(\omega-\omega'+\omega_1) \tag{3.105}$$

- The product of the delta functions yields

$$\delta(\omega' - \omega_1)\delta(\omega - \omega' + \omega_1) = \delta(\omega' - \omega_1)\delta(\omega), \tag{3.106}$$

hence

$$\tilde{E}_j(\omega_1)\tilde{E}_k(\omega - \omega_1) = \tilde{E}_j(\omega_1)\tilde{E}_k^*(\omega_1)\delta(\omega' - \omega_1)\delta(\omega) \tag{3.107}$$

- Substituting this result in $P_{NL}^{(2)}(\omega)$ gives

$$P_{\mathrm{NL},i}^{(2)}(\omega) = \epsilon_0 \chi_{ijk}^{(2)}(0;\omega_1,-\omega_1)\tilde{E}_j(\omega_1)\tilde{E}_k^*(\omega_1)\delta(\omega) + \cdots, \tag{3.108}$$

i.e. a contribution that is frequency independent.

- This process is called optical rectification. It causes a DC voltage to be generated during the propagation of intense radiation through a non-linear medium.

- Conversely, applying a static electric field to a nonlinear crystal produces a polarization that oscillates with frequency ω. From the equation (3.108), we note that this process does not depend on frequency, which means that a nonlinear medium can produce a static electric field.

- Therefore, consider an electric field

$$\mathbf{E}(t) = \mathbf{E}_0 + \tilde{\mathbf{E}}(\omega_1)\mathrm{e}^{-\mathrm{i}\omega_1 t} + \tilde{\mathbf{E}}^*(\omega_1)\mathrm{e}^{\mathrm{i}\omega_1 t}$$

. The nonlinear polarization drives a wave of frequency ω_1 whose strength depends on the constant field E_0, i.e., DC voltage. This is the *Pockels effect*, which causes the refractive index to depend on the amplitude E_0. For the sake of simplicity assume that the direction of propagation is in one dimension, then the refractive index becomes

$$n = \sqrt{1 + \chi^{(1)} + 2\chi^{(2)}E_0}. \tag{3.109}$$

- Pockels cell, e.g., electro-optic modulator works on this principle, i.e., changing the refractive index as a function of the applied electric field.

3.3.1.3 Sum and Difference Frequency Generation

- Sum frequency generation (SFG) or up conversion is a type of nonlinear optical process in which two input laser beams of different frequencies interact with a material or interface, and generate a new beam at the sum of their frequencies, approximately very similar with second harmonic generation, but in sum

frequency generation the two input waves different frequencies. The remaining terms in (3.100) that contain contributions from the two monochromatic fields

$$E_j(\omega')E_k(\omega-\omega') = \tilde{E}_j(\omega_1)\tilde{E}_k(\omega_2)\delta(\omega'-\omega_1)\delta(\omega-\omega'-\omega_2), \tag{3.110}$$

hence

$$P^{(2)}_{\mathrm{NL},i}(\omega) = \epsilon_0\chi^{(2)}_{ijk}(\omega_1+\omega_2;\omega_1,\omega_2)\tilde{E}_j(\omega_1)\tilde{E}_k(\omega_2)\delta(\omega-\omega_1-\omega_2) \tag{3.111}$$

- The difference frequency generation (DFG) or down conversion is another type of nonlinear optical process that is similar to sum frequency generation (SFG), but instead of generating a new beam at the sum of frequencies, it generates a new beam at the difference of frequencies.

$$E_j(\omega')E_k(\omega-\omega') = \tilde{E}_j(\omega_1)\tilde{E}^*_k(\omega_2)\delta(\omega'-\omega_1)\delta(\omega-\omega'+\omega_2), \tag{3.112}$$

thus

$$P^{(2)}_{\mathrm{NL},i}(\omega) = \epsilon_0\chi^{(2)}_{ijk}(\omega_1-\omega_2;\omega_1,\omega_2)\tilde{E}_j(\omega_1)\tilde{E}^*_k(\omega_2)\delta(\omega-\omega_1+\omega_2). \tag{3.113}$$

- The frequencies are either converted up or down (frequency up-conversion and frequency down-conversion).
- Since the effect of two monochromatic waves with frequencies ω_1 and ω_2 results the generation of new waves with the frequencies

$$\omega_+ = \omega_1 \pm \omega_2. \tag{3.114}$$

- Moreover, it should be noted here that all nonlinear optical processes happen if energies and momenta are conserved.
- Let's now take a closer look at the up-conversion process. The relation

$$\omega_1+\omega_2 = \omega_3 = \omega_+ \tag{3.115}$$

reflects the energy conservation of the process.

- For propagating waves, the spatial factors must also be taken into account. The combination of two waves entering the medium

$$\mathrm{e}^{\mathrm{i}(\mathbf{k}_1\cdot\mathbf{r}-\omega_1 t)}\mathrm{e}^{\mathrm{i}(\mathbf{k}_2\cdot\mathbf{r}-\omega_2 t)} = \mathrm{e}^{\mathrm{i}(\mathbf{k}_+\cdot\mathbf{r}-\omega_+ t)} \tag{3.116}$$

implies the momentum conservation

$$\boxed{\mathbf{k}_1+\mathbf{k}_2 = \mathbf{k}_3 = \mathbf{k}_+} \tag{3.117}$$

or, *phase matching condition*.

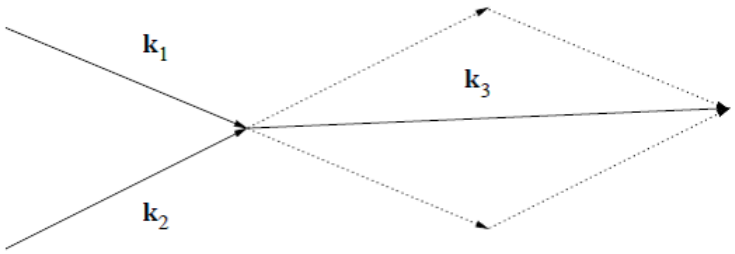

Fig. 3.7: Phase matching in three-wave mixing.

- This phase matching means that special processes can be selected out of possible nonlinear processes. This is particularly important when dispersion in the medium has to be taken into account because the refractive index is frequency dependent. To fulfill phase matching condition, birefringence crystals are used.
- Now let's imagine light with frequencies ω_1 and ω_2 are mixed into a wave with frequency $\omega_3 = \omega_1 + \omega_2$ using phase matching. This new wave with ω_3 can now generate a wave with the difference frequency $\omega_2 = \omega_3 - \omega_1$ in addition to the existing wave frequency ω_1, since this process is also phase-matched. The radiation generated at ω_3 can also produce a difference frequency ω_1 with ω_2.
- All three waves are mutually coupled to one another within the framework of a three-wave mixing. Such a process is also known as *parametric* interaction. These parametric processes are involved in

  1. Optical frequency conversion (OFC): Processes such as sum and difference frequency generation ($\omega_3 = \omega_1 + \omega_2$ or $\omega_2 = \omega_3 - \omega_1$) and frequency doubling ($\omega_3 = 2\omega_2$).
  2. Optical parametric amplification (OPA): A process in which a high-energy pump laser beam at frequency ω_3 amplifies the signal laser beam at frequency $\omega_1 = \omega_3 - \omega_2$ via difference frequency generation process, where ω_2 is the frequency of unwanted laser beam or *idler*.
  3. Optical parametric oscillator (OPO): OPA with feedback (resonator) to produce ultrashort laser pulses.
  4. Spontaneous Parametric Down-Conversion (SPDC): a quantum mechanical process where a single photon (pump) split into two photons of lower frequency (longer wavelength), known as signal and idler photons. The polarization and direction of the generated photons are correlated and entangled.

3.3.2 Third-order Nonlinear Processes

- Second-order nonlinearities are not particularly common because they are often excluded by symmetry. In our model for the potential, for example, this means that the potential is anharmonic and therefore the correction up to fourth order reads

$$V(x) = V(x_0) + \frac{1}{2!}V''(x_0)(x-x_0)^2 + \frac{1}{4!}V''''(x_0)(x-x_0)^4 + \cdots \tag{3.118}$$

- In the phenomenological description, this means that the non-linearity is denoted as:

$$\mathbf{P}^{(3)}_{\mathrm{NL}}(t) = \epsilon_0 \int_0^\infty \mathrm{d}\tau_1 \int_0^\infty \mathrm{d}\tau_2 \int_0^\infty \mathrm{d}\tau_3 \vdots\mathbf{E}(t-\tau_1)\mathbf{E}(t-\tau_2)\mathbf{E}(t-\tau_3) \tag{3.119}$$

and in index notation,

$$P^{(3)}_{\mathrm{NL},i}(t) = \epsilon_0 \int_0^\infty \mathrm{d}\tau_1 \int_0^\infty \mathrm{d}\tau_2 \int_0^\infty \mathrm{d}\tau_3 \chi^{(3)}_{ijkl}(\tau_1,\tau_2,\tau_3)E_j(t-\tau_1)E_k(t-\tau_2)E_l(t-\tau_3). \tag{3.120}$$

- We note here that $\chi^{(3)}$ is third rank tensor, and in frequency space the third order nonlinear optical susceptibility becomes

$$P^{(3)}_{\mathrm{NL}}(\omega) = \epsilon_0 \int_{-\infty}^\infty \mathrm{d}\omega_1 \int_{-\infty}^\infty \mathrm{d}\omega_2 \chi^{(3)}_{ijkl}(\omega;\omega_1,\omega_2,\omega_3)E_j(\omega_1)E_k(\omega_2)E_l(\omega_3), \tag{3.121}$$

where the energy conservation $\omega = \omega_1 + \omega_2 + \omega_3$ holds.

3.3.2.1 Optical Kerr Effect and Intensity-Dependent Refractive Index

- We now look at some important special cases and start with a monochromatic wave propagating in a given direction through homogeneous $\chi^{(3)}$ nonlinear medium. Among many nonlinear processes we investigate the contribution where

$$\mathbf{E}(t) = \frac{1}{2}\tilde{\mathbf{E}}(\omega_0)\mathrm{e}^{-\mathrm{i}\omega_0 t} + \frac{1}{2}\tilde{\mathbf{E}}^*(\omega_0)\mathrm{e}^{\mathrm{i}\omega_0 t},$$

and its Fourier transform

$$\mathbf{E}(\omega) = \frac{1}{2}\tilde{\mathbf{E}}(\omega_0)\delta(\omega-\omega_0) + \frac{1}{2}\tilde{\mathbf{E}}^*(\omega_0)\delta(\omega+\omega_0)$$

.

- Dropping all vector indices we write

$$\mathbf{P}_{\mathrm{NL}}^{(3)}(\omega) = \frac{3}{4}\epsilon_0 \chi^{(3)}(\omega;\omega,\omega,-\omega)|\tilde{E}(\omega)|^2\tilde{E}(\omega) \tag{3.122}$$

  which oscillates at the same frequency as the irradiated monochromatic wave.

- Substituting Eq. (3.122) into wave equation (3.92) and using FOURIER Transformation we found

$$\Delta\tilde{E} + \frac{\omega^2}{c^2}\left[1 + \chi^{(1)}(\omega) + \frac{3}{4}\chi^{(3)}(\omega;\omega,\omega,-\omega)|\tilde{E}(\omega)|^2\right]\tilde{E}(\omega) = 0, \tag{3.123}$$

  so the light propagates in medium having effective refractive index

$$n = \sqrt{1 + \chi^{(1)}(\omega) + \frac{3}{4}\chi^{(3)}(\omega;\omega,\omega,-\omega)|\tilde{E}(\omega)|^2}. \tag{3.124}$$

- The index of refraction is now dependent on the intensity. Therefore the propagation of light inside the medium depends on its (instantaneous) intensity. We can write for small nonlinearities

$$n(\omega, I) = n_{\mathrm{L}}(\omega) + \Delta n I(\omega) \quad n_{\mathrm{L}} = \sqrt{1 + \chi^{(1)}(\omega)} \tag{3.125}$$

  where the change in refractive index is given by

$$\Delta n = \frac{3}{8n_{\mathrm{L}}}\chi^{(3)}(\omega;\omega,\omega,-\omega). \tag{3.126}$$

- This is the case of *self-KERR effect*, i.e., the intensity-dependent refractive index due to the same monochromatic wave. This effect is responsible for self-phase modulation and self-focusing.

3.3.2.2 Self Focusing

- Take a beam with transverse intensity profile

$$I(r) = I_0 \mathrm{e}^{-r^2/r_0^2}, \tag{3.127}$$

  hence

$$n(r) = n_{\mathrm{L}} + \frac{3}{8n_L}\chi^{(3)} I_0 \mathrm{e}^{-r^2/r_0^2} \tag{3.128}$$

  which is an effective graded-index profile depending on the lateral position of the beam.

- Plane wave-front curves towards the propagation axis and the intensity concentrates further at propagation axis.

3.3.2.3 Self Phase Modulation

- The phase velocity $v_p = c/n$ of a wave propagating in z-direction changes with intensity $I(t)$.
- Phase modulation
$$\phi(z,t) = -\omega \Delta n I(t) \frac{z}{c} \tag{3.129}$$
whose time derivative is the instantaneous pulse frequency
$$\frac{\mathrm{d}\phi}{\mathrm{d}t} = -\frac{z\omega\Delta n}{c}\frac{\mathrm{d}I}{\mathrm{d}t}, \tag{3.130}$$
where the chirp frequency is
$$\frac{\mathrm{d}\omega}{\mathrm{d}t} = -\frac{z\omega\Delta n}{c}\frac{\mathrm{d}^2 I}{\mathrm{d}t^2}. \tag{3.131}$$
- For a GAUSSIAN pulse $I(t) = I_0 \mathrm{e}^{-t^2/t_0^2}$, the chirp is positive ($\mathrm{d}\omega/\mathrm{d}t > 0$) in the center of the pulse and negative ($\mathrm{d}\omega/\mathrm{d}t < 0$) in the wings of the pulse.

3.3.2.4 Four Wave Mixing

- Four-wave mixing (FWM) is a nonlinear optical process that occurs in a medium has $\chi^{(3)}(\omega)$ when multiple input laser beams interact with each other. In FWM, three input beams with frequencies ω_1, ω_2 and ω_3 are combined in a nonlinear medium to generate a fourth beam at frequency ω_4. This effect produce nonlinear polarization has the following formula
$$\mathbf{P}^{(3)}_{\mathrm{NL},i}(\omega_4) = \epsilon_0 \chi^{(3)}_{ijkl}(\omega_4; \omega_1, \omega_2, -\omega_3) \tilde{E}_j(\omega_1) \tilde{E}_k(\omega_2) \tilde{E}^*_l(\omega_3) \tag{3.132}$$
- The FWM effect is a type of nonlinear mixing, which means that the output signal is not simply a linear combination of the input signals. Instead, the FWM process involves the conservation of energy and momentum
$$\omega_4 + \omega_3 = \omega_1 + \omega_2 \tag{3.133}$$
$$\mathbf{k}_1 + \mathbf{k}_2 = \mathbf{k}_3 + \mathbf{k}_4 \tag{3.134}$$
from the input beams to the generated output beam, which can have a different frequency, phase, and polarization compared to the input beams.

- The nonlinearity of the vacuum is responsible for the interaction of four photons, which in free-space quantum electrodynamics is hardly to occur since its probability depends on the factor α^2 (α is the fine structure constant).

E We model a four-level laser by the rate equations

$$\begin{aligned} \dot{n}(t) &= kn(t)\Delta N(t) - \gamma_{\mathrm{R}} n(t) \\ \Delta\dot{N}(t) &= -kn(t)\Delta N(t) - \gamma_2 \Delta N(t) + P_2, \end{aligned}$$

with photon number $n(t)$, population inversion $N(t)$, pump rate P_2, upper level decay rate γ_2, resonator decay rate γ_{R}, and atom-photon coupling constant k, which absorbs all the details like the atomic cross-section, mode volume, etc.

1. Find the stationary solution of the rate equations. Write the steady state of the photon number as $n_{\mathrm{ss}} = (r-1)\gamma_2/k$ ($r =?$) and explain the physical meaning of r to the laser.
2. Suppose the laser exhibits a small distortion from its steady state

$$\begin{aligned} n(t) &= n_{\mathrm{ss}} + n_1(t), \quad n_1(t) \ll n_{\mathrm{ss}}, \\ \Delta N(t) &= \Delta N_{\mathrm{ss}} + \Delta N_1(t), \quad \Delta N_1(t) \ll \Delta N_{\mathrm{ss}}. \end{aligned}$$

   Show that the rate equations for the small distortions reduce to the linear form

$$\begin{aligned} \dot{n}_1(t) &= (r-1)\gamma_2 \Delta N_1(t) \\ \Delta\dot{N}_1(t) &= -\gamma_{\mathrm{R}} n_1(t) - r\gamma_2 \Delta N_1(t). \end{aligned}$$

3. The solutions take the form Ce^{st} (except for critical damping). Compute $s_{1,2}$.
4. Show that if $(r\gamma_2/2)^2 \gg (r-1)\gamma_2\gamma_{\mathrm{R}}$ the solutions take the form $s_1 \approx -r\gamma_2$, $s_2 \approx -[(r-1)/r]\gamma_{\mathrm{R}}$.

E A Laser has a gain bandwidth of 2 GHz centered at 500 nm and the longitudinal mode spacing (FSR) is 100 MHz. The round trip small signal gain is $g_0 = 0.1\,\mathrm{cm}^{-1}$ and the total round trip losses are $0.03\,\mathrm{cm}^{-1}$. You wish to use an etalon made of glass ($n = 1.5$) to encourage the laser to run on a single longitudinal mode.

1. What thickness would the etalon have to have?
2. Discuss the finesse and the surface refectivity needed if the laser is inhomogeneously broadened!

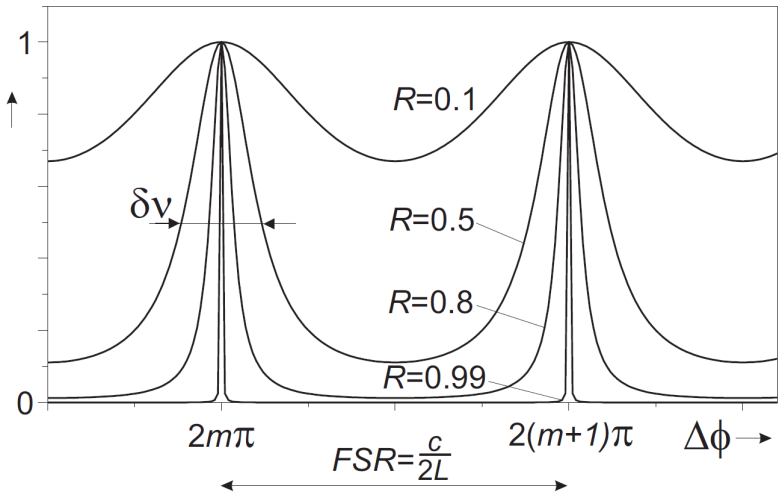

Fig. 3.8: Transmission of an etalon with thickness L.

Control Questions: These questions are designed to give you an overview over most of the lecture, and help the students to test their understanding of it.

- What main components does a laser typically consist of? Sketch their arrangement in a general laser model.
- Name some additional optical components you might find inside a real laser.
- Intuitively, how does a laser work?
- What are typical features of laser radiation?
- One of the important features of laser light is a high degree of coherence.
  a) Qualitatively, what is meant by coherence?
  b) How could you measure spatial coherence?
- What are EINSTEIN coefficients and what processes do they describe?
- What is population inversion and why is it required for laser operation?
- Historically, the first maser was built 7 years before the first laser, because it was easier to realize. Why?
- To achieve lasing, the electric field inside the cavity needs to fulfill the phase and amplitude condition. What are these conditions, and why are they required?
- Sketch and explain the two-, three- and four-level laser scheme. Why is a two-level laser (mostly) impossible in reality?

- The figure bellow shows the gain curve, cavity modes and lasing threshold of an exemplary laser.

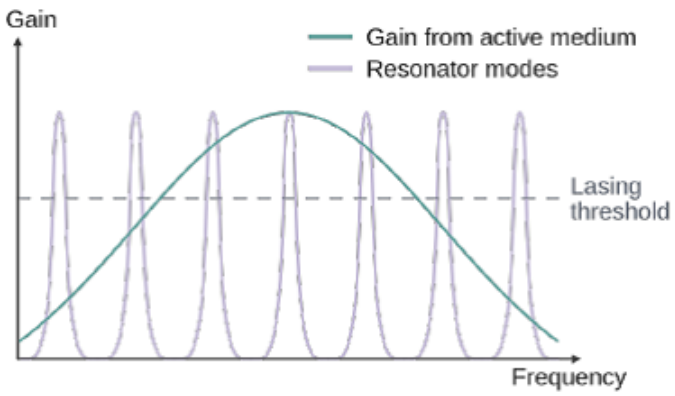

  a) Explain where these three curves come from.
  b) Sketch the resulting laser spectrum you would expect from these curves.
  c) What approximate output would you expect instead when the laser is only slightly pumped, so that the gain curve is entirely below the threshold?

- The width of any spectral line of a gain medium is usually broadened due to several mechanisms.

  a) What do "homogeneous broadening" and "inhomogeneous broadening" mean in this context? Explain using natural line width and Doppler broadening as examples.
  b) What is saturation broadening (aka. gain saturation)? Sketch how it affects homogeneously and inhomogeneously broadened lines.

- Most single-mode Lasers will output a Gaussian beam. What does such a beam look like? What happens when you focus a Gaussian beam with a lens?

- What is happening inside a Fabry-Pérot interferometer? What does its transmission spectrum look like and how does it depend on the reflectivity and distance of the mirrors?

- Sketch a stable and an instable resonator geometry. Draw the g_1-g_2-diagram for resonator stability and place your resonators on it.

- The figure bellow shows comparison of two wave packets in vacuum and in medium. Sketch how we are sure that there is no superluminal signalling.

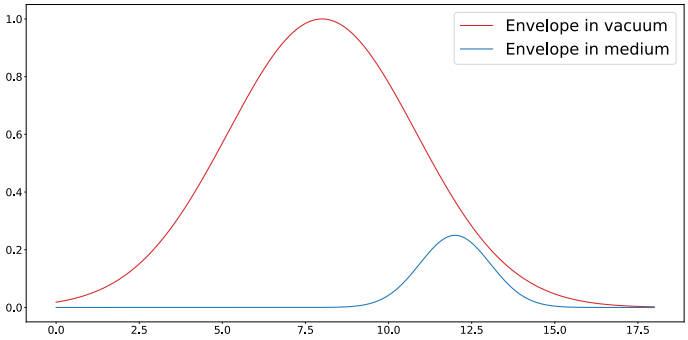

- What do Kramers-Kronig relations state?
- Write down the wave equation for light propagating in arbitrary media.
- What is the origin of nonlinear optical effects, and why can they often be neglected? What are second harmonic generation (SHG), sum frequency generation (SFG), and difference frequency generation (DFG)?
- What do these optical elements do? Explain the basics of their working principle and name a typical application in laser physics.

  a) Etalon.

  b) Reflective grating.

  c) Optical isolator

  d) Acousto-optic modulator (AOM).

  e) Pockels cell.

- Besides CW operation, lasers are also often run pulsed. Why might pulsed lasers be desirable?

Bibliography

[1] A E. Siegman, "Lasers", University Science Books (1986).

[2] O. Svelto, "Principles of Lasers", Fifth edition, Springer (2010).

[3] W T. Silfvast, "Laser Fundamentals", Second edition, Cambridge University Press (2004).

[4] P W. Milonni, J H. Eberly "Laser Physics", Wiley (2010).

[5] H. Haken, "Laser Theory", Springer (1984).

[6] W. Koechner, M. Bass, "Solid-State Lasers", Springer (2002).

[7] S. Hooker, C. Webb, "Laser Physics", Oxford University Press (2011).

[8] C C. Davis, "Lasers and Electro-Optics", Second edition, Cambridge University Press (2014).

[9] A. Szameit, "Laser Physics", Lecture Notes, Rostock University (2017).

[10] S. Scheel, B. Hage "Fundamentals of Photonics", Lecture Notes, Rostock University (2016).

[11] H. Abramczyk "Introduction to Laser Spectroscopy", Elsevier (2005).

[12] D. Meschede "Optics, light and lasers", Second edition, Wiley (2007).

[13] R. Menzel, "Photonics : linear and nonlinear interactions of laser light and matter", Berlin Springer, 2007.

[14] G. New, "Introduction to nonlinear optics", Cambridge University Press, (2011).

[15] G A. Reider, "Photonics: An introduction", Springer (2016).

[16] B E A. Saleh, M C. Teich "Fundamentals of Photonics", Third edition, Wiley (2019).

[17] A. Yariv, "Quantum Electronics", Third edition, Wiley (1988).